نشریه علمی - پژوهشی

پژوهشهای علوم و صنایع غذایی ایران

جلد ۱۴ شماره ۳

سال ۱۳۹۷

شماره پیاپی ۵۰

شاپا: ۴۱۶۱-۱۷۳۵

عنوان مقالات

نشریه علمی- پژوهشی پژوهشهای علوم و صنایع غذایی ایران جلد۱۴ شماره ۳ سال ۱۳۹۷ 2018 Vol.14 No.3 Iranian Food Science and Technology Research Journal

نشریه پژوهش های علوم و صنایع غذایی ایران

با شماره پروانه 124/847 و درجه علمی – پژوهشی شماره 3/11/810 از وزارت علوم، تحقیقات و فناوری
88/5/10

جلد 14 شماره 3 مرداد- شهریور 1397

درجه علمی- پژوهشی این نشریه طی نامه 3/11/47673 از وزارت علوم، تحقیقات و فناوری تا سال 1393 تمدید شده است.
90/4/14

ناشر: دانشگاه فردوسی مشهد **چاپ:** چاپخانه دانشگاه فردوسی مشهد

شمارگان: 250 نسخه **قیمت**: 5000 ریال (دانشجویان 2500 ریال)

نشانی: مشهد- کد پستی 91775 صندوق پستی 1163

دانشگاه فردوسی مشهد، دانشکده کشاورزی - گروه علوم وصنایع غذایی - دفتر نشریه پژوهش های علوم وصنایع غذایی ایران.

تلفن: 20-8795618 داخلی 321 نمابر: 8787430

این نشریه درپایگاههای زیر نمایه شده است:

پایگاه استنادی علوم ایران(ISC)، پایگاه اطلاعات علمی جهاد دانشگاهی(SID)، بانک اطلاعات نشریات کشور (MAGIRAN)

پست الکترونیکی: ifstrj@um.ac.ir

این نشریه در سایت http://jm.um.ac.ir/index.php/food_tech/index به صورت مقاله کامل نمایه شده است.

بسم الله الرحمن الرحیم

مندرجات

Iranian Food Science and Technology Research Journal
Vol. 14, No. 3, Aug. Sep. 2018, p. 1-16

نشریه پژوهشهای علوم و صنایع غذایی ایران
جلد 14، شماره 3، مرداد - شهریور 1397، ص. 16-1

Effect of temperature on the textural, thermal and microstructural properties of wheat flour/high amylose corn starch gels

Lida Shahsavani Mojarad[1], Ali Rafe[2*]

Received: 2017.07.31
Accepted: 2018.04.09

Abstract

Textural, thermal and microstructural properties of single component gels and binary composite gels (BCG) of high amylose corn starch (Hylon VII) mixed with wheat flour at different wheat flour/Hylon VII (WF/H) ratios (95:5, 90:10 and 85:15) and temperatures (100, 121 and 135ºC) were investigated. The visual appearance showed that as Hylon VII was increased in BCG, the stronger gel was achieved. Textural results confirmed by increasing Hylon VII, the firmness was increased, but the springiness, cohesiveness and adhesiveness were reduced. Moreover, the BCG at high temperatures showed the higher level of Hylon VII, the higher water solubility index would be achieved. The gelatinization enthalpy (ΔH) and peak gelatinization temperature (T_p) increased by improving the content of amylose in BCG. Hylon VII showed the lowest peak viscosity and the BCG gel containing high amount of Hylon VII indicated a reduction in the paste viscosity. The differences in the microstructure of WF and HylonVII gels were also reflected the pasting properties of the gels. Consequently, BCG of WF/H develops the stronger gel which can withstand at high thermal processing such as retort to improve the shelf-life of the final product.

Keywords: Composite gel; pasting properties; texture; microstructure; gelatinization.

Introduction

The most abundant polysaccharide and most important dietary source of carbohydrates is plant starch. Among different kinds of starch, corn starch is an interesting ingredient with a precious position in the food, nutraceutical, textile and biomedical industries due to its thickening, gelling and bulking characteristics (Sandhu & Singh, 2007). The granules of starch are comprised of two types of α-glucans including amylose and amylopectin, which are approximately 98 to 99% of the dry weight of starch (Carvalho *et al.*, 2007). Amylose is the chief material in gel forming which can also be linked with intact starch granules or fragments (Ott & Hester, 1995), whereas the swelling and gelation are associated with amylopectin (Maningat & Seib, 2010; Atwell, 2001; Krogars *et al.*, 2002). Corn starch can be classified into three groups based on the ratios of amylose to amylopectin. Normal corn starch has about 27% amylose, whereas "waxy starch" and "high amylase corn starch" possess less than 15% and more than 40% amylose, respectively. "High amylose corn starch" is a derivative form of the hybrid corn, which can be improved the strength and crunchiness of the product (Huang, 1995). A superior instance of high amylose corn starch is Hylon VII which contains about 70% amylose (Carvalho *et al.*, 2007; Kibar *et al.*, 2010).

Starch gels are an interesting issue from a colloidal chemical standpoint as well as their relation to other carbohydrate gels such as agar or cellulose. They are generally known as composite systems, consisting of swollen particles embedded in a three-dimensional (3-D) network of aggregated amylose chains. When starch granules are heated in excess water at a particular temperature, the swelling gets to be irrevocable and the structure of the granule is significantly modified. The structure of the gel is depends on the starch concentration, amount of leached-out

1 and 2. Ph.D Graduate and Associate Professor, Department of Food Science and Technology, Research Institute of Food Science and Technology (RIFST), Mashhad, Iran.
(*- Corresponding Author Email: a.rafe@rifst.ac.ir)
DOI: 10.22067/ifstrj.v14i3.66501

components, configuration of swollen granules and the ratio of amylose/amylopectin as well as their interactions (Luo *et al*., 2012; Carvalho *et al*., 2007).

Functionality of starch solutions during thermal processing is critical in food operations. The inexpensiveness techniques such as micro visco-amylograph (MVA) and rapid visco-analyser (RVA) can be utilized to track the important quality changes during thermal processing (Suh & Jane, 2003). However, RVA has been previously applied to develop gels to determine fundamental rheology of starch systems and survey the extent of interaction among a mixture of food components (Zhang & Hamaker, 2003; Shim & Mulvaney, 2001).

Although, the functionality changes of starch upon processing and monitoring of its physicochemical modification were previously studied (Zhang & Hamaker, 2003; Sriburi & Hill, 2000), but the effect of thermal processing on the paste viscosity of starch systems particularly in presence of Hylon-VII is still unknown. Furthermore, numerous studies have been reported on the individual physicochemical properties of high amylose corn starch (Cieśla & Eliasson, 2003) and Hylon VII (Kibar *et al.*, 2010; Shi *et al*., 1998), but the mixture of wheat flour with Hylon VII starch at different temperatures and concentrations did not investigate yet.

Therefore, the aim of current work was to evaluate the textural, gelling, pasting, thermal and microstructural properties of the single component gel (SCG) and binary composite gel (BCG) of wheat flour and Hylon VII starch at different ratios and temperatures. Certainly, the understanding of the functional properties of the gel mixture will be useful in selecting the appropriate ratio for high heat treatments such as cooking and improving the eating quality of final products like as noodle.

Material and methods

High amylose corn starch as Hylon VII (~70%) was donated by National Starch & Chemical Company (10 Finderne Avenue Bridgewater, New Jersey, USA). Wheat flour type 000 without any additives was purchased from Zarin Company (Mashhad, Iran). The approximate protein, fat, moisture and mineral content were measured following the methods of Association of Official Analytical Chemist Society (AOAC, 2000). The carbohydrate was also calculated by subtracting the amount of other ingredients from 100.

Gel preparation

Single component gels (SCG) and binary composite gels (BCG) were prepared according to the procedure of Foo *et al.* (2013) and Tan *et al*. (2015) with slight modifications. The stock solution of individual biopolymer of Hylon VII and wheat flour (10% w/w) was dispersed in distilled water. The BCG of Hylon VII and wheat flour at different ratios of WF/H including 95:5, 90:10 and 85:15 were prepared at the total biopolymer concentration of 10%. All the solutions were stirred for 5 min and left overnight to ensure complete hydration. Excessive stirring was avoided to ensure that no fragmentation was imparted to the samples. Then, the samples were put in retort for 30min at temperatures 100, 121, 135 ºC for SCG of Hylon VII starch gel and 100, 121 ºC for BCG of WF/H at different ratios of 95:5, 90:10 and 85:15.

When the solutions were still warm, they transferred into the cut off plastic syringes (20 ml; inner diameter: 19 mm). A thin layer of paraffin oil was initially used to avoid adhesiveness of gels and reduce the friction between the gel and inner surface of the syringes during unmoulding. All the gels were cooled down to room temperature (25 ºC) and refrigerated at 4 ºC for at least 18 h. The gels were gradually removed from the syringe by pushing the plunger. Then, they were cut into 20 mm in length by using a sharp razor and were left to equilibrate at room temperature for at least 1 h prior to the textural analysis.

Texture profile analysis (TPA)

Textural properties of gels were evaluated by using a TA-TX2 Texture Analyser (Stable Micro Systems Ltd., Surrey, UK), attached

with a 5 kg load cell. The cylindrical sample was compressed by using a 75 mm diameter compression platen at constant speed of 1.0 mm/s to a distance of 4 mm. The deformation level was set at 80% strain of the original sample height (Koliandris *et al*., 2008). In order to avoid barrel effect during compression, the bottom plate and the top of the gel were covered with a thin layer of paraffin oil. The gel strength was evaluated according to the method provided by the Gelatin Manufacturers Institute of America (GMIA) testing standard. At least five measurements were recorded for each type of gel.

Textural characteristics of gels including modulus or modulus of deformability as a measure of firmness (Pons & Fiszman, 1996), hardness or the strength of gel structure as a measure of maximum force at any time during the first compression cycle (Rosenthal, 1999), and cohesiveness as the ratio of the area of work during the second compression to the area of work during the first compression were determined. The latter determines the degree of difficulty in breaking down the internal gel structure (Li *et al*., 2004). In this study, cohesiveness was expressed as the percentage ratio of the peak area during the second compression to the peak area during the first compression.

Pasting properties

The pasting properties of the samples were determined using a Rapid Visco-Analyzer (RVA) (TCW, Newport Scientific, NSW, Australia). Briefly, 3 g of samples (wheat flour, mixed with different levels of Hylon VII starch) were transferred into an RVA aluminum canister and was mixed with 25 mL of distilled water. The sample was dispersed at a shear rate of 960 rpm for 10 s followed by a constant shear rate at 160 rpm. The samples were pasted according to the programmed heating and cooling cycle and the approved method ICC Standard No. 162 (Sriburi & Hill, 2000). The temperature profile was hold at 50ºC for 1 min, ramped to 95ºC at rate of ~12ºC/min, hold at 95ºC for 2.70 min, cool back to 50ºC at the same rate, hold at 50 ºC for 2min. Each analysis took 13 min and was performed in triplicates.

The paste viscosity responses of RVA curves were: onset paste temperature (initial increase in viscosity) (PT), peak viscosity (maximum viscosity during heating) (PV), breakdown viscosity (the difference between the maximum and minimum peak viscosity after heating ramp), setback viscosity (difference between the maximum viscosity during cooling and the lowest viscosity after the heating ramp), trough (the lowest viscosity during holding time), final viscosity (FV) and peak time (PTM).

Water solubility and absorption index

The water solubility (WSI) and water absorption indices (WAI) were determined following the procedure described by Bujang (2006), with slight modifications. Gel was prepared according to the procedure explained by Teck (2012). The solution samples were put in the retort for 30 min at the temperatures from 100 to 121 ºC and transferred into a centrifuge tube. Then, the mixture was centrifuged at 3000 g for 10 min. The supernatant was dried in an aluminum plate in the oven at 70 ºC for 24 h. Then, it was cooled in desiccator and weighed. WSI is calculated by using the Eq. 1:

$$WSI\ (\%) = \frac{weight\ of\ dissolved\ solid\ in\ supernatant}{weight\ of\ dry\ solids\ in\ orginal\ sample} \times 100 \quad (1)$$

The sediment formed after centrifuged in WSI was used to calculate WAI as follows:

$$WAI = \frac{weight\ of\ sediment\ formed}{weight\ of\ dry\ solids\ in\ orginal\ sample} \quad (2)$$

Differential scanning calorimetry (DSC)

Thermal properties of the gels were determined using a differential scanning calorimeter (Q100, TA Instruments, Inc., New Castle, USA). Starch samples (3±0.01 mg) were weighed into a steel DSC pan and mixed with 9 µL of distilled water (starch/water ratio 1:3). Then, the samples (~13 mg) were carefully stirred, hermetically sealed and left

for 1 h at room temperature to equilibrate. Heating was applied out from 30 to 200 ºC at a rate of 5 °C/min. A sealed empty pan was also used as a reference. The onset temperature (T_o), peak gelatinization temperature (T_p), and conclusion temperature (T_c) were measured as well as the gelatinization enthalpy change (ΔH) from the area of the endotherm peak using the Universal Analysis 2000 Software (TA Instruments, Inc., New Castle, USA).

Scanning Electron Microscopy (SEM)

The gel samples were initially frozen to -50ºC and subsequently were freeze-dried. The freeze-dried gels were cut to the size of 0.5×0.5×0.5 cm using a razor blade, to expose the cross-sectional (CS) surface. A conductive double-sided tape was used to fix the gel samples to the round aluminum stub prior to spotting them with a thin layer of gold-palladium by using a sputter coater Quorum SEM coating system for about 90 s. The morphology of the gel was observed at 100× magnifications under a SEM (EVO, MA 10; ZEISS, German) with an accelerating voltage of 5 kV.

Statistical Analysis

All the experimental data were analyzed in triplicates and presented in mean ± standard deviation (SD). The statistical evaluation between the treatments were subjected to One-way analysis of variance (ANOVA), using SPSS version 19.0 for windows software. A significant level of $P < 0.05$ was maintained throughout the study.

Results and discussion

The visual appearance of the wheat flour, Hylon VII and BCG of WF/H at various ratios and temperatures are presented in Fig.1. It can be seen that Hylon VII develops self-standing or "hard gel" at concentration 10% at temperatures 121 and 135ºC. In addition, Hylon VII gels were opaque and white in color with sticky and elastic texture (Fig. 1 b,c). The similar findings were also reported for modified tapioca starch gels (13%) (Foo *et al*., 2013). In contrary, wheat flour produces yellowish color gel with the attributes of "soft gel" or yield free standing gels without sagging (Fig. 1 d, e). For BCG two regimes of temperatures including 100 and 121ºC were studied. As the amount of Hylon VII was increased in the mixed gel at 100 ºC, the more elastic and firm gel was obtained (Fig.1. f-h). Similarly, by increasing the level of Hylon VII in BCG at 121ºC, the stronger gel was achieved (Fig. 1. i-k). From technical point of view, it is more critical to have strong and elastic gels to endure the harsh conditions in retort and sterilization processing. Therefore, textural properties of SCG and BCG of WF/H at different ratios and temperatures were investigated to achieve the suitable composite gel for industrial applications.

Textural properties of gels

Gels can be defined as a substantially dilute cross-linked system, which may be weak or strong depending on their flow behaviour in steady-state (Gulrez *et al*., 1980). Textural properties of SCG of Hylon VII, wheat flour and BCS gel at different ratios and temperatures are shown in Table1. It was found that the gel development did not occur at 100 ºC (Fig. 1 a), which may be attributed to the limited swelling of the granules would leave unabsorbed water and as a result Hylon VII did not gelatinize during cooking at boiling water (100 ºC) (Rendleman 2000; Ott & Hester, 1965). In contrast, high-amylose corn starch has shown strong gel and less stickiness at higher temperatures (Kasemsuwan *et al*., 1998; Carvalho *et al*., 2007).

The maximum firmness was obtained for Hylon VII at 135 ºC (224 N) and followed by SCG of Hylon VII at 121 ºC (136 N). This phenomenon could be related to the required level of solubility of amylose in gel forming and structure (Ott & Hester, 1965). The gelation is the formation of a three-dimensional network and contains only amylose and water. The molecular connection that happens after cooling of the gelatinized starch, generally known as retrogradation, leads to the elimination of water from gel and

dehydration of the material (Sobolewska-Zielińska *et al*., 2010; Ott & Hester, 1965). The main reason for the rupture of starch gels is the retrogradation which is associated with the syneresis of water. Therefore, the starch gel showed severe syneresis and the lowest rupture at 121 ºC.

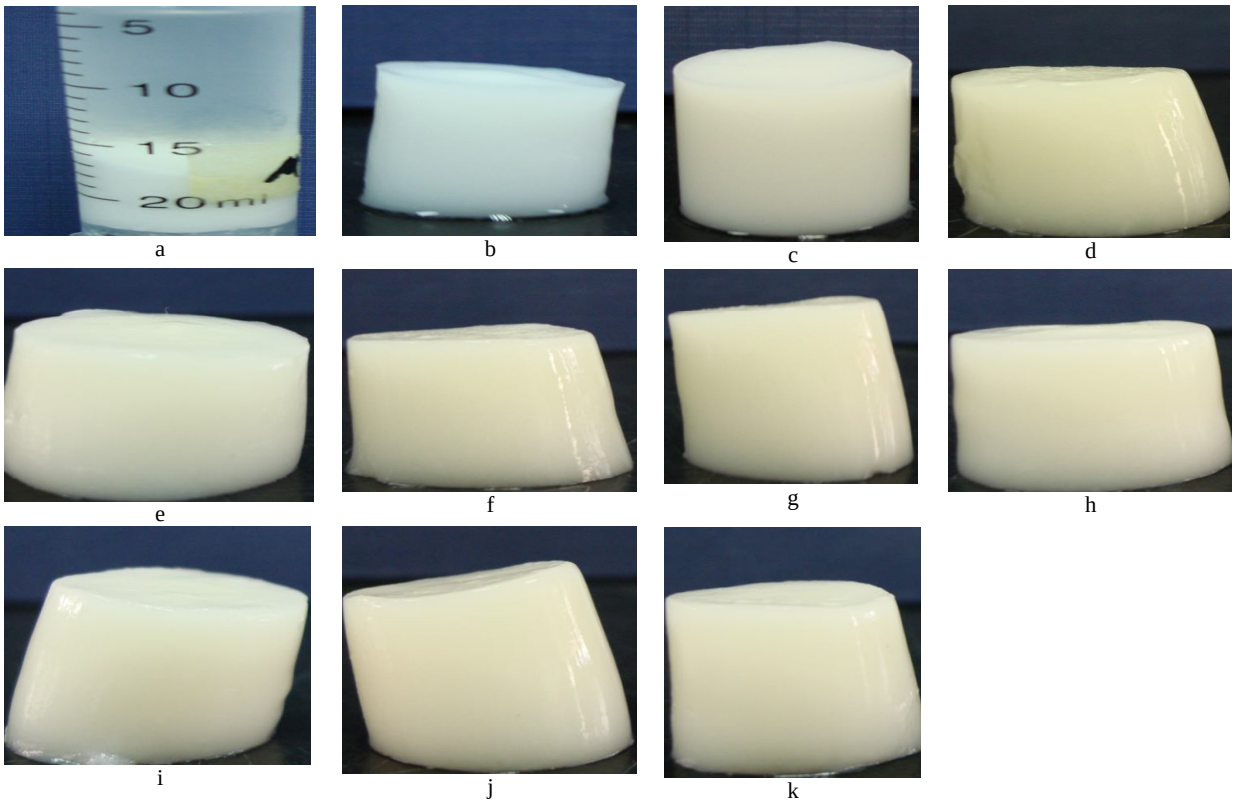

Fig. 1. Appearance of SCG of Hylon VII gels at :(a) 100 ºC, (b) 121 ºC, (c) 135 ºC; SCG of wheat flour gels at: (d) 100 ºC, (e) at 121 ˚C and BCG at different ratios and temperatures including: (f): WF/H 95:5 at 100 ˚C, (g) WF/H 90:10 at 100 ˚C, (h) WF/H 85:15 at 100 ˚C, (i) WF/H 95:5 at 121 ˚C, (j) WF/H 90:10 at 121 ˚C and (k) WF/H 85:15 at 121 ˚C.

Table 1. Textural properties of Hylon VII starch, wheat flour and BCG of WF/H at different temperatures.

WF/Hylon VII	Temperature (ºC)	Firmness (N)	Springiness (%)	Cohesiveness (%)	Adhesiveness (g)
0:100	121	136.77 ± 10.13 ^{b}	27.11±03^{a}	2.2±0.01^{e}	8.5 ± 0.72^{a}
0:100	135	222.40 ± 45.15 ^{a}	30.13±04^{a}	0.91±0.3^{f}	4.5 ± 0.74^{b}
100:0	100	32.5 ± 1.92^{a}	16.7±0.6^{a}	24.02±0.3^{a}	3.92 ± 0.59 ^{a}
95:5	100	32.92 ± 0.81^{a}	16.01±0.1^{b}	21.04±0.2^{b}	3.6 ± 0.45 ^{a}
90:10	100	33± 2.32^{a}	15.0± 0.4^{c}	22.34±0.1^{c}	3.4 ± 0.24 ^{a}
85:15	100	35.6 ± 1.90 ^{a}	13.22±0.1^{d}	22.11±0.4^{d}	4.1±0.64 ^{a}
100:0	121	18.85 ± 1.97^{c}	11.87±0.1^{e}	8.8±0.4^{a}	13.13 ± 1.80 ^{a}
95:5	121	23.05 ± 1.84^{b}	14.1±0.0^{d}	7.8±0.1^{b}	11.27 ± 1.59 ^{a}
90:10	121	30.2 ± 2.32^{a}	15.02±0.2^{c}	6.1±0.4^{c}	8.83 ± 1.04 ^{b}
85:15	121	36.65 ± 3.52^{a}	17.06±01^{b}	4.2±0.0^{d}	4.06±0.56 ^{c}

*. Values with similar letters in the same column do not differ significantly ($P < 0.05$).

Furthermore, results showed that adding Hylon VII at different ratios had no significant effect on the gel firmness at 100 ºC (Table 1), which may be related to the limited swelling of the high amylose corn starch. The starch granules of the wheat are gelatinized and swollen in excess water below 100ºC. Depending on the amount of the wheat

flour protein, the gluten network protein holds up the soluble wheat flour starch into the boiling water (Maningat & Seib, 2010). The granules of Hylon VII are diffused in water during boiling, but they are not swollen (Błaszczak *et al.*, 2007). Coagulation of gluten in wheat flour plays an important role in making gel, whereas Hylon VII starch may be considered as filler. On the other hand, the gel samples illustrated various results with different significances at 121 ºC. By increasing the content of Hylon VII to BCG, firmness increased and adhesiveness decreased. The lowest firmness was found for the sample did not have any Hylon VII (WF). This shows that all wheat starches have been gelatinized and the gel structure is "soft gel" and due to the high leaching of amylose, the highest adhesiveness was obtained for SCG of wheat flour. During heating, the thermal energy breaks hydrogen bounds among the molecules of the starches. Hylon VII starch granules were hydrated by diffusion of water. The granules swell and lose their structure; the amylose leaches out and leads to the gelation process. During cooling, retrogradation happened and the distances among the starch molecules decreased, and finally the water was taken out of the gel and dehydration occurred. So, the high gel strength values reported for Hylon VII starch are perhaps related to the retrogradation of amylose (Sobolewska-Zielińska *et al.*, 2010; Sandhu & Singh, 2007; Kibar *et al.*, 2010). The results showed that by increasing the level of Hylon VII starch, the firmness increased and the adhesiveness decreased (Table 1).

Pasting properties

Pasting behaviours of wheat flour mixed with different levels of Hylon VII are reported in Table 2. The paste viscosity profiles of all samples were smooth curves without sharp peaks. The highest PV as a measure of gelatinization (239.5 RVU) was observed for wheat flour (Fig. 2).Starch gelatinization as a complex phenomenonoccurs when the internal crystaline structure of the starch granules is lost by heating in the presence of excess water (Carvalho *et al.*, 2007). The higherPV indicates high amylopectin content and higher resistance to retrogradation (Van Hung *et al.*, 2006). As the Hylon VII was increased in the BCG of WF/H, the pasting properties were reduced (Fig. 3). Peak viscosity was decreased from 148, 127 and 107 RVU when wheat flour was substitutes with Hylon VII at 95:5, 90:10 and 85:15, respectively.

Holding samples at 95 ºC under constant shear rate caused the disruption of granules, leaching and alignment of strach molecules, which consequently let to viscosty breakdaown known as trough. The FV is the paste viscosity at the end of the cooling cylce and is largley determined by the retrogradation of soluble amylose by cooling (Delcour & Hoseney, 2010). Although, the setback viscosity is the recovery of viscosity during cooling of cooked strach and is known as FV minus the holding viscsoity (Islas-Rubio *et al.*, 2014). As expected, setback viscosity which is associated with the degree of retrogradation of starch paste was found higher for wheat flour (Fig. 2). Breakdown, FV and setback viscosities were decreased by substituting of wheat flour with Hylon VII, due to reduction of amylopectin from wheat flour caused by starch dilution effect, promoted by Hylon VII addition (Fig. 3). Similar findings were also found for BCG of rice flour/defatted soy flour and whey protein/ Hylon VII (Sereewat *et al.*, 2015; Carvalho *et al.*, 2007), which may be attributed to the competition of rice starch or whey proteinto hydration as well as the restraint action of amylose to swelling, which results to lower viscosity. The low gelatinization peak and the high onset tempreture of Hylon VII could be explained by the high amylose content and low level of amylopectin (Carvalho *et al.*, 2007).

Table 2. Paste behaviours of Hylon VII, WF and WF/H mixtures in RVA at 10% concentartion.*

WF:H	Peak viscosity (RVU)	Trough (RVU)	Breakdown (RVU)	Final viscosity (RVU)	Setback (RVU)	Peak time(min)	Pasting temperature (ºC)
100:0	239.5 ± 0.1[a]	134.5± 0.1[a]	105±1.4[a]	250±01[a]	115.5±0.2[a]	2.2±0.1[d]	43±0.0[c]
95:5	148.1± 1.0[b]	87.2 ±2.3[b]	61± 0.8[b]	180±0.5[b]	92.83±0.1[b]	2.5±0.4[c,d]	43±0.8[c]
90:10	127.6 ± 0.4[c]	78.9 ± 0.9[c]	48.66± 1.2[c]	160±0.4[c]	81.08±0.3[c]	3±0.0[b]	44±0.2[b]
85:15	107.7± 1.2[d]	69.7± 0.7[d]	38± 0.0[d]	140±0.7[d]	70.33±1.1[d]	3.4±0.1[a]	45±0.1[a]
0:100	n.a.	n.a.	n.a.	n.a.	n.a	n.a.	n.a.

*. Mean values in the same column with different letters are significantly different at $p < 0.05$.

*. All the viscosities are presented in Rapid Visco Unit (RVU), which equals to 12 cp. n.a. is not applicable

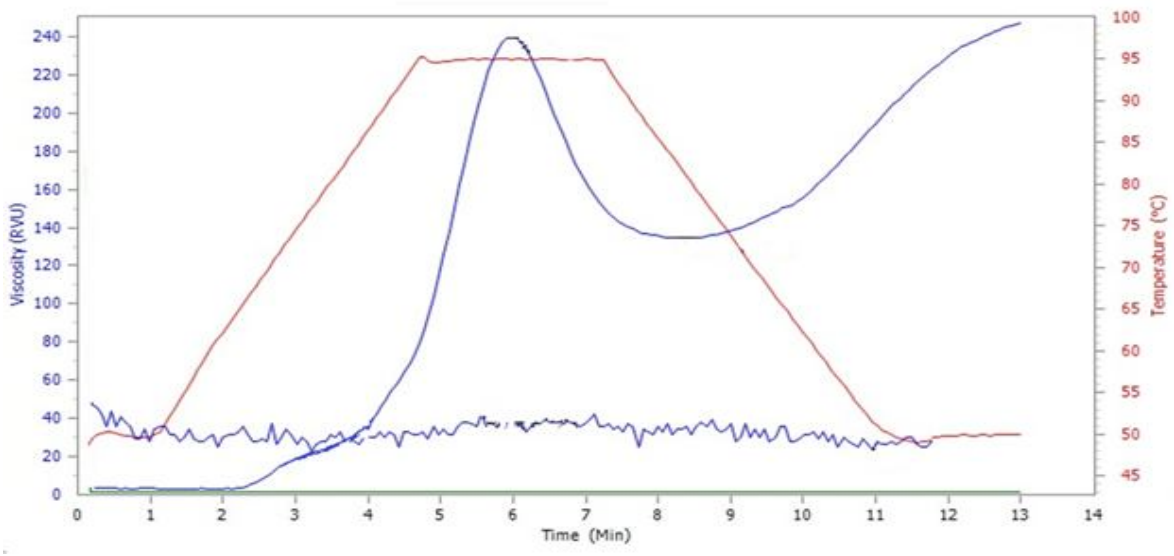

Fig.2. RVA pasting profiles of Hylon VII starch (the bottom graph) and wheat flour (WF) at 10%.

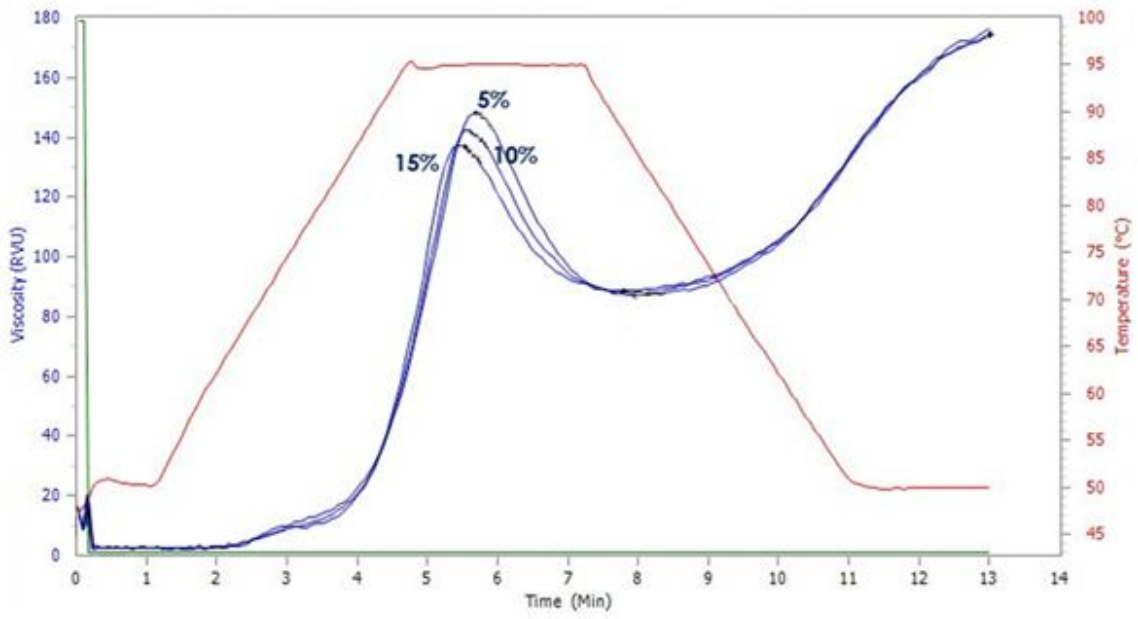

Fig. 3.RVA pasting profiles of BCG of wheat flour mixed with Hylon VII. 5%: WF/H (95:5), 10%: WF/H(90:10), 15%: WF/H

(85/15).

Water solubility and absorption index

For gel structure, the amount of amylose in the soluble is necessary (Ott & Hester, 1965). Water solubility index (WSI) was used as a scale of the degradation of starch components, and often determines the level of free molecules leached out from the starch granules. Water absorption index (WAI) measures the rate of water absorbed by starch. Water solubility index (WSI) shows mobility and amount of soluble polysaccharide released from the starch components. WAI and WSI can be used as index of starch gelatinization (Bujang, 2006). The reverse relationship between the water absorption and amylose content led to the result that as the amylose content increased, the water absorption increased and water solubility decreased (Kibar *et al.*, 2010; Rodriguez-Sandoval *et al.*, 2012). The gel forming and ability of heated composite flour and Hylon VII starch to absorb water is determined using water absorption index (WAI) and the fragment granules with residual amylose is responsible for water absorption (Hongsprabhas, 2007). The water solubility and water absorption indices for Hylon VII starch at various temperatures are provided in Fig. 4. The results revealed that both the water absorption and water solubility indices depend on the temperature. As temperature increases, WAI increases and WSI decreases. The low gelatinization temperature of Hylon VII may be due to the more water absorption by more amylose content. It can be found from Fig. 5, by increasing level of amylose, WSI decreased at 100 ºC. It may be due to the development of Hylon VII percentage, reduced amount of wheat flour and the reduction of starch gelatinization. While at a high temperature (121 ºC), the results indicated that by increasing the level of Hylon VII more water absorption and more gelatinization are observed (Fig. 5).

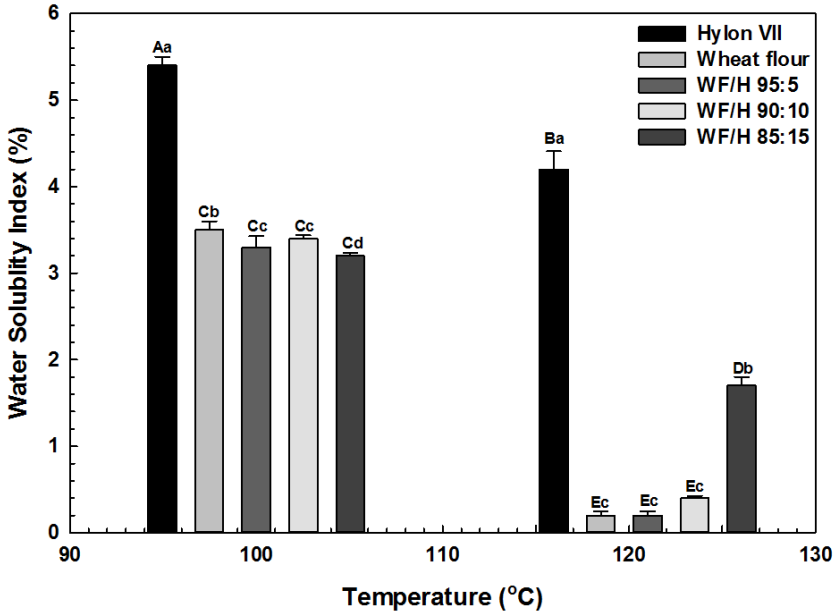

Fig. 4. The WSI of SCG and BCG of H/WF at different ratios and temperatures. The upper and lower case letter are corresponding to the statistical significant difference between treatments and within treatments, respectively ($p<0.05$).

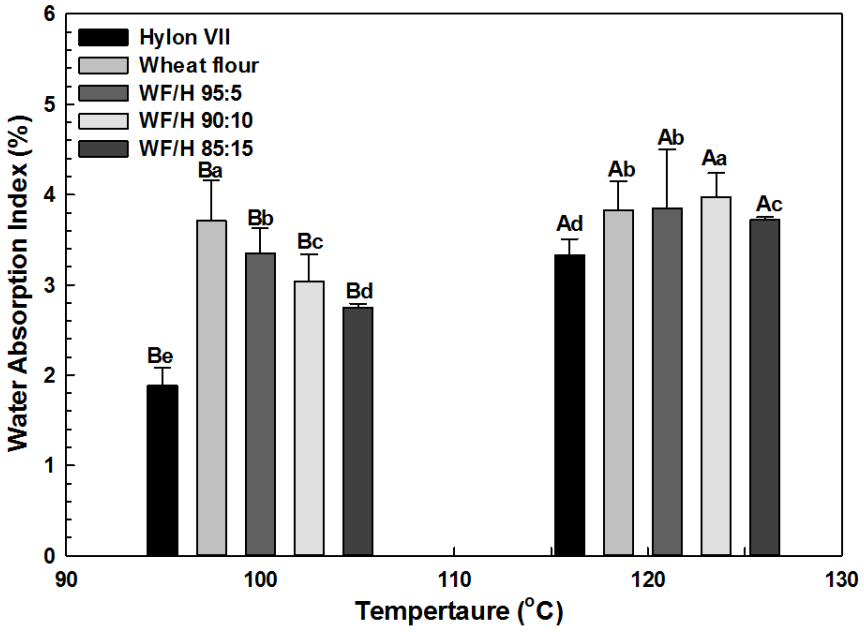

Fig. 5. The WAI of SCG and BCG of H/WF at different ratios and temperatures. The upper and lower case letter are corresponding to the statistical significant difference between treatments and within treatments, respectively ($p<0.05$).

Differential scanning calorimetry (DSC)

Thermal properties of the gels are summarized in Table 3 and their corresponding DSC thermograms are shown in Fig. 6. All the samples showed an endothermic peak, which shifted to higher temperatures as the wheat flour was substituted by Hylon VII. As a result, the WF/H of 85:15 was shown the higher T_o, T_p and T_c than that of the other samples (Table 3). Gelatinization temperature of the gels directly depend on the amylose content and increases with enhancing the amylose content (Table 3) (Matveev *et al.*, 2001; Zaidul *et al.*, 2008). The gelatinization temperature (T_p) of wheat flour and Hylon VII were observed at 61.91 and 107.50 ºC, respectively (Fig. 6).Whereas, the T_p of BCG of WF/H at ratio 95:5 (~107.83 ºC) was obviously closer to Hylon VII. However, the addition of Hylon VII to wheat flour caused enhancement of T_p, which issolely related to the gelatinization transition of the wheat flour starch granules (Zaidul *et al.*, 2008). Moreover, T_o, T_p and T_c of Hylon VII were greater than the others gels except BCG of WF/H at ratio 85:15, which may be attributed to β-Type crystalline form of amylopectin as well as the hydrogen bonding between the chains in high amylose structures, resulting in higher gelatinization temperatures (Kibar *et al.*, 2010). Therefore, water uptake of Hylon VII was limited due to this chemical hindrance and needs higher temperatures for complete gelatinization. In contrast, the lowest T_o (39.77 ºC) and T_c (92.09 ºC) were found for wheat flour, whereas the highest values of T_o and T_c were seen for BCG of WF/H at ratio 85:15 (Table 3).

Since, the BCG of WF/H at ratio of 85:15 had the highest amylose content, it would require more energy to initialize the starch gelatinization. Therefore, the more gelatinization enthalpy (ΔH) was observed for the sample. The enthalpy reduction of wheat flour can be attributed to its more fiber, which is in agreement with the findings of other workers (Duta & Culetu, 2015; Sabanis *et al.*, 2009; Katina *et al.*, 2006). As the amount of amylose was increased, T_p, T_o, T_c and the gelatinization enthalpy(ΔH) were raised. In fact, increasing the level of Hylon VII would reduce the gelatinized wheat flour starch (Fig. 6).

Table 3. DSC results of the gelatinization peak.

WF:Hylon VII	T_o(ºC)	T_p(ºC)	T_c (ºC)	ΔH(J/g)
100:0	39.77±0.15^{e}	61.91±0.7^{e}	92.09±0.10^{d}	245.4±0.8^{d}
95:5	100.75±013^{d}	107.83±0.3^{c}	130.00±0.2^{b}	483.70±0.2^{b}
90:10	102.5±0.2^{c}	109.12±0.2^{b}	132±0.1^{c}	512.3±0.6^{c}
85:15	108.75±0.3^{a}	118.11±0.0^{a}	145.00±0.0^{a}	845.6±0.2^{a}
0:100	101.74±0.2^{b}	107.50±0.4^{c,d}	130.01±0.6^{b}	238.8±0.1^{e}

*. Mean values in the same column with different letters are significantly different at $p < 0.05$.

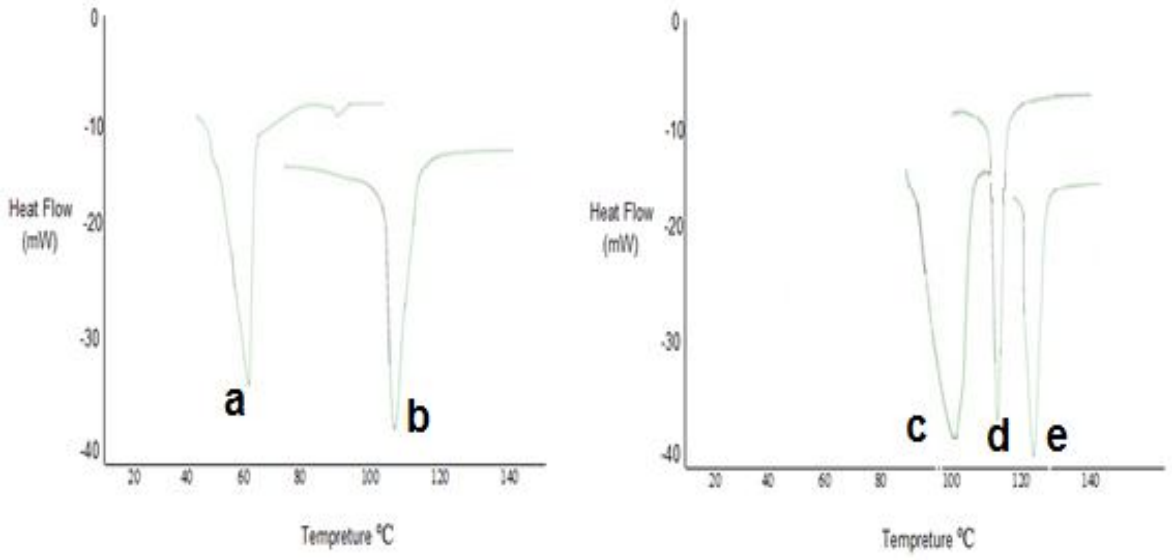

Fig. 6. DSC thermogram of gel samples, a: WF, b: Hylon VII, c: BCG of WF/H at ratio 95:5, d: BCG of WF/H at ratio 90:10, e: BCG of WF/H at ratio 85:15.

Microstructure of gels

The SEM images were obtained from cross-section of the gels, which illustrated the interior morphological structure of the gel network. The microstructural SEM images of SCG and BCG of wheat starch and Hylon VII at different temperatures are shown in Fig. 7. It can easily be seen very distinct structures in which SCG of wheat flour and Hylon VII has a smooth structure, well defined by the holes left where air and water entrapped in the gel (Fig 7 a, b and c, d). The wheat flour gel showed large fibrous strands with large void spaces and no remnant of granular structure which can entrapped water and produced a cream-yellowish gel. On the other side, the SCG of wheat flour was constructed of porous and cellular structure with interconnected thin walls (Fig.7 a). In comparison, SCG of Hylon VII illustrated a homogenous "honeycomb" network of interconnected pores with an average size of about 100 µm. The extensive amylose network was formed with granular structure indicating that it has more thermo-mechanical resistance structure (Fig. 7b). Due to the larger pore size, it lets the light pass easily through the structure, SCG of Hylon VII showed opaque gel with lighter color than that of wheat flour. As a result, it can be concluded that wheat flour gelatinized at lower temperature (~62 ºC) than HylonVII gels (107.5 ºC), which is in agreement with previous work on tapioca starch(66.2 °C), corn starch and maize starch (~69.9 °C) (*Carvalho et al.*, 2007; Carvalho & Mitchell, 2000; Tan *et al.*, 2015; Li *et al.*, 2007). Furthermore, it can be concluded that the fibrous thin network strands of wheat flour gels led to weak and soft gels as indicated by the low hardness in TPA. In contrary, the globular structure of

Hylon VII cause to strong and hard gel as confirmed by the textural studies. The differences in the microstructure of wheat flour and Hylon VII gels were also reflected the pasting properties of the gels.

Effect of Hylon VII on the BCG microstructure

As wheat flour substituted by Hylon VII, the gel structure was reinforced (Fig.1 c, d). Therefore, Hylon VII acted like as a filler between retrograded amylose entanglements and a more compact structure was formed (Fig. 7c, d). In contrast, the presence of wheat flour in BCG work a plasticizer by preventing molecular rearrangement of amylose leading to reduced rigidity. It was also similarly found for BCG of high amylose starch gels mixed with whey protein (Carvalho *et al*., 2007). However, the independent Hylon and wheat starch networks were not distributed evenly throughout the gel. As a result, the textural properties of BCG were relatively weaker than the respective SCG, particularly for Hylon VII-SCG. Similar findings were observed for maize starch-egg white and amylase-egg white gels (Tan *et al*., 2015; Li *et al*., 2007). The more densely packed structure of SCG was also in agreement with the work of Rodriguez-Hernandez *et al*., 2006 in which maize starch promoted segregation of gel led to a higher local polymer concentration and more compact networks for the mixed gels of waxy maize starch and gelatin.

Effect of temperature on the BCG microstructure

During cooking, the starch granules of the wheat flour become swollen and the granules gelatinized have lower resistance to enzyme which can be digested easier than high amylose starch (e.g. Hylon VII). High amylose starch is not gelatinized when cooked in water at 100ºC (Rendleman, 2000). The effect of different temperatures on the microstructure of SCG and BCG gels are illustrated in Fig.7 d, e and f. It indicates the potential interactions between the coagulated proteins and the gelatinized wheat starch components at different temperature (Fig.7). As shown, the surface structure becomes softer and sticky as the temperature increased. The surface areas interconnected by the fibrils that contain gluten protein and some material leached from the wheat starch granules. Starchy filamentous network and strongly swollen starch granules are visible. As it is clear, the granules are not gelatinized at 100 ºC. Dissolution in water is very slight at that temperature and the starch granules are not completely gelatinized at 121 ºC. Raw starch granules can still be observed at the core. This may be, due to the fact that Hylon VII does not swell and gelatinize during cooking in boiling water (100 ºC) and the swelling of Hylon VII starch granules is limited at higher temperatures. In this state, the Hylon VII starch gelatinization is not yet complete, and amylose enrichment occurs without more leaching, so the amylose is quite dense and still have crystalline. Therefore, by adding Hylon VII starch to wheat flour at 100ºC, the surface of gel structure becomes rougher than higher temperatures. Since, Hylon VII was showed high gel strength, particularly when mixed with wheat flour, it can withstand at high thermal processing such as retort processing.

Conclusion

The effect of high temperatures and high amylose corn starch on the pasting properties as well as textural, thermal and microstructural of wheat flour gels were studied. By increasing the Hylon VII level in the BCG of WF/H, due to reduction of amylopectin from wheat flour caused by starch dilution effect, the pasting properties were reduced. It can be concluded that the competition of wheat flour for hydration and the restraint action of amylose to swelling, results to lower viscosity. The low gelatinization peak and the high onset temperature of Hylon VII could be explained by the high amylose content and low level of amylopectin. The highest WAI was found for Hylon VII at 121 ºC, which may be related to higher diffusion of amylose to the granule surface. The combination that exhibit harder gels, tend to have more and higher Hylon VII level and the gel firmness is depend on retrogradation of starch gels. Hylon VII starch

has a low gelatinization level at 100 ºC, and dissolution in water at that temperature was slight. Increasing the amylose level in gels cause firmness, strength and tightness in the gel network structure at retort temperature (121ºC). Gel formation depends on the degree of hydration, the concentration of amylose in the soluble and rate of temperature. Thermal studies showed that the BCG of WF/H at ratio 85:15 had the greatest T_o, T_p and T_c than that of the other samples. Due to the more amylose content, it had more gelatinization enthalpy (ΔH). In fact, increasing the level of Hylon VII would reduce the gelatinized wheat flour starch. SEM results confirmed that the fibrous thin network strands of wheat flour gels led to weak and soft gels as indicated by the low hardness in TPA. In contrary, the globular structure of Hylon VII cause to strong and hard gel as confirmed by the textural studies. The differences in the microstructure of wheat flour and HylonVII gels were also reflected the pasting properties of the gels. As wheat flour substituted by Hylon VII, the gel structure was reinforced. As a result, the textural properties of BCG were relatively weaker than the respective SCG, particularly for Hylon VII-SCG. Cooked starch gels by increasing amylose, showed higher viscosities at higher shear rates. Consequently, BCG of WF/H develops the stronger gel which can withstand at high thermal processing such as retort to improve the shelf-life of the final product

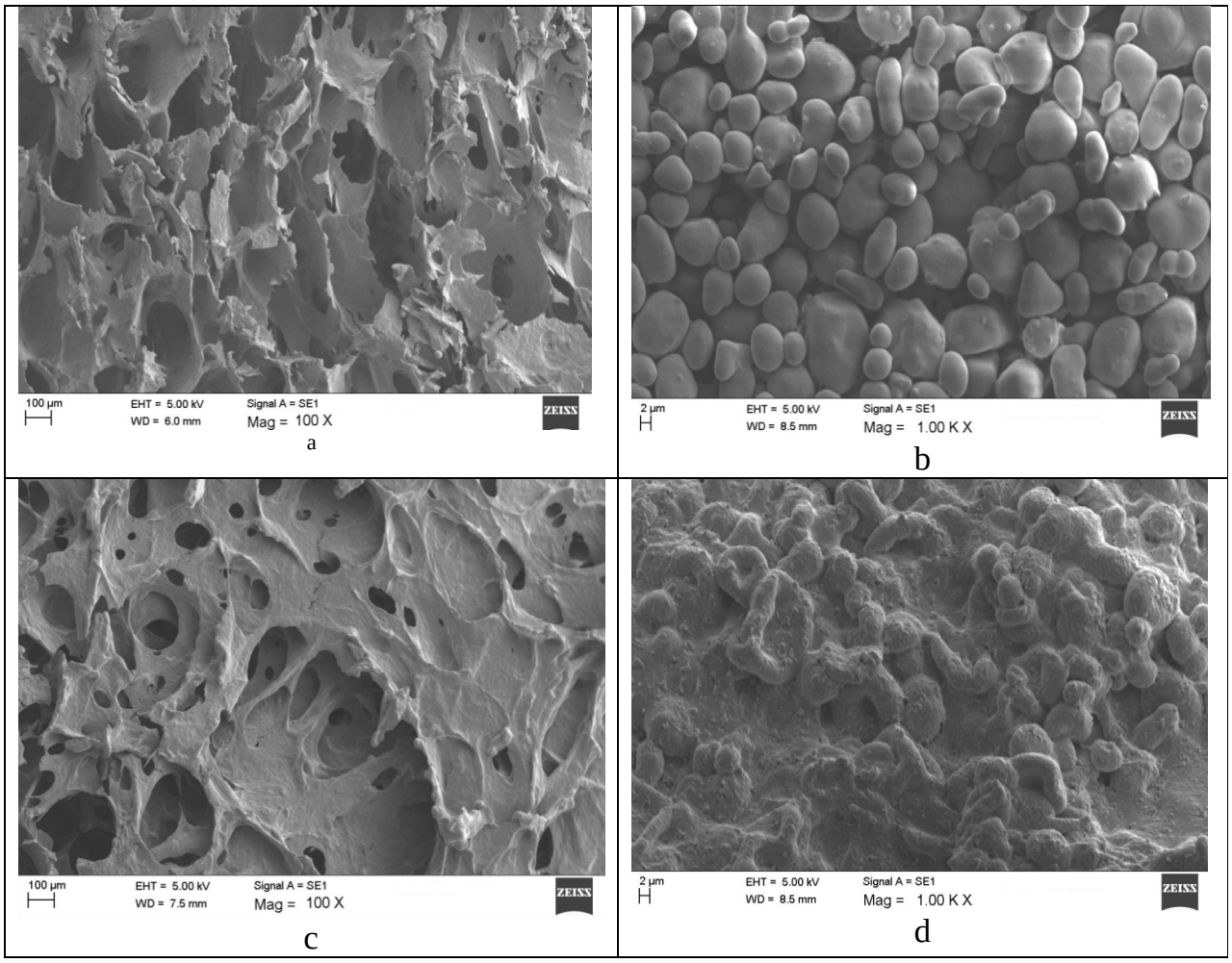

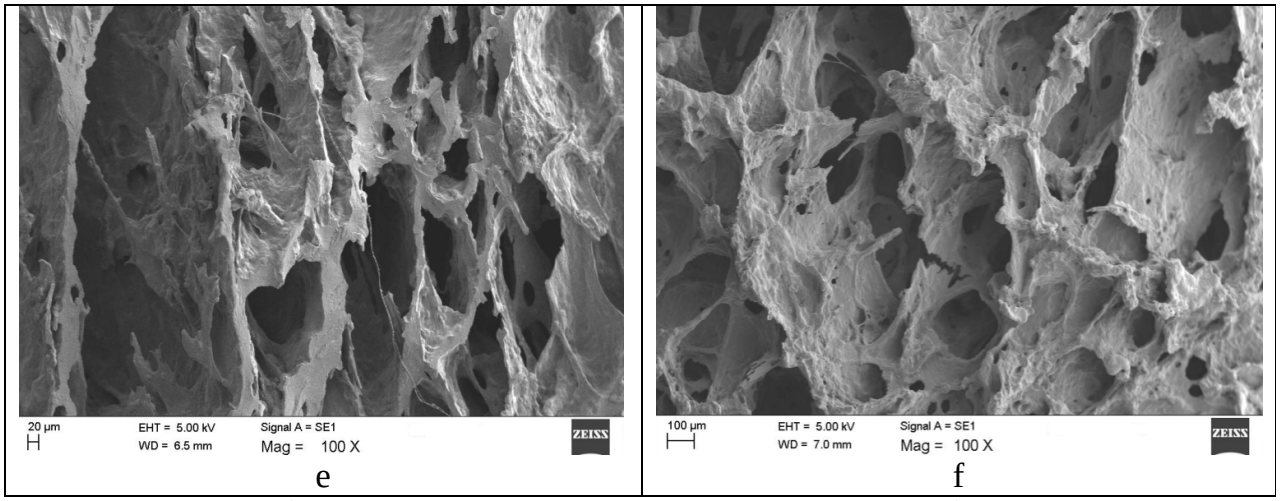

Fig. 7. SEM micrographs of the SCG at 100 ºC: (a) WF , (b) H; at 121 ºC: (c) WF , (d) H; BCG of (e) WF/H at ratio 85:15 at 100 ºC and (f) BCG of WF/H at ratio 85:15 at 121 ºC.

.

References

AOAC International.2000. Official Methods of Analysis of the AOAC International, 17th ed. Association of Official Analytical Chemists, Inc. Maryland, USA.

Atwell, W. A. 2001. *Wheat flour*: Eagan Press.

Błaszczak, W., Fornal, J., Kiseleva, V., Yuryev, V., Sergeev, A., and Sadowska, J. 2007. Effect of high pressure on thermal, structural and osmotic properties of waxy maize and Hylon VII starch blends. *Carbohydrate polymers* 68 (3):387-396.

Bujang, A. 2006. Effect of destructuring on the physicochemical and functional properties of Sago starch, Universiti Sains Malaysia.

Carvalho, C., Onwulata, C. and Tomasula, P. 2007. Rheological properties of starch and whey protein isolate gels. *Food Science and Technology International* 13 (3):207-216.

Delcour, J.A., Hoseney, R.C. 2010. Principles of Cereal Science and Technology, Third ed. AACC International, St. Paul, MN. USA.

Duta, D.E. and Culetu, A. 2015. Evaluation of rheological, physicochemical, thermal, mechanical and sensory properties of oat-based gluten free cookies. *Journal of Food Engineering*, 162, 1-8.

Foo, W.T., Liong, M.T. & Easa, A.M. 2013. Textural and strauctural breakdown properties of selected hydrocolloid gels. *Food Research International*, 52, 401-408.

Huang, D. 1995. New perspectives on starch and starch derivatives for snack applications. *Cereal foods world* 40 (8):528-531.

Islas-Rubio, A.R., Calderon de la Barca, A.M., Cabrera-Chavez, F., Cotagatelum, A.G. & Beta, T. 2014. Effect of semolina replacement with a raw: popped amaranth flour blend on cooking quality and texture of pasta. *LWT-Food Scienc and Technology*, 57, 217-222.

Koliandris, A., Lee, A., Ferry, A. -L., Hill, S., & Mitchell, J. 2008. Relationship between structure of hydrocolloid gels and solutions and flavour release. *Food Hydrocolloids*, 22, 623-630.

Kasemsuwan, T., Bailey, T. and Jane, J. 1998. Preparation of clear noodles with mixtures of tapioca and high-amylose starches. *Carbohydrate polymers* 36 (4):301-312.

Katina, K., Salmenkallio-Marttila, M., Partanen, R., Forssell, P., & Autio, K. (2006). Effects of sourdough and enzymes on staling of high fibre wheat bread. *LWT-Food Science and Technology*, 39, 479-491.

Kĭbar, E. A. A., I. Gönenç, and F. Us. 2010. Gelatinization of waxy, normal and high amylose corn

starches. *GIDA-Journal of Food* 35 (4):237-244.
Krogars, K., O. Antikainen, J. Heinämäki, N. Laitinen, and J. Yliruusi. 2002. Tablet film-coating with amylose-rich maize starch. *European journal of pharmaceutical sciences* 17 (1):23-30.
Luo, L., Tashiro, Y. and Ogawa, H. 2012. Relationship between the water molecules in fish-meat gel and the gel structure. *Fisheries Science* 78 (5):1137-1146.
Li, J.H., Vasanthan, T., Hoover, R. & Rossnagel, B.G. 2004. Starch from hull-less barley: IV. Morphological and structural changes in waxy, normal and high-amylose starch granules during heating. *Food Research International*, 37, 417-428.
Maningat, C.C., and Seib, P.A. 2010. Understanding the physicochemical and functional properties of wheat starch in various foods. *Cereal Chemistry* 87 (4):305-314.
Matveev, Y. I., Van Soest, J., Nieman, C., Wasserman, L., Protserov, V., Ezernitskaja, M., and Yuryev, V. 2001. The relationship between thermodynamic and structural properties of low and high amylose maize starches. *Carbohydrate polymers* 44 (2):151-160.
Ott, M., and Hester, E. E. 1965. Gel formation as related to concentration of amylose and degree of starch swelling. *Cereal Chem* 42:476-484.
Pons, M. & Fiszman, S.M. 1996. Instrumental texture profile analysis with particular reference to gelled systems. *Journal of Texture Studies*, 27, 597-624.
Rendleman Jr, J. A. 2000. Hydrolytic action of α-amylase on high-amylose starch of low molecular mass. *Biotechnology and applied biochemistry* 31 (3):171-178.
Rosenthal, A.J. 1999. Relation between instrumental and sensory measures of food texture. In: Food Texture Measurement and Perception (edited by A.J. Rosenthal). Pp. 1–17. Gaithersburg, MD, USA: Aspen Publishers.
Sabanis, D., Lebesi, D., & Tzia, C. 2009. Effect of dietary fibre enrichment on selected properties of gluten-free bread. *LWT-Food Science and Technology*, 42, 1380-1389.
Sandhu, K. S., and Singh, N. 2007. Some properties of corn starches II: Physicochemical, gelatinization, retrogradation, pasting and gel textural properties. *Food Chemistry* 101 (4):1499-1507.
Sereewat, P., Suthipinittham, C., Sumathaluk, S., Puttanlek, C., Uttapap, D. and Rungsardthong, V. 2015. Cooking properties and sensory acceptability of spaghetti made from rice flour and defatted soy flour. *LWT-Food Science and Technology*, 60(2):1061-1067.
Shim, J., & Mulvaney, S. J. 2001. Effect of heating temperature, pH, concentration and starch/whey protein ratio on the viscoelastic properties of corn starch/whey protein mixed gels. *Journal of the Science of Food and Agriculture. 81*, 706-717.
Sriburi P. and Hill S.E. 2000. Extrusion of cassava starch with either variations in ascorbic acid concentration or pH. *International Journal of Food Science and Technology*, 35(2): 141–154.
Sobolewska-Zielińska, Joanna, and T. Fortuna. 2010. Retrogradation of starches and maltodextrins of origin various. *Acta Sci. Technol. Aliment* 9 (1):71-81.
Tan, T.C., Foo, W.T., Lion, M.T. & Easa, A.M. 2015. Comparative assessment of textural properties and microstructure of composite gels prepared from gelatin or gellan with maize starch and/or egg white. *International Journal of Food Science and Technology*, 50, 592-604.
Teck, F. W. 2012. Comparative assessment of gelatin and gellan maize starch-egg white, Universiti sains Malaysia.
Van Hung, P., T. Maeda, and N. Morita. 2006. Waxy and high-amylose wheat starches and flours-Characteristics, functionality and application. *Trends in Food Science & Technology* 17 (8):448-456.
Zaidul, I., N. Absar, S. J. Kim, T. Suzuki, A. Karim, H. Yamauchi, and T. Noda. 2008. DSC study of mixtures of wheat flour and potato, sweet potato, cassava, and yam starches. *Journal of Food Engineering* 86 (1):68-73.
Zhang G.Y. & Hamaker B. R. 2003. A three component interaction among starch, protein, and free

fatty acids revealed by pasting profiles. *Journal of Agriculture and Food Chemistry*. *51(9),* 2797-2800.

نشریه پژوهشهای علوم و صنایع غذایی ایران
جلد 14، شماره 3، مرداد - شهریور 1397، ص. 16-1

Iranian Food Science and Technology Research Journal
Vol. 14, No. 3, Aug. Sep. 2018, p. 1-16

اثر دماهای بالا بر ویژگی‌های بافتی، حرارتی و ریزساختمانی ژل های ترکیبی آرد گندم/ نشاسته ذرت آمیلوز بالا

لیدا شاهسونی مجرد[1]- علی رافع[2*]

تاریخ دریافت: 1396/05/09
تاریخ پذیرش: 1397/01/20

چکیده

ویژگی‌های بافتی، حرارتی و ریزساختمانی ژل‌های تک جزئی نشاسته ذرت آمیلوز بالا و آرد گندم و ژل‌های دوجزئی (BCG) در نسبت‌های مختلف و دماهای 100، 121 و 135 درجه سانتی‌گراد مورد بررسی قرار گرفته است. نتایج نشان داد که ژل‌های دوجزئی با مقادیر بالای نشاسته قوی‌تر بودند. افزایش نشاسته منجر به سفتی بیشتر، کاهش فنریت، چسبندگی و پیوستگی ژل شد. افزون بر این، ژل‌های دوجزئی در دماهای بالا شاخص‌های جذب آب بالاتری را در مقادیر بالای نشاسته نشان دادند. آنتالپی ژلاتیناسیون و دمای پیک ژلاتیناسیون ژل دو جزئی با افزایش مقدار آمیلوز افزایش یافت. ژل نشاسته و پس از آن ژل دو جزئی با مقدار بالای آمیلوز، کمترین پیک ویسکوزیته را نشان دادند. اختلاف در ریزساختمان ژل‌های ارد گندم و نشاسته آمیلوز بالا خواص خمیری آنها را به‌خوبی منعکس می‌نماید. در نتیجه ژل دوتایی آرد گندم و نشاسته آمیلوز بالا ژل‌های قوی‌تری بودند و می‌توانند شرایط فراوری حرارتی بسیار شدید مانند استریلیزاسیون و اتوکلاو را تحمل نمایند که در نهایت به افزایش مدت زمان ماندگاری محصول نهایی منتهی می‌شود.

واژه‌های کلیدی: ژل ترکیبی، خواص خمیری، ریزساختمان، ژلاتیناسیون، بافت

1 و 2- به‌ترتیب دانش‌آموخته دکتری و دانشیار، موسسه پژوهشی علوم و صنایع غذایی.
(*- نویسنده مسئول : Email: a.rafe@rifst.ac.ir)

Iranian Food Science and Technology Research Journal
Vol. 14, No. 3, Aug. Sep. 2018, p. 17-28

نشریه پژوهشهای علوم و صنایع غذایی ایران
جلد 14، شماره 3، مرداد - شهریور 1397، ص. 28-17

Influence of Ultrasound-Assisted Extraction on Bioavailibity of Bene Hull (*Pistacia Atlantica* Subsp. *Mutica*) Extract: Testing Optimal Conditions and Antioxidant Activity

Mojtaba Delfanian[1], Mohammad Hossein Haddad Khodaparast[2*], Mohammad Ali Razavi[2], Reza Esmaeilzadeh Kenari[3]

Received: 2017.06.25
Accepted: 2017.09.23

Abstract

The central composite rotatable design by response surface methodology was applied for optimization of ultrasonic extraction conditions of Bene hull (*Pistacia atlantica* subsp. *Mutica*) polyphenols. The sonication time, temperature and ethanol-water ratio were independent parameters studied for the extraction optimization. Total polyphenols and antioxidant potentials of extracts in terms of ferric reducing antioxidant potential (FRAP), DPPH scavenging activity and oxidative stability index (OSI) were determined. The obtained data were well consistent with the polynomial equations by significant variation in linear, quadratic and interaction impacts of the process factors. The optimized extraction conditions were sonication time, 26.91 min, temperature, 50.42 °C and ethanol concentration, 55.84%. The total polyphenols, DPPH, FRAP an OSI of optimal extract were 304.47 mg GAE/g, 72.47%, 54.04 mmol/100g and 8.55 h, respectively. High performance liquid chromatography (HPLC) analysis of optimal extract detected presence of epicatechin, chlorogenic, sinapic, caffeic and gallic acids.

Keywords: Antioxidant activity; Bene hull; Polyphenols; Response surface methodology; Ultrasound-assisted extraction.

Introduction

Polyphenols such as flavonoids are important bioactive compounds in terms of antioxidant activity, antimicrobial activity and etc., in plants (Delfanian *et al.* 2016). The addition of antioxidants is effective to terminate or delay oxidation process by chelating free catalytic metals, scavenging free radicals and also by acting as electron donors (Anagnostopoulou *et al.* 2006). Many countries such as Canada and America have prohibited use of synthetic antioxidants (BHA, BHT and TBHQ) in food lipids due to increasing of cancer risk, so plants natural antioxidants can be used as a suitable alternative (Delfanian *et al.* 2015).

Pistacia atlantica belonging to the family of Anacardiaceae and has various subspecies: *mutica*, *kurdica*, *atlantica* and *cabulica*. Bene (*Pistacia atlantica* subsp. *Mutica*) tree grows in dry and semi dry regions of Iran such as Kerman, Khorasan and Sistan-Baluchestan provinces (Farhoosh *et al*. 2009). Bene is useful for treatment of the liver, spleen, night-blindness, peptic ulcer and rickets (Shaddel *et al.* 2014). Several studies confirmed the biological activity of Bene hull bioactive compounds such as anti-inflammatory, antimicrobial, antitoxic and antioxidant activities (Gourine et al. 2010, Hatamnia *et al*. 2014). Recent researches on Bene mainly considered the fatty acids, phytosterols, triacylglycerol and essential oils composition (Benhassaini *et al*. 2007, Farhoosh *et al*. 2008).

Ultrasound-assisted extraction (UAE) comparing to other extraction methods such as supercritical fluids, superheated water, accelerated solvent and microwave

1 And 2. PhD Student and Professor, Department of Food Science and Technology, Faculty of Agriculture, Ferdowsi University of Mashhad, Mashhad, Iran.
3. Associated professor, Department of Food Science and Technology, Faculty of Agricultural Engineering, Sari Agricultural Sciences and Natural Resources University, Sari, Iran
(*-Corresponding Author: khodaparast@um.ac.ir)
DOI: 10.22067/ifstrj.v14i3.65394

has many benefits including simplicity, shorter time and high efficiency (Xie *et al*. 2012). The cavitation generated in the solvent during sonication and thermal impacts lead to destruction of cell wall and increase the extraction efficiency (Xu and Pan *et al*. 2013). Different extraction parameters including solvent polarity, time, temperature, liquid-to-solid ratio and etc., are effective in extraction process of bioactive compounds (Liew *et al*. 2005).

Response surface methodology (RSM) is an effective statistical and mathematical tool for optimization of process conditions which can describe the effect of independent variables on response values. Recently, RSM is applied for optimization of antioxidants extraction conditions from various sources (Da Porto et al. 2013, Li *et al*. 2015, Rodríguez-Pérez *et al*. 2015, Szydłowska-Czerniak and Tułodziecka 2015). Currently, there is no available scientific document about optimization of UAE of phenolic compounds from Bene hull by RSM. Therefore, in the present study RSM was used for optimization of extraction parameters ethanol-water ratio, temperature and sonication time during ultrasonic irradiation in order to maximize antioxidant capacity and polyphenols content from Bene hull.

Materials and methods

Chemicals

All the solvents and chemicals used were of analytical or HPLC grade. Folin-Ciocalteu's phenol reagent, gallic acid, sodium carbonate anhydrous (Na_2CO_3), 2,2-diphenyl-1-picryl-hydrazyl (DPPH), iron (III) chloride anhydrous, 2,4,6-tripyridyl-s-triazine (TPTZ) and HPLC standards were purchased from Merck Co. (Darmstadt, Germany). Ethanol and hydrochloric acid (HCl) were obtained from Scharlau Co. (Barcelona, Spain).

Plant Materials

Bene fruits were collected in August 2015 from the fields of Khvaf, Razavi Khorasan, Iran. After air-drying (at 30°C for 72 h in shadow), the green hulls of samples were separated using a mechanical instrument. Samples were frozen in the dark at –18 °C for further experiments (Rezaie et al. 2015).

Ultrasound-Assisted Extraction (UAE)

The UAE was carried out in an ultrasonic bath (DT 102H, Bandelin, Germany) at 35 kHz (100% power). Dried samples (50 g) were placed into Erlenmeyer flasks and extracted with 250 mL of different ratios of aqueous ethanol (0-100%) at various temperatures (25-65°C) and times (varying from 5 to 50 min). The mixtures were filtered and evaporated at 35°C to remove solvents using a vacuum oven. Finally, concentrated samples were stored at -18°C (Hammi *et al.* 2015).

Determination of total polyphenols

Total polyphenols content (TPC) of samples were determined using Folin–Ciocalteu assay as described by *Sfahlan et al*. (2009). Briefly, 0.1 mL of different extracts (1 mg/mL) was mixed with 2.5 ml of 10-fold-diluted Folin-Ciocalteu reagent. The solution was mixed thoroughly and allowed to stand at room temperature. After 4 min, 2 mL of 7.5% sodium carbonate solution was added and then incubated at 45°C for 15 min. The estimation of phenolic compounds was done at 765 nm using a UV–Vis spectrophotometer (Model 160A Shimadzu, Japan) and calculated by a calibration curve (R^2=0.99) performed with gallic acid (0 to 0.4 mg/mL). The TPC was expressed as mg of gallic acid equivalents (GAE) per g of dried sample.

Determination of antioxidant capacity
DPPH Method

The ability of samples to scavenge DPPH$^{\bullet}$ radicals was evaluated following the procedures described by Delfanian *et al*. (2015). This parameter was assessed according to ability of the extracts to reduce free radicals. Accurately, 5 mL of DPPH$^{\bullet}$ ethanolic solution (0.004%) was mixed with 50 µL of extract (0.5 mg/mL) and the reaction mixture was shaken vigorously and incubated in the dark at ambient temperature for 30 min. The absorbance of the mixtures was estimated

at 517 nm against a blank. The radical scavenging activity of the extracts was expressed as a percentage of DPPH$^{\bullet}$ radical attraction calculated according to Eq. (1) below:

$$\%\ \text{Inhibition} - \left[1 - \frac{Abs_{sample}}{Abs_{blank}}\right] \times 100 \quad (1)$$

FRAP Method

The ferric reducing antioxidant power assay followed was according to Sulaiman et al. (2011). The FRAP reagent was prepared by mixing 300 mM sodium acetate anhydrous in distilled water pH 3.6, 20 mM ferric chloride hexahydrat in distilled water and 10 mM 2,4,6-tri(2-pyridyl)-s-triozine (TPTZ) in 40mM HCl in a proportion of 10:1:1. Then, 50 µL of diluted sample extract (0.5 mg/mL) was mixed with 50 µL distilled water and 900 µL of FRAP reagent. The absorbance of the solution was measured at 593 nm against a blank after 30 min incubation at 37 °C. In the case of the blank, 100 µL of distilled water was added to 900 µL of FRAP reagent. Calibration curve was prepared using Iron (II) sulfate ($FeSO_4$) at concentrations from 30 to 1000 µmol/mL. The results were expressed as mM of Fe^{+2}/100 g extract. All tests were carried out in triplicate.

Oxidative Stability Index (OSI)

Rancimat (Metrohm 743, Herisau, Switzerland) was applied for measurement of OSI. The test was performed at 110°C and an airflow rate of 15 l/h (3g refined soybean oil, containing 1000 ppm of extract) (Rezaie *et al*. 2015).

HPLC Analysis

Samples were analyzed according to the method approved for identification of polyphenols in olive oil by International olive Council (COI/T.20/Doc No29. 2009). The HPLC system which was used in this study was a Younglin (South Korea) equipped with an UV/Vis detector (Younglin, South Korea). The phenolic compounds in a 10 µL of sample solution were separated on a Hector C-18 column (150×4.6 mm, 5 µm) at room temperature and detected at 280 nm. The mobile phase consisted of solvent A (water-phosphoric acid, 0.2%) and solvent B (methanol-acetonitrile, 50%). Solvent gradient was used in four steps: 25 min, 4-50% B; 5min, 50-60% B; 25 min, isocratic elution of 100% B; back to initial status for two minutes. The total elution time flow rate was 72 min and 1.0 mL/min, respectively.

Experimental Design

Using the Design-Expert Version 6.0.2 software (Stat-Ease, Inc., USA) response surface methodology was applied for optimization of UAE parameters based on central composite rotatable design (CCRD). The effects of process factors: sonication time (X_1; min), temperature (X_2; °C) and ethanol concentration (X_3; %) were investigated on four dependent variables (as responses), namely TP, DPPH, FRAP and OSI. Table 1 is shown the experimental designs of the coded and un-coded extraction factors.

Table 1- Coded and uncoded levels of independent variables employed for optimization of the extraction of polyphenols

Independent variables	Symbols	Coded levels		
		-1	0	+1
Time (min)	X_1	5	27.5	50
Temperature (°C)	X_2	25	45	65
Ethanol concentration (%)	X_3	0	50	100

Range of sonication time, temperature and ethanol-water ratio was chosen based on preliminary experiments. Data was achieved from CCRD fitted by a second-order polynomial equation as follows:

$$Y = \beta_0 + \sum_{i=1}^{3} \beta_i X_i + \sum_{i=1}^{3} \beta_{ii} X_i^2 + \sum_{i=0}^{n} \sum_{j=2}^{3} \beta_{ij} X_i X_j \quad (2)$$

Where Y is the dependent factor, β_0, β_i, β_{ii} and β_{ij} are the coefficients for intercept, linear, quadratic and interaction, respectively and X_1, X_2, and X_3 represent the independent factors. The model fitness was estimated by analyzing of coefficient R^2, adjusted coefficient R^2_{Adj}, lack of fit and analysis of variance (ANOVA). All tests were done in triplicate and confidence level was 95.0%.

Results and discussion

Model fitting using RSM

The impacts of independents parameters including ethanol-water ratio, temperature and time under ultrasound-assisted extraction on responses were investigated by CCRD of RSM. Table 2 shows the experimental design and response values of TPC, FRAP, DPPH and OSI determined for Bene hull extracts. Experimental responses obtained from the CCRD were fitted into the second-order polynomial models and coefficients R^2 of the calculated equations were investigated by ANOVA. The adequacy of the model is determined by F-test, lack of fit, coefficients R^2, predicted R^2, adjusted R^2 and *P*-value (Yim et al. 2012). The ANOVA results indicated lower *P*-values with higher R^2, R^2_{adj} and R^2_{pre} (> 0.8) associated insignificant lack of fit (P>0.05) for experimental responses, show that there was an appropriate relationship between the response and independent factors (Tables 3 and 4). Regression coefficients R^2 for TPC, DPPH, FRAP and OSI were 0.9709, 0.9371, 0.9304 and 0.9473, respectively.

Response Surface Analysis

As it can be seen in Table 3, the response surface analysis (RSA) of the experimental results indicates that all three factors; sonication time, temperature and solvent ratio have quadratic effect on phenolic content with an appropriate coefficient R^2 (0.9709). The predicted data TPC for total phenolic content of extracts were calculated with the following equation:

$$TPC = 304.74 + 18.32X_3 - 114.32X_1^2 - 30.75X_2^2 - 45.4X_3^2 + 14.68\ X_1X_3 + 18.79X_2X_3 \quad (3)$$

Ethanol concentration (X_3) was only variable by significant linear impact ($P < 0.05$), while the variables sonication time (X_1), temperature (X_2) and ethanol concentration had quadratic impacts on TPC. Also, RSA revealed that interaction between variables time and solvent ratio and also temperature and solvent ratio were significant, whereas reciprocal interaction of time and temperature was not significant.

Table 2- Response surface central composite design, experimental and predicted responses for the dependent variables

Test	Independent variables			Dependent variables (Response)							
	Time (min), X_1	Temp (°C), X_2	Ethanol (%), X_3	Phenols (mg GAE/g)		DPPH (% Inhibition)		FRAP (mM of Fe^{+2}/100g)		OSI (h)	
				Expt.	Pred.	Expt.	Pred.	Expt.	Pred.	Expt.	Pred.
1	5.00	25.00	0.00	118.54±2.98	129.41	9.21±1.71	4.99	17.26±0.85	15.39	11.27±0.08	11.57
2	27.50	45.00	50.00	310.25±3.86	304.74	72.26±0.60	70.41	59.06±0.79	53.08	8.88±0.17	8.68
3	50.00	25.00	0.00	123.06±4.91	100.04	28.28±1.54	21.90	15.03±0.63	15.39	11.94±0.66	11.57
4	5.00	25.00	100.00	96.73±3.46	99.11	25.31±0.88	23.33	25.91±1.08	24.71	8.67±0.42	8.42
5	5.00	65.00	100.00	130.26±2.56	136.69	57.07±0.84	53.45	31.76±0.76	32.56	8.84±0.31	8.89
6	50.00	45.00	50.00	182.16±2.17	190.41	43.26±0.57	51.50	30.87±0.98	30.63	8.18±0.29	8.68
7	27.50	45.00	0.00	246.36±3.82	241.01	44.56±0.45	47.92	31.56±1.31	33.91	11.15±0.19	11.34
8	27.50	25.00	50.00	245.26±3.90	273.98	42.26±0.37	54.85	42.53±1.71	53.08	8.45±0.02	8.68
9	50.00	65.00	100.00	170.62±5.39	166.05	38.09±0.79	36.54	34.80±0.94	32.56	9.25±0.02	8.89
10	5.00	65.00	0.00	78.25±3.19	91.83	30.36±1.21	35.11	9.65±1.92	7.54	11.45±0.05	11.10
11	27.50	45.00	50.00	318.94±2.02	304.74	70.36±0.33	70.41	61.25±0.87	53.08	8.49±0.31	8.68
12	27.50	45.00	50.00	308.35±2.66	304.74	74.56±0.33	70.41	54.51±1.88	53.08	8.58±0.55	8.68
13	27.50	45.00	50.00	328.42±4.76	304.74	78.08±0.44	70.41	52.06±1.57	53.08	8.82±0.34	8.68
14	27.50	65.00	50.00	282.12±4.92	273.98	70.12±0.81	68.05	45.15±1.19	53.08	8.92±0.01	8.68
15	27.50	45.00	50.00	301.12±3.58	304.74	78.36±0.25	70.41	58.12±1.66	53.08	8.93±0.23	8.68
16	50.00	65.00	0.00	58.55±5.88	62.47	15.72±0.61	18.20	6.26±1.45	7.54	10.87±0.47	11.10
17	27.50	45.00	100.00	251.72±6.86	277.66	59.10±0.68	66.26	47.53±1.95	51.08	8.12±1.64	8.66
18	50.00	25.00	100.00	158.65±3.81	128.48	40.26±1.92	40.24	25.62±0.53	24.71	8.40±0.04	8.42
19	5.00	45.00	50.00	178.08±3.24	190.41	49.23±0.67	51.50	24.48±1.19	30.63	8.63±0.34	8.68
20	27.50	45.00	50.00	302.52±3.24	304.74	69.88±0.45	70.41	57.84±1.20	53.08	8.92±0.23	8.68

Table 3- Analysis of variance (ANOVA) of the quadratic model adjusted to the total phenolic content and DPPH• scavenging activity assays

Squares	Sum of Square	DF	Mean Square	F Value	P-value Prob F
Total phenolic content					
Model	1.489E+005	6	24817.46	72.29	< 0.0001
X_3	3356.96	1	3356.96	9.78	0.0080
X_1^2	35941.64	1	35941.64	104.69	< 0.0001
X_2^2	2600.76	1	2600.76	7.58	0.0165
X_3^2	5668.87	1	5668.87	16.51	0.0013
X_1X_3	1724.61	1	1724.61	5.02	0.0431
X_2X_3	2823.76	1	2823.76	8.23	0.0132
Residual	4462.93	13	343.30		
Lack of Fit	3921.48	8	490.19	4.53	0.0565
Pure Error	541.45	5	108.29		
Cor Total	1.534E+005	19			
R^2	0.9709				
Adj.R^2	0.9575				
Pred.R^2	0.9138				
DPPH• scavenging activity					
Model	8168.56	6	1361.43	32.30	< 0.0001
X_2	436.13	1	436.13	10.35	0.0067
X_3	840.89	1	840.89	19.95	0.0006
X_1^2	982.94	1	982.94	23.32	0.0003
X_2^2	220.82	1	220.82	5.24	0.0395
X_3^3	487.98	1	487.98	11.58	0.0047
X_1X_2	571.90	1	571.90	13.57	0.0028
Residual	547.87	13	42.14		
Lack of Fit	478.69	8	59.84	4.32	0.0618
Pure Error	69.18	5	13.84		
Cor Total	8716.42	19			
R^2	0.9371				
Adj.R^2	0.9081				
Pred.R^2	0.8172				

Fig.1A shows the reciprocal interaction effect of sonication time and ethanol-water ratio on the TPC. TPC increased by increasing ethanol concentration to 50%, while it increased with extraction time until 27.5 min and then declined, confirming reverse quadratic impact of solvent ratio and time. Moreover, this plot demonstrates the positive reciprocal interaction impacts of solvent ratio and time on TPC. As clearly seen in Fig. 1B, at 50% aqueous ethanol, the total polyphenols increased by increasing temperature to 45 ℃, and then decreased at higher temperatures (>45°C). In general, maximum of polyphenols (328.42 mg GAE/g) was extracted with 50% aqueous ethanol, at 45 ℃ for 27.5 min.

Water can conveniently penetrate into the plant cells, while protein is denatured in high proportion of ethanol and prevents the dissolution of polyphenols (Yang *et al*. 2010). Water is not an appropriate solvent for extraction of carbonaceous compounds, hence mixture of water and alcohols can increase the extraction efficiency (Delfanian *et al*. 2015). According to the ‘‘like dissolves like’’ principle, extraction efficiency of polyphenols increased by increasing of solvent polarity (Zhang *et al.* 2007, Zhang *et al*. 2008). We found that the recovery of polyphenols was higher in mixtures of ethanol/ water (1:1) compared to pure ethanol and water. These results were in agreement with the results reported by Hemwimol *et al*. (2006); Delfanian et al. (2015) and Hammi *et al*. (2015).

DPPH• scavenging activity is a valid and reliable assay for evaluation of antioxidant properties of extracts (Li *et al.* 2006). According to ANOVA results there was a quadratic relationship between DPPH and sonication variables with high coefficient R^2 (0.9371) (Table 3). The following Eq. (4) demonstrates the real model for the DPPH• scavenging ability:

$$DPPH = 70.41 + 6.6X_2 + 9.17X_3 - 18.91X_1^2 - 8.96X_2^2 - 13.32X_3^2 - 8.46X_1X_2 \quad (4)$$

DPPH equation indicates that the sonication temperature and ethanol concentration were linear effects and all three variables were quadratic effects on response. Also, there was a significant interaction among irradiation time and temperature (P<0.05). The model was fitted and adequate for DPPH with non-significant lack of fit and high coefficients R^2 (Table 3). According to Fig. 1C the DPPH inhibition declined with rising process time at shorter or longer durations than 27.5 min, supporting the reverse quadratic impact of time. Generally, our results revealed that the highest value of DPPH$^{\bullet}$ inhibition was obtained with 50% ethanol, at 45 °C for 27.5 min. In order to minimize process time and cost-saving may be preferred combination of the lowest levels of extraction parameters in the optimum zone. This result were in agreement by MorelliPrado (2012); *Yim et al*. (2012) and Setyaningsih et al. (2016) that noted the highest DPPH$^{\bullet}$ inhibition in extracts was obtained in moderate extraction time and temperature.

The real model correlating the FRAP in term of significant independent variables is given below:

$$FRAP= 53.08+ 8.59\ X_3 – 22.45X_1^2 – 10.58X_3^2 + 3.93X_2X_3 \quad (5)$$

FRAP equation shows that the irradiation time and ethanol concentration were quadratic impacts, whereas solvent variable had also a linear effect on FRAP values. There was a significant interaction among ethanol concentration and temperature at 95% confidence level.

According to ANOVA results (Table 4) model were significant and valid for FRAP values with non-significant lack of fit and high regression coefficient. Therefore, model can be applied for prediction of data as respects there was a high correlation between the predicted and experimental data.

Table 4- Analysis of variance (ANOVA) of the quadratic model adjusted to the FRAP and OSI assays

Squares	Sum of Square	DF	Mean Square	F Value	P-value Prob F
FRAP					
Model	5365.01	4	1341.25	50.10	< 0.0001
X_3	737.19	1	737.19	27.54	< 0.0001
X_1^2	1612.72	1	1612.72	60.24	< 0.0001
X_3^2	358.15	1	358.15	13.38	0.0023
X_2X_3	123.32	1	123.32	4.61	0.0486
Residual	401.55	15	26.77		
Lack of Fit	346.80	10	34.68	3.17	0.1076
Pure Error	54.75	5	10.95		
Cor Total	5766.56	19			
R^2	0.9304				
Adj.R^2	0.9118				
Pred.R^2	0.8987				
OSI					
Model	27.07	3	9.02	95.84	< 0.0001
X_3	17.96	1	17.96	190.71	< 0.0001
X_3^2	8.66	1	8.66	91.97	< 0.0001
X_2X_3	0.46	1	0.46	4.84	0.0428
Residual	1.51	16	0.094		
Lack of Fit	1.33	11	0.12	3.41	0.0932
Pure Error	0.18	5	0.035		
Cor Total	28.58	19			
R^2	0.9473				
Adj.R^2	0.9374				
Pred.R^2	0.9112				

Fig. 1D illustrates the level of FRAP was increased by increasing of ethanol-water ratio up to 50% and degrades at high ratio of ethanol during long extraction times. The highest FRAP value was observed under the center point variables (50% aqueous ethanol at 45°C for 27.5 min). These results were in agreement by

Moyo *et al.* (2003) and Yim *et al.* (2012) whom explained linear effects of extraction variables are less than their interactions which occurs in reality.

Rancimat assay is often applied for estimate the oxidative stability index (OSI) of samples based on changes in water electrical conductivity resulting from the production of volatile acids such as formic acid (Farhoosh *et al*. 2009). Longer oxidative stability index values demonstrate higher antioxidant ability. The obtained mathematical equation that indicates the relationship among the OSI and the significant process variables is given below:

$$OSI = 8.68 - 1.34\ X_3 + 1.32X_3^2 + 0.24X_2X_3 \quad (6)$$

Ethanol concentration showed significant linear and quadratic impact, while irradiation time and temperature did not have any significant linear or quadratic impacts on OSI (P>0.05). Model indicated that significant interaction effect was observed only between ethanol concentration and temperature. As seen in Fig. 1E, the OSI decreased with decreasing of ethanol concentration from 100 to 50%, and then it increased with further increase of water proportion through different extraction temperatures. Thus, the highest level of OSI (11.94 h) was obtained with pure water at 25°C for 50 min.

Solvent polarity is the most important parameter for extraction of polyphenols compared to other extraction variables (Wang et al. 2008). Assessment of extracts in the polar environment such as DPPH and FRAP tests revealed than samples extracted by ethanol-water 50% were the highest antioxidant activities compared to pure ethanol and water. Whereas, samples in Rancimat assay showed different behavior and extracts extracted with water had the maximum of OSI. This reason can be explained by presence of short chain polyphenols with high thermal stability in water. Our results water concurred with Rezaie *et al*. (2015) that reported water extract of Bene hull had more OSI compared to ethanolic extract.

Optimization of UAE Conditions

The optimization of independent factors for ultrasound-assisted extraction (UAE) of Bene hull bioactive compounds were estimated through considering the polynomial models and surface plots. The optimized process conditions were 26.91 min sonication time, 50.42°C temperature and 55.84% aqueous ethanol with desirability of 0.903. The maximum TPC, DPPH$^{\bullet}$ scavenging activity, FRAP and OSI predicted by RSM were 304.47 mg GAE/g, 72.47%, 54.04 mmol/100g and 8.55 h, respectively. Under these optimal conditions the experimental values for TPC, DPPH, FRAP and OSI were 305.62 mg GAE/g, 74.26%, 55.12 mmol/100g and 8.82 h, which were very close to the predicted values by RSM. These results were in agreement by (Kadam *et al*. 2015, Rodríguez-Pérez et al. 2015, Saikia *et al.* 2015) that reported use of ultrasound heat at 45-60°C can increase extraction efficiency of bioactive compounds in shortest time. Because, thermal effects and created cavitation in the liquid phase during sonication lead to cell wall damage, reduction of particle size and subsequently increase of process efficiency (Xu and Pan *et al*. 2013).

HPLC Analysis of the Extracted Polyphenols

The high performance liquid chromatography analysis was performed for identification the major polyphenols in extracted sample under optimal UAE conditions (Fig. 2). Five polyphenols were found in Bene hull extract containing gallic acid, chlorogenic acid, caffeic acid, epicatechin and sinapic acid with retention times 5.18, 15.73, 16.9, 20.41, 23.56 min, respectively. Among the five identified and quantified polyphenols, gallic acid was the major polyphenols in Bene hull extract (1236.65 ppm) and the content of epicatechin, caffeic acid, chlorogenic acid and sinapic acid were 189.39, 64.56, 46.20 and 31.48 ppm, respectively. Therefore, the high level of antioxidant potential of Bene hull is probably due to the presence of large amount of gallic acid. In recent studies, the presence of luteolin, gallic acid, quercetin 3-rutinoside, 2″-O-

galloylisoquercitrin, epicatechin, flavanomarein, ethyl vanillin, and apigenin 7-glucoside were confirmed in Bene hull extract obtained by maceration and subcritical water methods (Shaddel et al. 2014, Rezaie *et al.* 2016). Although, chlorogenic acid, caffeic acid and sinapic acid was not identified in these published works.

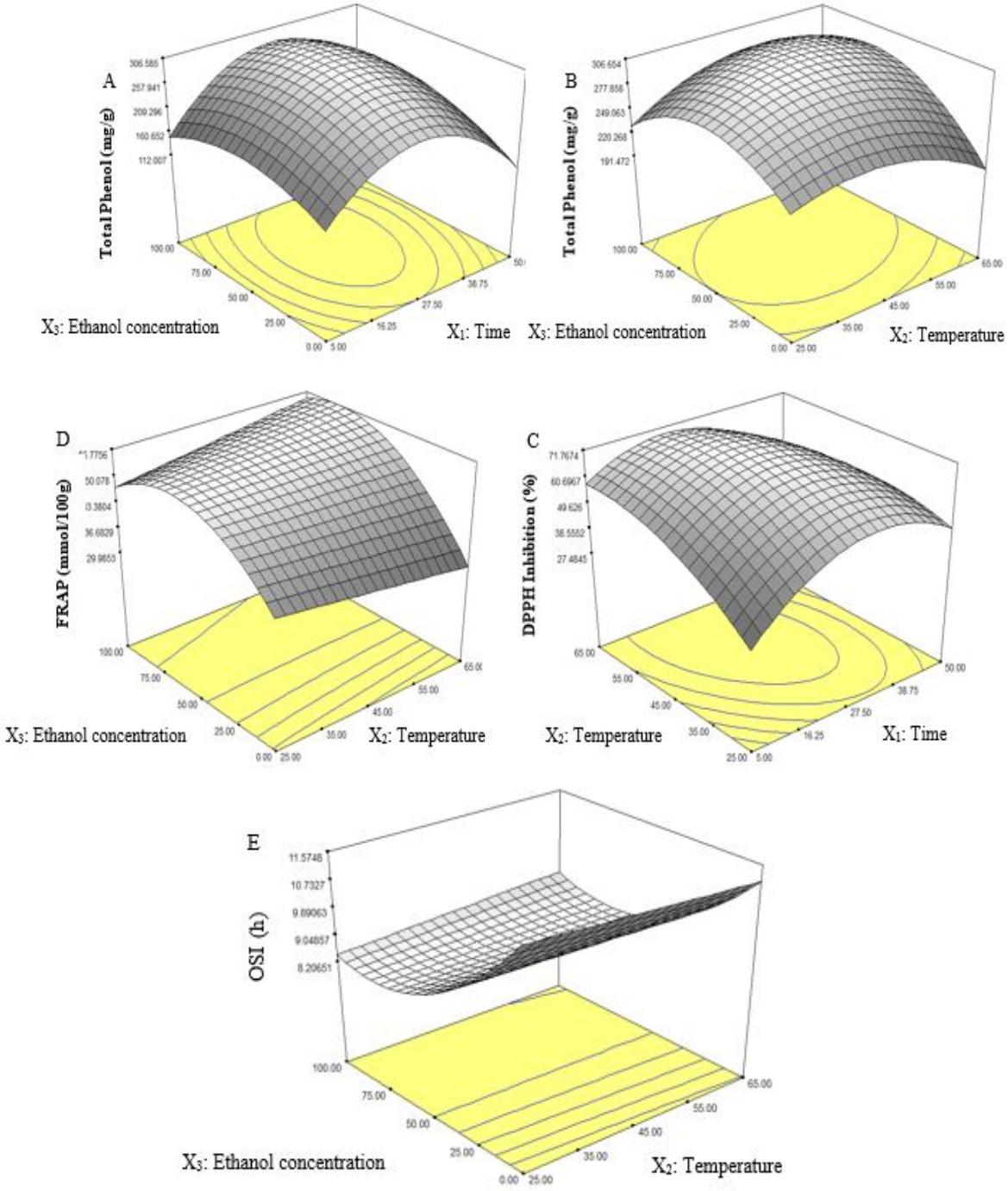

Fig. 1. Response surface plots showing the effect of interaction between independent variables on TPC (A, B), DPPH (C), FRAP (D) and OSI (E) values.

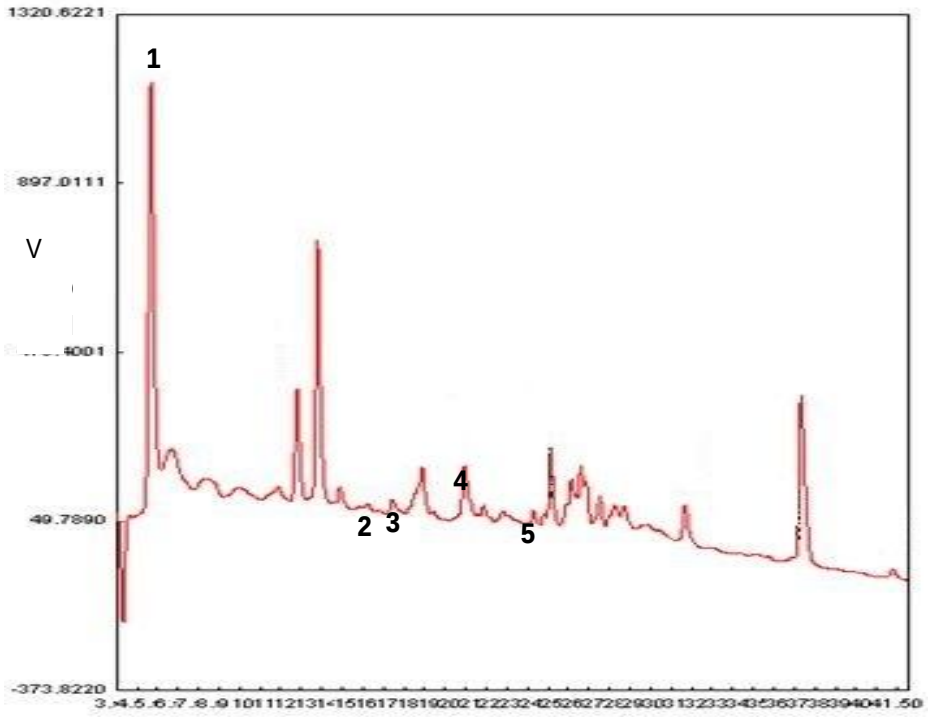

Fig. 2. HPLC chromatogram of phenolic compounds present in bene hull extract. Compounds were identified as follows: (1) gallic acid; (2) chlorogenic acid; (3) caffeic acid; (4) epicatechin; (5) sinapic acid.

Conclusions

Response surface analysis by central composite rotatable design was found as an excellent statistical method for evaluating the effects of extraction variables on total polyphenols and biological activity of Bene hull extract. The experimental values were fitted with second-order polynomial equations. The optimum operating conditions for ultrasound-assisted extraction were 55.84% aqueous ethanol at 50.42°C for 26.91 min based on maximum total polyphenols and antioxidant activity. The TPC, DPPH, FRAP and OSI of optimal extract were 304.47 mg GAE/g, 72.47%, 54.04 mmol/100g and 8.55 h, respectively. Thus, the amount of ethanol in aqueous solvent was important factor for extraction of polyphenols. In addition, HPLC analysis allowed the detection and quantification of five phenolic compounds caffeic acid, chlorogenic acid, gallic acid, epicatechin and sinapic acid in optimal extract

References

Maria A Anagnostopoulou, Kefalas Panagiotis, Papageorgiou Vassilios P, Assimopoulou Andreana N and Boskou Dimitrios (2006). Food Chemistry 94, 19-25.

H Benhassaini, Bendahmane M and Benchalgo N (2007). Chemistry of Natural Compounds 43, 121-124.

Carla Da Porto, Porretto Erica and Decorti Deborha (2013). Ultrasonics Sonochemistry 20, 1076-1080.

Mojtaba Delfanian, Esmaeilzadeh Kenari Reza and Sahari Mohammad Ali (2015). Food Science and Nutrition 3, 179-187.

Mojtaba Delfanian, Esmaeilzadeh Kenari Reza and Sahari Mohammad Ali (2015). *Journal of Food Processing and Preservation* 40, 386-395.

Mojtaba Delfanian, Kenari Reza Esmaeilzadeh and Sahari Mohammad Ali (2015).

I*nternational Journal of Food Properties* 18, 2813-2824.
Mojtaba Delfanian, Kenari Reza Esmaeilzadeh and Sahari Mohammad Ali (2016). *Journal of Food Science And Technology*, in press.
Reza Farhoosh, Kenari Reza Esmaeilzadeh and Poorazrang Hashem (2009). Journal of the *American Oil Chemists' Society* 86, 71-76.
Reza Farhoosh, Khodaparast Mohammad Hossein Haddad and Sharif Ali (2009). *European Journal of Lipid Science And Technology* 111, 1259.
Reza Farhoosh, Tavakoli Javad and Khodaparast Mohammad Hossein Haddad (2008). *Journal of the American Oil Chemists' Society* 85, 723-729.
N Gourine, Yousfi M, Bombarda I, Nadjemi B, Stocker P and Gaydou EM (2010). *Industrial Crops and Products* 31, 203-208.
Khaoula Mkadmini Hammi, Jdey Ahmed, Abdelly Chedly, Majdoub Hatem and Ksouri Riadh (2015). *Food Chemistry* 184, 80-89.
Ali Asghar Hatamnia, Abbaspour Nasser and Darvishzadeh Reza (2014). *Food Chemistry* 145, 306-311.
Surasak Hemwimol, Pavasant Prasert and Shotipruk Artiwan (2006). Ultrasonics Sonochemistry 13, 543-548.
Shekhar U Kadam, Tiwari Brijesh K, Smyth Thomas J and O'Donnell Colm P (2015). *Ultrasonics Sonochemistry* 23, 308-316.
An-Na Li, Li Sha, Xu Dong-Ping, Xu Xiang-Rong, Chen Yu-Ming, Ling Wen-Hua, Chen Feng and Li Hua-Bin (2015). *Food Analytical Methods* 8, 1207-1214.
Yunfeng Li, Guo Changjiang, Yang Jijun, Wei Jingyu, Xu Jing and Cheng Shuang (2006). *Food Chemistry* 96, 254-260.
SL Liew, AB Ariff, AR Raha and YW Ho. *International Journal of Food Microbiology* 102, 137-42.
Lucíula Lemos Lima Morelli and Prado Marcelo Alexandre (2012). *Ultrasonics Sonochemistry* 19, 1144-1149.
S Moyo, Gashe BA, Collison EK and Mpuchane S (2003). I*nternational Journal of Food Microbiology* 85, 87-100.
Mitra Rezaie, Farhoosh Reza, Iranshahi Mehrdad, Sharif Ali and Golmohamadzadeh Shiva (2015). *Food Chemistry* 173, 577-583.
Mitra Rezaie, Farhoosh Reza, Pham Ngoc, Quinn Ronald J and Iranshahi Mehrdad (2016). *Journal of Pharmaceutical and Biomedical Analysis* 117, 352-362.
Mitra Rezaie, Farhoosh Reza, Sharif Ali, Asili Javad and Iranshahi Mehrdad (2015). *Journal of Food Science And Technology* 52, 6784-6790.
C Rodríguez-Pérez, Quirantes-Piné R, Fernández-Gutiérrez A and Segura-Carretero A (2015). *Industrial Crops and Products* 66, 246-254.
Sangeeta Saikia, Mahnot Nikhil Kumar and Mahanta Charu Lata (2015). *Food Chemistry* 171, 144-152.
W Setyaningsih, Duros E, Palma M and Barroso CG (2016). *Applied Acoustics* 103, 129-135.
Ali Jahanban Sfahlan, Mahmoodzadeh Ahmad, Hasanzadeh Abdollah, Heidari Reza and Jamei Rashid (2009). *Food Chemistry* 115, 529-533.
Rezvan Shaddel, Maskooki Abdolmajid, Haddad-Khodaparast Mohammad Hossein, Azadmard-Damirchi Sodeif, Mohamadi Morteza and Fathi-Achachlouei Bahram (2014). *Food Science and Biotechnology* 23, 1459-1468.
Shaida Fariza Sulaiman, Sajak Azliana Abu Bakar, Ooi Kheng Leong and Seow Eng Meng (2011). *Journal of Food Composition and Analysis* 24, 506-515.
Aleksandra Szydłowska-Czerniak and Tułodziecka Agnieszka (2015). *Food Analytical Methods* 8, 778-789.
Jing Wang, Sun Baoguo, Cao Yanping, Tian Yuan and Li Xuehong (2008). *Food Chemistry* 106, 804-810.
Xu Yuan and Pan Siyi (2013). Ultrasonics sonochemistry 20,1026-1032.
Jian-Hua Xie, Shen Ming-Yue, Xie Ming-Yong, Nie Shao-Ping, Chen Yi, Li Chang, Huang

Dan-Fei and Wang Yuan-Xing (2012). Carbohydrate Polymers 89, 177-184.

Yu-Chun Yang, Li Ji, Zu Yuan-Gang, Fu Yu-Jie, Luo Meng, Wu Nan and Liu Xiao-Lei (2010). *Food Chemistr*y 122, 373-380.

Hip Seng Yim, Chye Fook Yee, Koo Sze May, Matanjun Patricia, How Siew Eng and Ho Chun Wai (2012). *Food and Bioproducts Processing* 90, 235-242.

Bin Zhang, Yang Ruiyuan and Liu Chun-Zhao (2008). *Separation and Purification Technology* 62, 480-483.

Zhen-Shan Zhang, Li Dong, Wang Li-Jun, Ozkan Necati, Chen Xiao Dong, Mao Zhi-Huai and Yang Hong-Zhi (2007). S*eparation and Purification Technology* 57, 17-24.

نشریه پژوهشهای علوم و صنایع غذایی ایران
جلد 14، شماره 3، مرداد - شهریور 1397، ص. 28-17

Iranian Food Science and Technology Research Journal
Vol. 14, No. 3, Aug. Sep. 2018, p. 17-28

تأثیر استخراج با فراصوت بر فعالیت بیولوژیکی عصاره پوست بنه (*Pistacia Atlantica* Subsp. *Mutica*): بررسی شرایط بهینه و فعالیت آنتی‌اکسیدانی

مجتبی دلفانیان[1]- محمدحسین حدادخداپرست[2*]- سید محمدعلی رضوی[2]- رضا اسماعیل‌زاده کناری[3]

تاریخ دریافت: 1396/04/04
تاریخ پذیرش: 1396/07/01

چکیده

در این تحقیق از طرح مرکب مرکزی محوری قابل چرخش در روش سطح پاسخ برای بهینه‌یابی شرایط استخراج با فراصوت ترکیبات پلی‌فنلی پوست بنه (*Pistacia atlantica* subsp. *Mutica*) استفاده شد. پارامترهای زمان، دما و نسبت حلال اتانول/ آب از پارامترهای مستقل بررسی شده برای بهینه‌یابی شرایط استخراج بودند. میزان ترکیبات پلی‌فنلی تام و قدرت آنتی‌اکسیدانی عصاره‌ها از نظر قدرت احیاکنندگی آهن (FRAP)، جذب رادیکال‌های آزاد DPPH و شاخص پایداری اکسایشی (OSI) تعیین شد. داده‌های حاصل با معادلات درجه دوم با اثرات خطی، درجه دوم و متقابل فاکتورهای فرآیند به خوبی سازگار بود. شرایط بهینه استخراج در زمان 26/91 دقیقه، دمای 50/42 درجه سانتی‌گراد و با نسبت اتانول 55/84 درصد ایجاد شد. میزان ترکیبات پلی‌فنلی تام و قدرت جذب رادیکال‌های آزاد DPPH، قدرت احیاکنندگی آهن (FRAP)، و شاخص پایداری اکسایشی عصاره استخراجی در شرایط بهینه به ترتیب 304/47 میلی‌گرم گالیک اسید بر گرم، 72/47 درصد، 54/04 میلی‌مول بر 100 گرم و 8/55 ساعت بود. آنالیز عصاره بهینه با کروماتوگرافی مایع با عملکرد بالا (HPLC) حضور اپی‌کاتچین، کلروژنیک اسید، سیناپیک اسید، کافئیک اسید و گالیک اسید را شناسایی کرد.

واژه‌های کلیدی: پوست بنه، فعالیت آنتی‌اکسیدانی، پلی‌فنل، روش سطح پاسخ، استخراج با فراصوت

1 و2- به‌ترتیب دانشجوی دکترا و استاد، گروه علوم و صنایع غذایی، دانشکده کشاورزی، دانشگاه فردوسی مشهد
3- دانشیار، گروه علوم و صنایع غذایی دانشگاه علوم کشاورزی و منابع طبیعی ساری، ساری، ایران
(*- نویسنده مسئول : Email: khodaparast@um.ac.ir)

Iranian Food Science and Technology Research Journal
Vol. 14, No. 3, Aug. Sep. 2018, p. 29-40

نشریه پژوهشهای علوم و صنایع غذایی ایران
جلد 14، شماره 3، مرداد - شهریور 1397، ص. 40-29

Chemical quality and microbiological content of Kutum (*Rutilus frisii kutum*) roe processed in different brine concentration during storage

Parastoo Pourashouri[1*], Bahareh Shabanpour[2], Zeinab Noori Hashem Abad[3]

Received: 2017.10.14
Accepted: 2018.03.15

Abstract

Caviars represent the best-known form of fish roe products. The conventional method of roe processing includes saturated brine salting. However, despite the importance of these products, there is relatively little technical information available about their chemical composition, product quality and food safety attributes.

Three experimental treatments were provided with kutum roe brined in 10, 18 and 24% sodium chloride solutions for 14 days (24°C). Then, the brined-roes were removed from the solution and stored at 4°C for 90 days in refrigerator. The contents of proximate compositions, salt, volatile base nitrogen (VBN), total psychrotrophic bacteria and histamine forming bacteria, color were measured. Sampling was carried out at the first and at the end of days 30, 60 and 90 of storage period.

The samples brined in 10% solution putrefied during the brining and removed from study. The moisture and total volatile nitrogen content of 24% brined roes were lower than 18% treatment. The pH and histamine forming bacteria number at the end of storage and total psychrotrophic bacteria number after 60 days of storage were higher. The increase of L* value and the decrease of a* value in samples of brine 18% were observed on days 60 and 90 of storage, but this increase was induced only on the day 90 for samples of brine 24%.

18%brined roe showed acceptable chemical and microbial results in refrigerated condition, and 24% brine roe appeared optimal during storage period.

Keywords: Kutum, roe, Shelf life, Brine concentration

Introduction

Marine by-products have been reported as good sources of nutraceuticals as well as functional food ingredients (Rao, 2014). Fish eggs (roes) are highly perishable with short shelf-life and hence to be processed immediately (Narsing Rao *et al*., 2012). The considerable quantity (about 27% of the total body weight) of fish roes could be produced during spawning season. Roes are rich in polyunsaturated fatty acids (PUFA), amino acids and proteins depending on the variety of fish (RAO, 2014; Balaswamy *et al*., 2007; Lapa-guimarães *et al*., 2011). Caviar is a processed food originated from the aquatic animal's roes that salted and cured after separation of connective tissues. Sturgeon fish caviar is a well-known product traditionally comes from Caspian Sea littoral states (Bledsoe *et al*., 2003). Many other fish species (e.g., catfish, salmon, lumpfish, flying fish, herring, capelin, mullet and cod) have been used for making different kinds of caviar and consumed in the worldwide (Lapa-guimarães *et al*., 2011; Bledsoe *et al*., 2003; Shin *et al*., 2007).

Salting is one of the preserving techniques of fish and fishery products. This method has been used over the centuries (Chaijan, 2011). It mainly causes to the reduction of water activity and thus inhibits the growth of spoilage microorganisms (Goulas and Kontominas, 2005). Two main types of salting methods include dry and wet salting. The wet salting allows fish and roe to immerse in a strong brine or pickle. Higher brine concentration lead to increase the water phase salt content of fish products (Chaijan, 2011).

In northern fish markets of Iran, a large part of Kutum (*Rutilus frisii kutum*) roes are an underutilized by-product which is removed

1, 2 and 3. Assistant professor, Professor and PhD student, Department of Seafood Processing, Faculty of Fisheries and Environment, Gorgan University of Agricultural Sciences and Natural Resources, Gorgan, Iran.
(*-Corresponding Author: Pourashouri.p@gmail.com)
DOI: 10.22067/ifstrj.v14i3.67959

during processing. The roes are highly perishable. Preparation of traditional salted roe from fully developed kutum gonads (i.e. Ashbal) for storing at room temperature and its physicochemical properties were studied earlier (Pourashouri *et al.*, 2015). The traditional processing affected the proximate and fatty acid composition. However, the fresh roes were found to be more acceptable than heavy salted roes in terms of healthy product. On the other hand, it was reported that the light salt processing (3.5- 4.8%, w/w) did not affect the proximate composition, total amino acids and fatty acids composition compared to fresh roes (Balaswamy *et al*., 2007). The kutum roes containing 61-63% moisture, 28-29% protein and 1.3% ash. The lipid content is 6-7%, which following the composition: 4.37% docosahexaenoic acid and 5.13% eicosapentaenoic acid (Pourashouri *et al.*, 2015).

Some studies showed that light brine salting promotes better yield and water holding capacity than saturated brines (Martinez-alvarez *et al*., 2005). Furthermore, to the best of our knowledge, no work was carried out previously by different salt concentrations on chemical and microbiological properties of kutum roe pickle during storage. The objective of the present work was to study the effect of different brine concentrations (10, 18 and 24%) on kutum roes and assess the physicochemical and microbiological properties and shelf-life during storage.

Material and method

Preparation of samples

The roes of sixty kutum (*Rutilus friisi kutum*) were obtained from a local fish market (March 2013, Bandar-Anzali, Gilan Province) immediately after dressing of live fish. The roes (350± 40 g) were thoroughly cleaned to remove adhering fat deposits, blood vessels and washed in fresh water. Roes were not separated from skin (a sac which covers roes). Each roes (as a replicate) were subjected separately to the pre-treatments and then soaked in one of the brines consisted of 10, 18 and 24% sodium chloride solution in plastic containers (2 weeks). The containers were kept at room temperature (24± 2°C); solid to liquid ratio was maintained at 1:4 (w/w) (Balaswamy *et al*., 2010). Subsequently, the roe was allowed to drain using plastic baskets for 1 h, wrapped in polyethylene bags and stored in refrigerator (4± 1°C) for 90 days. Sampling was carried out on days of 1, 30, 60, and 90 of the storage.

Chemical analyses

The moisture, crude protein and ether extract contents of the brined-roe were measured according to the AOAC (1990). The pH was measured by using single electrode of a digital pH meter (Metrohm 713 pH meter, Germany) (AOAC, 1990). The amount of salt present in the samples was determined by silver nitrate titration for the chloride ion (Hwang *et al*., 2012). Total volatile basic-nitrogen (TVB-N) was determined in two steps, according to the method of Howgate (1976). At first, to obtain protein-free extracts of brined-kutum roe, 10 g of sample were homogenized with 20 ml 5% trichloroacetic acid for 1 min using an Ultra-Turrax apparatus. The homogenate was centrifuged (1200 x g, 4 min, 18°C) and the extract filtered through filter paper. The precipitate was washed twice with 10 ml 5% TCA, centrifuged and filtered again. The extracts were collected and diluted to 50 ml with 5% TCA in a volumetric flask and kept refrigerated at 4°C until required for further analysis. Then, the deproteinized kutum roe extracts (20 ml each) were steam distilled using a Kjeldahl instrument and the ammonia collected in 4% boric acid containing methyl red/bromocresol green (indicator). The solution was titrated with 0.02 M HCl solution and quantified by mg TVB-N/100g of tissue.

Color measurements

Color measurements of samples were objectively secured using Lovibond (CAM system500). Samples were placed in Petri to occupy the center of the dish. The unit was calibrated using a standard plate supplied by the manufacturer. Individual measurements

were conducted using 5 different roe samples, from which mean measurements were statistically computed. Color measurements employed CIE (Commission Internationale d'Eclairage of France) color system using L* (lightness), a* (redness), and b* (yellowness) color values (Tahergorabi *et al*., 2012).

Microbiological analysis

Changes in bacterial population of the brined-kutum roes were monitored at the same time with chemical analyses. To enumerate the bacterial population, 25 grams of the brined roe was homogenized by a stomacher (P.B.I. Milan, Italy) at high speed for 4 min in 225 ml of sterile saline phosphate buffer (0.05 M, pH 7.0). Serial dilution was made and diluted bacteria then spread onto agar plate. Total psychrotrophic bacteria were enumerated on plate count agar (Merck, Germany) at 4°C for 5 days. Enumeration of coliforms and *Escherichia coli* were carried out respectively on violet red bile agar (Merck, Germany) and MacConkey agar (Merck, Germany) and the plates were incubated in anaerobic jars (Anaerocult A; Merck, Darmstadt, Germany) at 37°C for 48 h. For quantitative detection of histamine-forming bacteria, 0.1 ml aliquots of the appropriate dilutions was spread on a specific medium introduced by Niven et al (1998) and consisted of 0.5% tryptone, 0.5% yeast extract, 2.7% L-histidine.2HCL, 0.5% NaCl, 0.1% CaCO3, 2.0% agar, and 0.006% bromocresol purple (pH 5.3). Histamine-forming bacteria cultured on the agar plates for 4 days at 35°C. After counting the number of colonies on each plate, the number so obtained was multiplied by the inverse of the dilution and the result was stated as the number of colony forming unit (cfu) in 1 gram of the sample (Downes *et al*., 2001).

Statistical analysis

The data were subjected to a completely randomized design with repeated measures. Comparison of means was performed using a Tukey method. All statistical analyses were performed with the SAS system (2003) with the significance level set at $\alpha = 0.05$ and the variability was expressed as standard error of mean (SEM).

Results and discussion

In the present experiment, NaCl concentrations of brine noticeably affected the roe shelf life; as the samples brined in 10% NaCl-solution putrefied during the brining with the change of their appearance and stench and so removed from the study. The results of the two other experimental treatments (18 and 24% brine concentration) during the storage on moisture, and chemical characteristics of salted kutum roe are presented in Table 1.

Table 1- Changes of moisture, dry and salt contents of salted kutum roe during storage

treatment	Day 1	Day 30	Day 60	Day 90
Moisture (%)				
18%	0.57 ± 64.50	0.85 ± 64.00	0.53 ±63.62	1.28 ± 63.45
24%	0.98 ± 62.04	0.51 ± 62.16	0.57 ± 61.92	0.41 ± 61.74
Salt (%)				
18%	0.10 ± 3.35	0.06 ± 3.37	0.07 ± 3.47	0.02 ± 3.52
24%	0.03 ± 4.15	0.03 ± 4.18	0.05 ± 4.23	0.03 ±4.26
Lipid (%)				
18%	0.57 ± 6.24	2.78 ± 6.29	0.60 ±6.24	1.28 ± 6.07
24%	0.98 ± 6.25	0.18 ± 6.63	2.07 ± 6.19	0.15 ± 6.16
Protein (%)				
18%	0.64 ± 22.56	0.23 ± 22.42	0.21 ± 22.53	0.19 ± 22.47
24%	0.32 ± 22.41	0.23 ± 22.57	0.07 ± 22.38	0.17 ± 22.35

[a,b] Different letters within each column represent significant differences($p<0.05$).
[A,B] different letters within each row represent significant differences ($p<0.05$).

The protein and lipid content of the samples were not affected by brine concentration and/or storage time (Table 1). In contrast to the moisture, samples of 24% brine treatment

had a greater salt content than 18% brined-roes. According to the authors' observation on putrefied samples, it found that the light NaCl concentration is not suitable for salting of kutum roe, and had no positive effect as a preservative on crude roe. In agreement with our results and findings of Shabanpour *et al* (2017), which suggested higher percentage of pure and mixed salt for preserving of trout roe (5.5 %). Salt penetrates into the roe by dialysis and water diffuses out of the roe by the osmotic pressure. They have shown that higher protein aggregating which could led to dehydration of more salted samples and so decrease water holding capacity (Shabanpour *et al.*, 2017). Moreover, lower moisture content in the samples of brine 24% could be explained by dynamic mutual diffusion process (Madadlou *et al.*, 2007) induced between the brine salt and roe moisture according to their gradient differences. Therefore, higher simultaneous uptake of NaCl in the concentrated brine increased the salt content in roes and thus led to water diffusion out through them (Madadlou *et al.*, 2007).

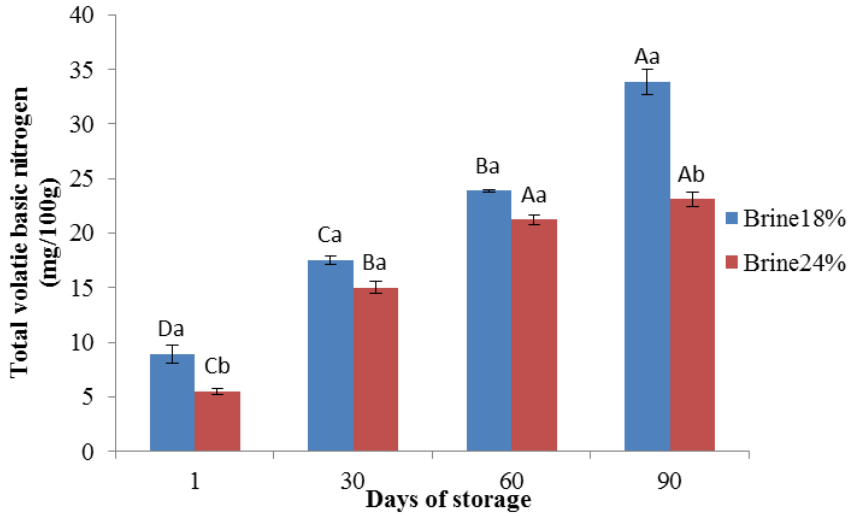

Fig. 1. Total volatile basic nitrogen (mg/100g) value of salted kutum roe during storage. Error bars indicate SEM. Different small letters are significantly different (P< 0.05) between treatments. Different capital letters are significantly different (P< 0.05) during storage.

The interaction of brine concentration× storage day was significant for TVB-N and its content in brined-roes increased during storage (P< 0.05). Amount of TVBN in 18% brined samples was higher (8.93 to 33.83 mg/100g) than 24% brined samples (5.46 to 23.1 mg/100g). The TVB-N has been used as quality indicators for aquatic protein sources and includes several compounds such as ammonia, and also mono-, di-, and tri-methylamine, which can be formed by bacterial or endogenous enzymatic (Lapa-guimarães *et al.*, 2011). According to the literature processing, condition and length of the storage have a significant effect on TVB-N content of fresh crude roe (Lapa-guimarães *et al.*, 2011; Kung *et al.*, 2009). Periago *et al.*(2003) reported that the amount of tuna fish roe TVB-N doubled during the 8 weeks of refrigeration at 4°C. Although, it has not been reported a safe range for the amount of TVB-N in fish roe product (Lapa-guimarães et al., 2011), the European Community has determined the maximum limit of TVB-N for consumption of 35 mg of TVB- N per 100 g of fish muscle. Furthermore, The Chilean Official Organization established the maximum TVB-N level in salted and dried fish products at 150 mg N/100 g of sample (Lapa-guimarães et al., 2011). There are relationship between amount of volatile nitrogen base and increasing of pH and bacterial activity (Shabanpour *et al.*,

2015).

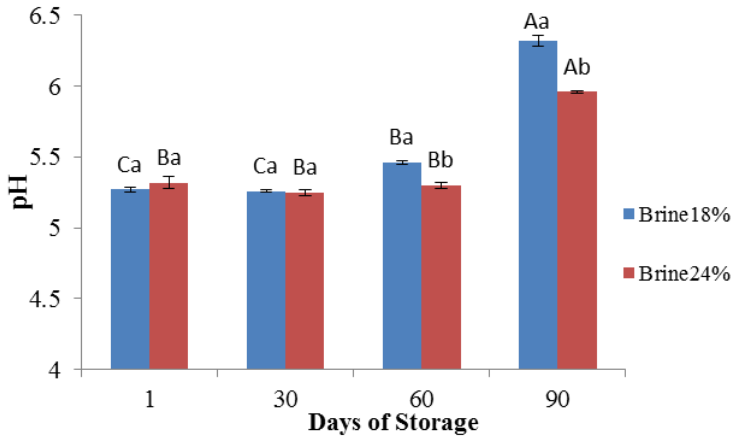

Fig. 2. pH of salted kutum roe of salted kutum roe during storage.
Error bars indicate SEM. Different small letters are significantly different ($P < 0.05$) between treatments.
Different capital letters are significantly different ($P < 0.05$) during storage.

The effects of treatments on pH value and microbial content of salted kutum roe are shown in Fig. 2- 4. The pH value of samples of brines 18% and 24%, significantly increased on days 60 and 90 of storage, respectively. It was increased progressively during the storage of the samples. In 18% brined samples pH increased from 5.27 to 6.32 while in 24% brined samples, pH increased from 5.33 to 5.96. The percentage of salt in 18% and 24% brined samples at the end of storage was 3.52 and 4.26%, respectively. This was presumably due to the production of volatile basic components, such as ammonia, trimethylamine. By the addition of salt, pH reduction which is the result of increasing the ionic strength of the solution inside of the cells occurs (Goulas and Kontominas, 2005). Shabanpour *et al.* (2015) reported pH value of dry-salted roe of rainbow trout by 3.5 % pure salt reached to 7.5 after 60 days of storage. They proposed higher percentage (5.5%) of salt for preserving of salted roe. It's previously reported that the pH value of brined roe has an increasing trend to the basic scale during long-cold storage, which is depending on brine concentration (Inanli *et al.*, 2010).

The sensitivity of microorganisms to NaCl concentrations was found to be different because of static or cidal effects of salt ion osmotic pressure (Hwang *et al.*, 2012; Bassin *et al.*, 2011).

None of these samples contained *Coliforms* or *E. coli*. The total counts of psychotropic bacteria in 18% brined roe during 30 days of cold storage was markedly higher than in the 24% brined roe (3.39 and 2.24 log cfu/g, respectively). For 18% treatment, after 90-day-storage, psychrotrophic bacteria was enhanced (3.48 to 4.42 $\log^{10}$ cfu/g) compared with the 24% brined sample (2.07 to 3.74 log cfu/g), respectively. At the end of storage, there were no significant difference of psychrotrophic bacteria between two treatments (4.42 & 3.74 logcfu/g, respectively). The accepted amount of psychrotrophic bacteria in caviar 5 log cfu/g have been determined (Iranian National Standards, 1995). According the results, the total bacterial counts in all samples were within acceptable limits (less than 5 log cfu/g). Shabanpour *et al* (2015) found that salted roe by higher percentage of salt (5.5%) (5.17 log cfu/g) had lower psychrotrophic bacteria than 3.5% dry-salted roe. According to Shabanpour *et al* (2015) as a result of osmotic exposure of water and salting in effect limited bacterial growth and increased the shelf life of salted roe. Inanli *et al* (2011) reported that the adding

of acetic acid on salted rainbow trout roe had significant effect on reducing of psychotrophic bacteria.

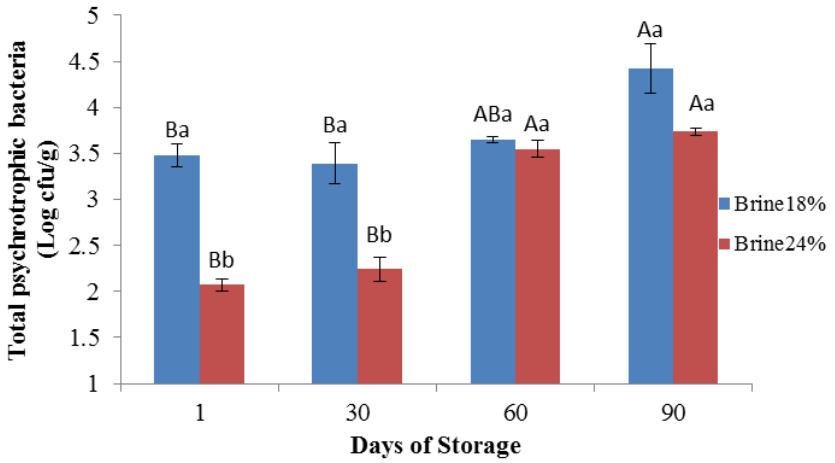

Fig. 3. Total psychrotrophic bacteria (Log_{10} cfu/g) of salted kutum roe during storage. Error bars indicate SEM. Different small letters are significantly different ($P< 0.05$) between treatments. Different capital letters are significantly different ($P< 0.05$) during storage.

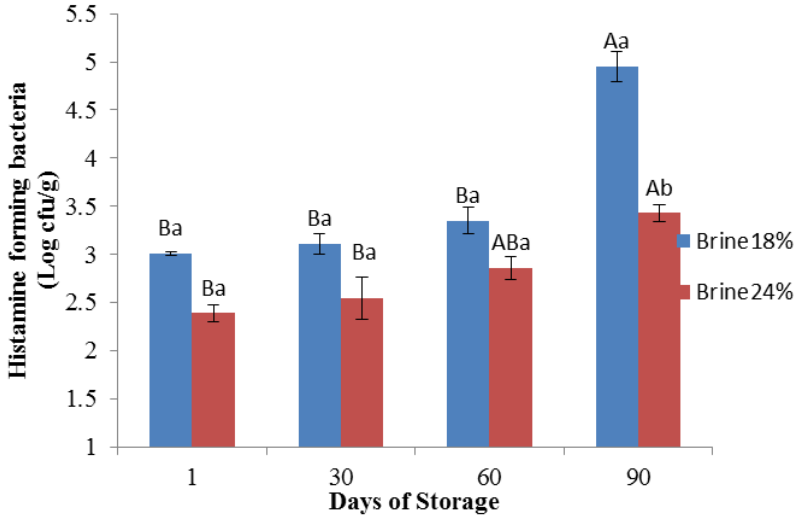

Fig. 4. Histamin forming bacteria (Log_{10} cfu/g) of salted kutum roe during storage. Error bars indicate SEM. Different small letters are significantly different ($P<0.05$) between treatments. Different capital letters are significantly different ($P<0.05$) during storage.

The presence of histamine-forming bacteria of 18% brined-roe significantly increased at the end of storage and was higher than 24% brined-roe (4.95 & 3.43 logcfu/g, respectively). Histamine-forming bacteria numbers of 24% brine samples on day 90 increased compared to the first of storage (2.39 to 3.43 logcfu/g). In this study, the effect of different brine concentrataions on HFB was also determined. The content of the histamine-forming bacteria in the 24% brined samples was less than 18% samples. This was according of Tsai *et al.*, (2007), reported that NaCl concentrations of 1.5% and 3.5% had a stimulatory effect on histamine formation, whereas concentrations of NaCl in excess of 7.5% inhibited its growth and histamine formation. Taylor and Speckard (1983) report that 0.5-2.0% NaCl did not inhibit the growth of *M. morganii* and *K.pneumoniae* or inhibit

their histamine production. Periago *et al.* (2003) reported the presence of total aerobic bacteria and histamine forming bacteria in salted (up to 15%) tuna roe. Also, Hwang *et al.* (2012) cultured, isolated and identified some of histamine forming bacteria in salted escolar roe products. Kung *et al.* (2015) have been isolated some histamine forming bacteria of various dried-salted fish products such as salted sardine and Spanish anchovies.

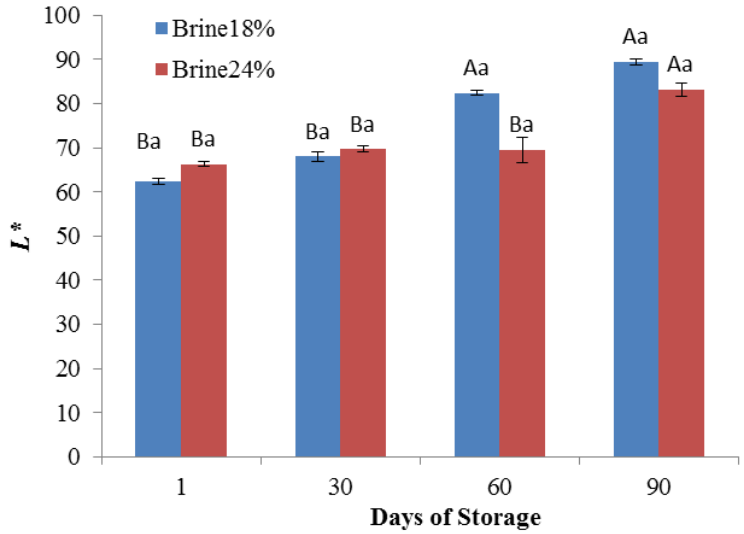

Fig. 5. Lightness (L*) of salted kutum roe during storage.
Error bars indicate SEM. Different small letters are significantly different ($P < 0.05$) between treatments.
Different capital letters are significantly different ($P < 0.05$) during storage.

The effects of experimental treatments on the color change of salted kutum roe during storage are presented in Figures 5-7. The interaction of brine concentration× storage was significant for color values. In storage period, L* value significantly increased in 18% brined roe (62.38 to 82.42 and 89.38). From the result, the lightness (L*) of salted roe in both treatments was found in the ranges of 62.38–89.38 during 90 days of storage (Fig. 5). No differences in L* value of roe treated with 18 and 24 % brine at the same time ($p>0.05$) were noticeable. However, the L* value tended to increase with increasing time for both concentration after 2 months of storage.

The redness-greenness (a*) of salted roe during storage are shown in Fig. 6. The results showed that a* value of in the ranges of 11.76 and 12 (18 and 24% treatment, respectively) at the first of storage, which then decreased throughout the storage (3.44 and 4.51) ($p<0.05$). This index in 24 % brined roe was higher than 18% brined samples at the end of storage. Thereafter, no differences in the a* value between salted roe prepared by both concentration were observed ($p>0.05$). For the yellowness–blueness (b* value) (Fig. 7), no significant differences was between treatments and during storage ($p>0.05$). The decrease in a*value at the end of the storage was possibly due to the excessive oxidation of both lipid resulting in the discolouration of roe samples (Chaijan, 2011). Shabanpour *et al* (2017) reported the redness value of rainbow trout roe decreased during storage and it was related to lipid oxidation and decrease of colorant. They also showed higher lightness in 5.5 of dry-salted treatments. The yellowness of dry-salted rainbow trout roe decresed during storage, that it was different with the current study which there is no significant diffrenes in this index.

Color measurement is an important quality parameter in processed fish products and effective on consumer preference. Carotenoids, such as lutein, astaxanthin, canthaxanthin, zeaxanthin, β- carotene, and β-

cryptoxanthin are the main source of the pigments in fish roe (Bekhit *et al.*, 2009), which could be affected by fish species, diet, age and maturity stage (Bledsoe *et al.*, 2003). On the other hand, some of carotenoids (e.g., Lutein) appear yellow at low concentrations and orange-red at high concentrations (William & Kalpana, 2014).

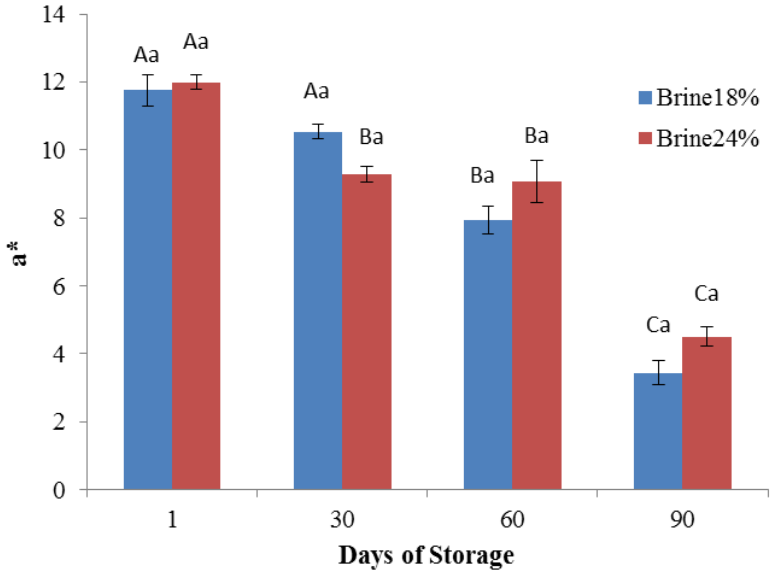

Fig. 6. Redness (a*) of salted kutum roe during storage.
Error bars indicate SEM. Different small letters are significantly different ($P < 0.05$) between treatments.
Different capital letters are significantly different ($P < 0.05$) during storage.

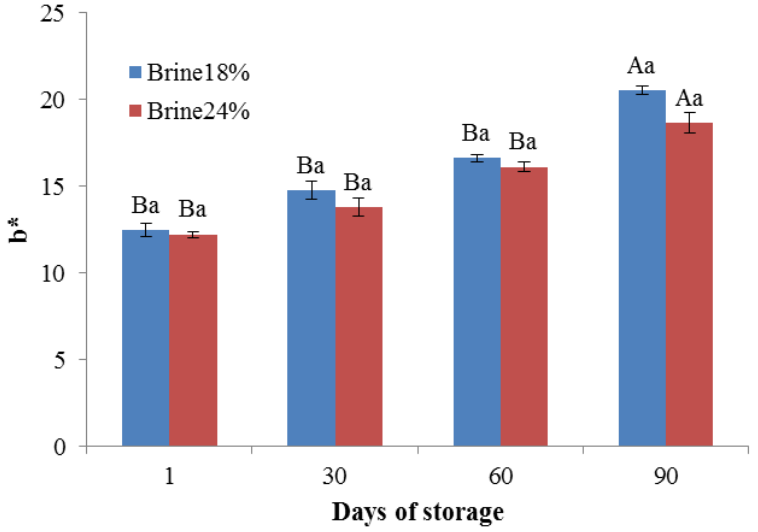

Fig. 7. Yellonewss (b*) of salted kutum roe during storage.
Error bars indicate SEM. Different small letters are significantly different ($P<0.05$) between treatments.
Different capital letters are significantly different ($P<0.05$) during storage.

Table 2. Color parameters of salted kutum roe during storage

treatment	Storage	ΔE	C^*_{ab}	h^*_{ab}
18%	1	3.62 ± 0.04^{De}	2.46 ± 0.08^{Dd}	180.81 ± 0.51^{Dc}
	30	3.69 ± 0.04^{Cd}	2.51 ± 0.05^{Cc}	180.95 ± 0.15^{Cc}
	60	3.85 ± 0.04^{Bb}	2.53 ± 0.05^{Bc}	181.12 ± 0.56^{Bab}
	90	3.92 ± 0.07^{Aa}	2.63 ± 0.06^{Aa}	181.40 ± 0.40^{Aa}
24%	1	3.67 ± 0.04^{Ce}	2.46 ± 0.04^{Bd}	180.79 ± 0.45^{Abc}
	30	3.70 ± 0.05^{Bc}	2.44 ± 0.04^{Bd}	180.97 ± 0.81^{Abc}
	60	3.71 ± 0.05^{Bc}	2.53 ± 0.05^{Ac}	181.05 ± 0.78^{Abc}
	90	3.89 ± 0.07^{Ab}	2.56 ± 0.05^{Ab}	181.33 ± 0.35^{Aab}

Different capital letters in each column show significant difference in each treatment ($P < 0.05$)
Different small letters in each column show significant difference between treatment ($P < 0.05$)

Therefore, a part of the change of a* value in the brined roe during the storage period (Fig 6) could be explained by the decrease of carotenoids concentration after their oxidation (William & Kalpana, 2014). However, the higher L* value of 18% brined roe could be due to the positive relation between moisture content and L* value (Bekhit et al., 2009). Regardless of the brine concentration, the ΔE value of salted roe (Table 2) increased significantly with the time of storage. On the other hand, chroma value of the samples (Table 2) also increased significantly ($P<0.05$) with storage. According to the color parameters, 18% brined-roe changed more than 24% brined samples. In general, both treatment at the first of storage showed a less yellowish appearance with in lower h* when compared to the end of storage. Total color differences was higher in 18% treatment in comparison of 24% brined samples ($P<0.05$).

The results obtained in this study demonstrated that 10% brine concentration has no protective effect on crude kutum roe. However, 18% brined roe showed acceptable chemical and microbial results in refrigerated condition, and 24% brine roe appeared optimal during storage period. Future studies on brined kutum roe should investigate the levels of histamine in this product and provide an appropriate packaging method to more control of carotenoids oxidation and microbial growth.

Acknowledgments

This work was financially supported by Gorgan University of Agriculture Sciences and Natural Resources (grant No: 92-314-84).

Conflict of Interest

Authors have no conflict of interest to declare.

References

AOAC. (1990). Official Methods of Analysis of AOAC Int. Association of Official Analytical Chemists, 15th edn. Arlington, VA, USA.

Balaswamy, K., Jyothirmayi, T., & Rao, D.G. (2007). Chemical composition and some functional properties of fish egg (roes) protein concentrate of rohu (*Labeo rohita*). *Journal of Food Science and Technology*, 44, 293-296.

Bassin, J.P., Pronk, M., Muyzer, G., Kleerebezem, R., Dezotti, M., & van Loosdrecht, M.C.M. (2011). Effect of elevated salt concentrations on the aerobic granular sludge process: linking microbial activity with microbial community structure. *Applied and Environmental Microbiology*, 77,7942-7953

Bekhit, A.E.A., Morton, J.D., Dawson, C.O., & Richard, S. (2009). Optical properties of raw and

processed fish roes from six commercial New Zealand species. *Journal of Food Engeering*, 91,363-371.

Bledsoe, G.E., Bledsoe, C.D., & Rasco, B. (2003). Caviars and fish roe products. *Critical Reviews in Food Science and Nutrition*, 43,317-356.

Chaijan, M. (2011). Physicochemical changes of tilapia (*Oreochromis niloticus*) muscle during salting. *Food Chemistry*, 129, 1201–1210.

Downes, F.P., & Ito, K. (2001). Compendium of methods for the microbiological analytic examination of foods, fourth ed. American Public Health Association, Washington, DC. USA. 995 Pages.

Gallart-Jornet, L., Barat, J.M., Rustad, T., Erikson, U., Escriche, I., & Fito, P. (2007). Influence of brine concentration on Atlantic salmon fillet salting. *Journal of Food Engineering*, 80,267-275.

Howgate, P. (1976). Determination of total volatile bases. Aberdeen: Torry Research Station. TD 564. Appendix 4.

Hwang, C.C., Lin, C.M., Huang, C.Y., Huang, Y.L., Kang, F.C., Hwang, D.F., & Tsai, Y.H. (2012). Chemical characterisation, biogenic amines contents, and identification of fish species in cod and escolar steaks, and salted escolar roe products. Food Control, 25, 415-420.

Inanli, A.G., Coban, O.E., & Dartay, M. (2010). The chemical and sensorial changes in rainbow trout caviar salted in different ratios during storage. *Fish Sciences*, 76,879-883.

Inanli, A.G., Oksuztepe, G., Ozpolat, E. & Emir Coban, O. (2011). Effects of acetic acid and different salt concentrations on the shelf life of caviar from rainbow trout (*Oncorhynchus mykiss* W. 1792). *Journal of Animal and Veterinary Advances*, 10(23), 3172-3178.

Iranian National Standards. 1995. Caviar 186, 27p. (in Persian).

Jittinandana, S., Kenney, P.B., Slider, S.D., & Kiser, R.A. (2002). Effect of brine concentration and brining time on quality of smoked rainbow trout fillets. *Journal of Food Science*, 67,2095-2099.

Kung, H.F., Wang, T.Y., Huang, Y.R., Lin, C.S., Wu, W.S., Lin, C.M., & Tsai, Y.H. (2009). Isolation and identification of histamine-forming bacteria in tuna sandwiches. *Food Control*, 20,1013-1017.

Kung, H.F., Huang, C.Y., Lin, C.M., Liaw, L.H., Lee, Y.C., Tsai, Y.H. (2015). The histamine content of dried flying fish products in Taiwan and the isolation of halotolerant histamine-forming bacteria. *Journal of Food And Drug Analysis*, 23,335-342.

Lapa-Guimarães, J., Trattner, S., Pickova, J. (2011). Effect of processing on amine formation and the lipid profile of cod (*Gadus morhua*) roe. *Food Chemistry*,129,716-723.

Madadlou, A., Khosrowshahi asl, A., Ebrahimzadeh Mousavi, M., & Farmani, J. (2007). The influence of brine concentration on chemical composition and texture of Iranian White cheese. *Journal of Food Engineering*, 81,330-335.

Martinez-Alvarez, O., & Gómez-Guillén, M. (2005). The effect of brine composition and pH on the yield and nature of water-soluble proteins extractable from brined muscle of cod (*Gadus morhua*). *Food chemistry*, 92,71-77.

Narsing Rao, G., Balaswamy, K., Satyanarayana, A., & Prabhakara, R.P. (2012). Physico-chemical, amino acid composition, functional and antioxidant properties of roe protein concentrates obtained from *Channa striatus* and *Lates calcarifer*. *Food Chemistry*, 132, 1171-1176.

Nguyen, M.V., Arason, S., Thorarinsdottir, K.A., Thorkelsson, G., & Gudmundsdóttir, A.(2010). Influence of salt concentration on the salting kinetics of cod loin (*Gadus morhua*) during brine salting. *Journal of Food Engeerning*, 100,225-231.

Niven, C.F., Jeffrey, J.M.B., & Corlett, D.A. (1981). Differential Plating Medium for Quantitative Detection of Histamine-Producing Bacteria. *Applied Environmental Microbiology*, 41,321-322.

Periago, M.J., Rodrigo, J., Ros, G., Rodríguez-Jérez, J.J., & Hernández-Herrero, M. (2003). Monitoring volatile and nonvolatile amines in dried and salted roes of tuna (*Thunnus thynnus* L.) during manufacture and storage. *Journal of Food Protection*, 66,335-340.

Pourashouri, P., Yeganeh, S., & Shabanpour, B. (2015). Chemical and microbiological changes of salted Caspian Kutum (*Rutilus frisii kutum*) roe. *Iranian Journal of Fisheries Sciences*, 14,176-187.

Rao, G.N. (2014). Physico-chemical, functional and antioxidant properties of roe protein concentrates from *Cyprinus carpio* and *Epinephelus tauvina*. *Journal of Food and Pharmaceutical Sciences*, 2,15-22.

Safari, R. and Yosefian, M. (2006). Changes in TVN (total volatile nitrogen) and psychotrophic bacteria in Persian sturgeon caviar (*Acipenser persicus*) during processing and cold storage. *Journal Applied Ichthyology*, 22(1),416–418.

SAS (Statistical Analysis System) (2003) SAS/STAT User's Guide: 2003 Edition: SAS Institute Inc., Cary, Nc.

Shabanpour, B., Ghorbanian, G., Ojagh, S. M., Pourashouri, P. and Aghili Negad, S.M. (2015). Effect of different concentrations of pure and mixed salt on the shelf life of salted rainbow trout (*Oncorhynchus mykiss*) roe during refrigerated storage. *Food Hygiene*, 6(4), 31-44.

Shabanpour, B., Ghorbanian, G., Ojagh, S. M., Pourashouri, P. and Aghili Negad, S.M. (2017). Effect of different concentrations of pure and mixed salt on sensory and microbial quality of salted rainbow trout (*Oncorhynchus mykiss*) roe during refrigerated storage. *Journal of Food Science and Technology*, 64 (14),191-201.

Shin, J.H., & Rasco, B.A. (2007). Effect of Water Phase Salt Content and Storage Temperature on Listeria monocytogenes Survival in Chum Salmon (*Oncorhynchus keta*) Roe and Caviar (Ikura). Journal of Food Science, 2,160-166.

Tahergorabi, R., Beamer, S.K., Matak, K.E., & Jaczynski, J. (2012). Functional food products made from fish protein isolate recovered with isoelectric solubilization/precipitation. *LWT- Food Science and Technology*, 48,89-95.

Tsai, Y.H., Kung, H.F., Chen, H.C., Chang, S.C., Hsu, H.H., Wei, C.I.(2007). Determination of histamine and histamine-forming bacteria in dried milkfish (*Chanos chanos*) implicated in a food-born poisoning. *Food Chemistry*, 105,1289-96.

William, J.R., & Kalpana, D.P. (2014). Reversibility of chronic disease and hypersensitivity: the effects of environmental pollutants on the organ system. CRC Press, UK. 723 Pages.

نشریه پژوهشهای علوم و صنایع غذایی ایران
جلد 14، شماره 3، مرداد - شهریور 1397، ص. 40-29

Iranian Food Science and Technology Research Journal
Vol. 14, No. 3, Aug. Sep. 2018, p. 29-40

کیفیت شیمیایی و بارمیکروبی تخم عمل‌آوری شده ماهی سفید (*Rutilus frisii kutum*) با غلظت‌های مختلف آب نمک در طی نگهداری

پرستو پورعاشوری[1*]- بهاره شعبانپور[2]- زینب نوری هاشم آباد[3]

تاریخ دریافت: 1396/07/12
تاریخ پذیرش: 1396/12/24

چکیده

خاویار به‌عنوان شناخته شده‌ترین شکل از محصولات تخم ماهیان است. تخم ماهی به‌طور سنتی و رایج در آب نمک اشباع نمک سود می‌شود. علیرغم اهمیت این محصولات اطلاعات تکنیکی اندکی در مورد ترکیب شیمیایی، کیفیت محصول و امنیت غذایی این محصولات وجود دارد. تخم ماهی سفید (*Rutilus frisii kutum*) به مدت 14 روز در سه تیمار آزمایشی در محلول‌های 10، 18 و 24 درصد آب نمک قرار گرفت. پس از خروج از آب نمک تخم ماهی سفید به مدت 90 روز در دمای یخچال (4 درجه سانتی‌گراد) نگهداری گردید. pH، ترکیبات تقریبی، نمک و بازهای نیتروژنی فرار (TVN)، باکتری‌های سرمادوست، کلی‌فرم‌ها، باکتری‌های تولیدکننده هیستامین و شاخص رنگ محصول مورد ارزیابی قرار گرفت. آزمایشات در ابتدای تولید و پس از 30، 60 و 90روز نگهداری انجام شد. تیمار 10% در طی مرحله نمک سود فاسد شد و مورد آزمایش قرار نگرفت. میزان رطوبت و TVN در تیمار 24% کمتر از تیمار 18% بود. pH و HFB در انتهای نگهداری و تعداد باکتریهای کل سرمادوست در روزهای 60 و 90 بیشتر بودند. افزایش شاخص *L و کاهش مقدار *a در نمونه‌های 18% در روزهای 60 و 90 مشاهده شد اما این افزایش در تیمار 24% تنها در روز 90 نگهداری مشاهده شد. فرآوری تخم ماهی سفید در آب نمک 18 درصد دارای شاخص‌های شیمیایی و میکروبی قابل‌قبولی در شرایط یخچال بود و تخم نمک سود شده در آب نمک 24 درصد شرایط بهینه را در طی نگهداری نشان داد.

واژه‌های کلیدی: تخم ماهی، ماهی سفید، مدت ماندگاری، غلظت آب نمک‌گذاری

1، 2 و3- به‌ترتیب استادیار، استاد و دانشجوی دکتری، گروه فرآوری محصولات شیلاتی، دانشکده شیلات و محیط زیست، دانشگاه علوم کشاورزی و منابع طبیعی گرگان، ایران
(*- نویسنده مسئول : Email: Pourashouri.p@gmail.com)

Iranian Food Science and Technology Research Journal
Vol. 14, No. 3, Aug. Sep. 2018, p. 41-51

نشریه پژوهشهای علوم و صنایع غذایی ایران
جلد 14، شماره 3، مرداد - شهریور 1397، ص. 51-41

The effects of ultrasound waves on yield, texture and some qualitative characteristics of cheese

Seyed Mahdi Hosseini Bahri[1], RezaEsmaeilzadeh Kenari[2*]

Received: 2017.07.11
Accepted: 2018.03.15

Abstract

In this study, the effects of bath and probe ultrasound treatments were investigated on yield, texture (hardness, adhesion, cohesion, springiness and chewiness), pH and moisture content of fresh white cheese. The times 2, 4, 6 minutes and 5, 10, 15 minutes were used in probe treatment (frequency 20 kHz) and bath treatment (frequency 37 kHz), respectively, at temperatures of 40, 50 and 60°C in two stages (raw cow milk and cheese matrix). The results showed that applying ultrasound treatment significantly (P<0.05) increases cheese making yield and moisture content and decreases pH compared with the control sample, so that the highest moisture content and efficiency were related to probe ultrasound treatment in 2 minutes at 30°C. Results of the texture analysis showed that the cheese sample hardness significantly (P<0.05) reduced with the increasing time and temperature of ultrasound treatment compared to control samples. Also parameters of the adhesiveness and chewiness decreased as a result of ultrasound treatment compared to the control samples, but parameters of cohesiveness and springiness did not have discernable change trends.

Keywords: ultrasound bath and probe, yield, quality characteristics, texture characteristics, cheese

Introduction

The processes of thermal pasteurization and sterilization are the most common methods used in processing of dairy products in order to eliminate and inactivate microorganisms. However, heat may result in drop of sensory properties and nutritional value of dairy products. One of the most important components of milk that can be altered by heat is protein. It can be said that protein is the most valuable compartment of milk due to its high nutritional value and unique physical and chemical properties. These unique properties of protein play a key role in the production of dairy products, such as cheese or yogurt (Cameron *et al.*, 2009). Coincided with an increase of consumer's information, the demand for the use of novel methods of food processing with minimal impact on reducing nutritional value and overall quality of food has been increased. Among the new technologies that have been proposed to improve the dairy products shelf life, ultrasound alone or in combination with heat (thermosonication) or with pressure (manosonication) can efficiently disable many bacterial species and improve quality of the products (Marchesini et al., 2012). Low frequency ultrasound technology (18-100 kHz) has many potential applications in the dairy industry, such as homogenization, crystallization, and anti-foam properties; facilitating the isolation of milk fat with high frequency equal to or higher than 400 kHz). The sound range in ultrasound is divided to ultrasound with high frequency, low intensity (respectively higher than 1 MHz and less than 1Wcm^{-2}) and with low frequency and high intensity (respectively 20-100 kHz and 10-1000 Wcm^{-2}) which both are applied in food technology. However, high-intensity, low-frequency is usually used in the food industry. The first type is non-destructive and can be used to

1. PhD student, Department of Food Science and Technology, Faculty of Agricultural Engineering, Sari Agricultural Sciences and Natural Resources University, Sari, Iran- Greenhouse Cultivation Research Department,Tehran Agricultural and Natural Resources Research and Education Center, AREEO,Varamin, Iran .
2. Associated professor, Department of Food Science and Technology, Faculty of Agricultural Engineering, Sari Agricultural Sciences and Natural Resources University, Sari, Iran.
(Corresponding Author Email: reza_kenari@yahoo.com)
DOI: 10.22067/ifstrj.v14i3.66004

analyze and characterize the compounds, while the latter can be used to modify cellular structures and a number of other processes such as foam inhibitors, emulsification, inhabitation or activation of the enzyme and crystallization. The ultrasound frequency is directly effective on the number of bubbles created in the system so that the higher frequency will lead to smaller number and size of bubbles. As a result, the power generated by cavitation will reduce (Alarcon-Rojo *et al*., 2015).

During the ultrasound treatment, mechanical power and high temperature caused by cavitation lead to great structural changes in milk. Some of these structural changes can be noted as reduction in the size of fat globules, cracking cell membrane of milk fat and breaking down milk casein micelles into smaller components (the components which are connected with triacylglycerol). Free radicals and other reactive species may be formed during ultrasound treatment. These chemicals can lead to oxidation reactions and production of volatile compounds in the environment which plays an important role in compromising the quality of milk. The production of these series of destructive compounds caused by ultrasound treatment highly depends on treatment conditions (frequency, intensity, range and temperature). It is important to determine the optimum process conditions. All of these structural changes caused by ultrasound treatment can lead to positive or negative qualitative and technological impaction dairy products (Marchesini *et al*., 2012). The use of ultrasound has found many applications in the dairy industry. Low-frequency waves between 100-18 KHz are used in operations such as homogenization, crystallization and de-foaming and the waves with higher frequencies up to 400 kHz are used to accelerate the separation of milk fat. Many food components are sensitive to thermal process and are vulnerable against biological and chemical changes and reducing these food components and long processing time and energy consumption in conventional processing methods are among the disadvantages of these methods. Using innovative technology methods such as ultrasound can largely reduce energy consumption and process time and costs and also prevent the vulnerability and sensitivity of nutrient products (Chemat and Khan, 2011). Among the new technologies used to improve the health and durability of milk, ultrasound technique causes the inactivation of many bacterial species more efficiently, better performance of starter bacteria in cheese making, further release of starter enzymes before and after the addition of the starter and also increases efficiency and improve quality of cheese (Piyasena *et al*., 2003). So far, relatively few studies have been conducted on the application of ultrasound in cheese making and in this context doing more research should be considered. Marchesini *et al* (2012) showed that the use of ultrasound significant increases the amount of free fatty acids, reduces the pH of the raw milk by increasing lipolysis reactions, decreases the number of somatic cells and improves the quality of milk, as well as decreasesthe formation process of clots in the cheese-making stage. So far, no study has been provided that attempted to evaluate the ultrasound treatment changing the texture of cheese. In this study, the effects of ultrasound bath (at a frequency of 37 kHz) and probes (20 kHz) are investigated on yield of cheese, textural properties (hardness, cohesiveness, adhesiveness, springiness and chewiness) and qualitative characteristics of the cheese (pH and moisture content) in two step process: 1) applying ultrasound on raw milk before adding starter and 2) applying ultrasound to the matrix cheese (after the formation of cheese clots) at 40, 50 60°C for 2, 4 and 6 minutes in probe technique and 5, 10 and 15 minutes in the bath technique.

Materials and methods

Supplying raw milk

In order to conduct the cheese-making

process, 20 kg of raw cow milk was prepared at the local market in Sari immediately after milking and was maintained at 4°C until the testing time (24 hours). Enough rennet tablets were purchased (IIEC, Iran Industrial Enzymes Company).

Applying ultrasound process to the raw cow milk used in cheese making

500 ml of raw milk was pasteurized in a non-continuous way at 62°C for 10 minutes to produce each ultrasound, before applying ultrasound and then, was affected by ultrasound in two methods of probes (at 40, 50 and 60°C for 2, 4 and 6 minutes) and bath (at 40, 50 and 60°C for 5, 10 and 10 minutes). In the probe method, ultrasound cell disruptor (Model KS-250F, China, Ningbo Zhejiang) was used with a frequency of 20 kHz and range of 45% and power of 250 watts and in the bath method Elma Ultrasonic cleaning device (model S 30 H, Germany) with a frequency of 37 kHz and power of 280 watts. Then, after applying the ultrasound process the temperature of milk was brought to 42°C and the amount of 0.1 grams rennet per liter was added to the milk. After the clot formation (about 20 minutes), the cheese matrix was cut and dehydrated. And after all these the compression operation was performed for 2 hours. And finally fresh white cheese was packed in plastic packages containing salt water solution 4%. All tests were performed three days after the production and brining (Villamiel and de Jong, 2000).

Applying ultrasound process to the cheese matrix

After the pasteurization of milk, as described above, the temperature of the milk was brought to 42 °C and the amount of 0.1 grams rennet per liter was added to the milk. Cheese matrix was affected by ultrasound in two methods of probes (at 40, 50 and 60°C for 2, 4 and 6 minutes) and bath (at 40, 50 and 60°C for 5, 10 and 10 minutes) after the clot formation (20 minutes). And operations like drainage, compressing, packaging and brining were donerespectively. Milk control samples were prepared from pasteurized milk without an ultrasound process (Villamiel and de Jong, 2000).

Measuring moisture content

25 grams of cheese was weighed and the moisture content of the samples was measured using an electric oven according to the following formula (Benedito *et al*., 2000):

Moisture content= (intial sample weight- dried sample weight)/ intial sample weight (1)

Measuring pH

The pH value of the samples was measured using a digital electrode pH meter PB 11 (Sartorius, Germany).

Determining the yield of cheese

Based on the amount of milk and cheese production, cheese yield is calculated as follows:

$$\text{Cheese yield}=\frac{\text{consumed milk}}{\text{produced cheese}} \quad (2)$$

Texture Profile Analysis

Analysis of tissue (TPA) by Brookfield CT3 Texture Analyzer (Brookfield Engineering Laboratories, USA) was pressed in order to study the changes resulting from the ultrasound process on the textural characteristics of the cheese samples, during the two-cycle compression using cylinder probe (50 mm diameter) up to 20% of the original thickness. Pre-test, test and returning speed were 1, 1 and 60 mm per minute, respectively. In the following we are going to evaluate the qualitative characteristics of the texture including; Hardness (the highest amount of force required for the first compression stage (N)); Cohesiveness (ratio of the force curve area during the second compression cycle to the ratio of the force curve area during the first compression cycle); Adhesiveness (negative force area for unloading in the first compression cycle); Springiness(ratio of the distance that the sample restores after the first compression (mm)); Chewiness (multiplication of hardness in cohesiveness and springiness (Nmm)) (O'Callaghan and Guinee, 2004).

Statistical analysis

All experiments were performed at least in three replications. Statistical analysis included one-way analysis of variance (ANVOA) and the significance mean (*post hoc* Duncan test) carried out at the significance level of $P<0.05$ using version 9 of SAS software. Stochastic statistical design was used in this work.

Results and discussion

The effects of ultrasound treatment on cheese pH

The pH is one of the most important cheese quality parameters of the texture which directly affects many chemical, structural and functional characteristics of cheese compounds. Reduction of pH leads to an increase in soluble calcium content and consequently increases the vulnerability of milk and helps to facilitate the process for cheese making. Decrease in pH causes the contraction of the protein matrix and helps the withdrawal of the whey (Pastorino *et al.*, 2003).

Tables 1 and 2 respectively show probe and bath ultrasound treatment effect on the cheese pH (applying ultrasound on raw milk for the cheese making and cheese matrix). Ultrasound treatment significantly reduces the pH of the cheese samples compared to control samples ($p<0.05$). In general, with increasing ultrasound treatment time, a significant decrease in cheese pH ($p<0.05$) was observed. It was also found that cheese samples prepared by applying ultrasound to the raw milk has less pH than the cheese samples prepared by applying treatment to the cheese matrix. In fact, applying ultrasound treatment on raw milk cheese is leading to a further reduction in pH. As can be seen in Tables 1 and 2, in general, samples treated with ultrasound probe have less pH than the ones treated with ultrasound bath this could be due to the more intense effect of ultrasound probe than the ultrasound bath on the milk composition structure. Increasing temperature of the ultrasound treatment initially leads to an increase in pH but ultrasound treatment reduced the pH of cheese at higher temperatures. The same behavior was noticed by Marchesini et al. (2012). They stated that temperature rise initially leads to an increase in the pH, due to the acceleration of CO_2 emissions from the milk but as the temperature increases, pH decreases due to the intensification of the Maillard reaction.

Ultrasound treatment can cause fat globule membrane damage caused by cavitation and release of free fatty acids, triglycerides, phospholipids and cholesterol from the center of the fat globules. The release of triglycerides in milk leads to an increase in lipolysis reaction and consequently an increase in free fatty acids of milk and ultimately reducing the pH due to an increase in lipolysis enzyme effect. Intensification of lipolysis reactions results in improved flavor in cheese ripening as well. The lower the pH, the faster the cheese ripening happens (Bermúdez-Aguirre *et al.*, 2008).

The effects of ultrasound treatment on moisture content of the cheese:

Moisture content is a very important parameter in the process of cheese making is directly related to cheese making yield. The higher the moisture content, the faster the ripening process happens and also the cheese yield would be higher. Higher moisture content leads to an increase in the amount of lactose in the cheese and therefore it produces more lactic acid in the ripening stage and the cheese becomes more acidic (Britz and Robinson, 2008, Walstra *et al*., 2005).

The results of the ultrasound bath and probe treatment on the content of the cheese (ultrasound applied on raw milk and cheese matrix), are presented in Tables 1 and 2. Moisture content of the sample was 54.20%. As can be seen in Tables 1 and 2, applying ultrasound treatment significantly increases moisture content compared to the control sample ($p<0.05$). Moisture content of the samples treated with ultrasound was in the range of 58.60-54.26 %. In general, an increase in ultrasound treatment time and temperature

significantly decreases the moisture content of the cheese ($p<0.05$). The moisture content of the cheese samples produced by ultrasound treatment on raw milk was more than the samples produced by ultrasound treatment on the cheese matrix (after inoculation).

Table 1- The effect of bath ultrasound on the pH and moisture content of raw milk and cheese matrix

ultrasound treatment type		pH	Moisture (%)
Raw milk	*5 min, 30 °C*	5.04±1.22^{gh}	57.84±1.42^{b}
	5 min, 40°C	5.16±2.35^{cde}	57.15±2.20^{c}
	5 min, 50°C	5.10±2.17^{efg}	56.15±1.42^{g}
	10 min, 30 °C	4.96±2.11^{i}	56.94±2.16^{d}
	10 min, 40°C	5.08±1.24^{fg}	56.45±2.15^{f}
	10 min, 50°C	4.99±1.31^{hi}	56.12±1.33^{g}
	15 min, 30 °C	4.85±1.33^{j}	56.55±1.21^{e}
	15 min, 40°C	4.98±0.62^{i}	56.13±1.16^{g}
	15 min, 50°C	4.88±1.40^{j}	55.60±0.51^{j}
Cheese matrix	*5 min, 30 °C*	5.20±1.42^{bcd}	57.94±2.12^{a}
	5 min, 40°C	5.24±0.60^{ab}	55.94±1.62^{h}
	5 min, 50°C	5.21±1.23^{abc}	55.15±0.13^{l}
	10 min, 30 °C	5.13±1.31^{ef}	56.48±0.71^{f}
	10 min, 40°C	5.15±0.22^{de}	55.34±0.46^{k}
	10 min, 50°C	5.13±0.85^{ef}	54.78±0.33^{n}
	15 min, 30 °C	5.04±0.52^{gh}	55.72±1.23^{i}
	15 min, 40°C	5.10±1.40^{fg}	54.92±1.34^{m}
	15 min, 50°C	5.05±1.50^{g}	54.54±0.50^{o}
Ultrasound treatment		5.26±0.28^{a}	54.20±1.52^{p}

Mean (*n=3*) values with different letters represents the significant case at $P<0.05$.

Table 2- The effect of probe ultrasound on the pH and moisture content of raw milk and cheese matrix

Ultrasound treatment type		pH	Moisture (%)
Raw milk	*2 min, 30 °C*	4.88±0.22^{j}	58.60±1.42^{a}
	2 min, 40°C	5.02±0.35^{fg}	55.95±2.20^{e}
	2 min, 50°C	4.94±2.17^{hi}	54.94±1.42^{j}
	4 min, 30 °C	4.78±2.11^{l}	57.88±2.16^{b}
	4 min, 40°C	4.90±1.24^{ij}	55.38±2.15^{h}
	4 min, 50°C	4.83±1.31^{k}	54.55±1.33^{m}
	6 min, 30 °C	4.65±1.33^{mn}	56.92±1.21^{c}
	6 min, 40°C	4.69±0.62^{m}	54.85±1.16^{k}
	6 min, 50°C	4.61±1.40^{n}	54.26±0.51^{p}
Cheese matrix	*2 min, 30 °C*	5.16±1.42^{bc}	56.80±2.12^{d}
	2 min, 40°C	5.18±0.60^{b}	55.32±1.62^{i}
	2 min, 50°C	5.14±1.23^{bc}	54.45±0.13^{n}
	4 min, 30 °C	5.08±1.31^{de}	55.58±0.71^{f}
	4 min, 40°C	5.13±0.22^{bcd}	54.64±0.46^{l}
	4 min, 50°C	5.12±0.85^{cd}	54.44±0.33^{n}
	6 min, 30 °C	4.98±0.52^{gh}	55.53±1.23^{g}
	6 min, 40°C	5.04±1.40^{ef}	54.31±1.34^{o}
	6 min, 50°C	5.01±1.50^{fg}	54.42±0.50^{n}
Ultrasound treatment		5.26±0.28^{a}	54.20±1.52^{p}

Mean (*n=3*) values with different letters represents the significant case at $P<0.05$.

It is recognized that ultrasound treatment reduces the size of casein micelles that in this regard, the exact ultrasound mechanism is not clear. It is also observed that after the ultrasound treatment, the serum protein of the solution increases and the reason for this has been attributed to the breakdown of the connection between serum casein and protein (kappa-casein and beta-lactoglobulin connection), which is the result of pasteurization heat. Breaking down serum protein-casein connection facilitates the effect of renin enzyme on the kappa-casein and contributes to the formation of cheese clots (Chandrapala *et al.*, 2012). Increasing the moisture content of cheese samples after ultrasound

treatment may be attributed to the casein micelles' break down and reduction in the size and thus increasing the active surface and absorbing more water. Also reduction in the moisture content of the cheese by increasing the treatment time and temperature can be due to possible denaturation of serum protein and caseins. In fact increase in ultrasound treatment temperature and time results in denaturation of milk proteins and surface exposure of hydrophobic groups. This can decrease the moisture content of cheese samples compared to less ultrasound treatment temperature and time.

The effect of ultrasound treatment on the yield of cheese making:

Figure 1 shows the effect of bath and probe ultrasound treatment on the yield of cheese making (ultrasound applied on raw milk and cheese matrix). As can be seen in Figure 1, generally ultrasound treatment resulted in a significant increase in cheese making yield ($p<0.05$). In general we can say that with increasing ultrasound treatment time and temperature there was a significant reduction in cheese making yield ($p<0.05$). It was also found that applying ultrasound treatment on raw milk leads to more cheese making yield compared to applying ultrasound treatment on cheese matrix. These results showed overlap with the moisture content data (Tables 1 and 2). Since the content of moisture is one of the most important parameters that directly affect cheese yield. The highest yield of cheese (0.25%) was for the ultrasound treatment applied to the raw milk for 2 minutes at 30°C (Figure 1 c). It is recognized that due to mechanical stresses caused by cavitation, the fat globules of the milk are crushed and the sizes are increased and the numbers increased so that the size of fat globules are the same size as casein micelles. In such circumstances the globule membrane no longer will be able to cover all fat globules. And the fat globules with the hydrophobic part will be coated with casein particles. It results in the creation of a new membrane with different combinations and connection of casein micelle to the fat globules (Meyer et al., 2006). These series of protein-fat binding helps clustering and accumulating casein and serum proteins and therefore provides an ideal structure for cheese making. Smaller fat globules provide a suitable substrate for the rennet enzyme activity due to their physical properties and reduce coagulation time and also increase the time for the clot to become stiff (Villamiel et al., 1999). Increasing cheese making yield through ultrasound treatment can be attributed to several reasons: (1) increasing the moisture content of the samples after applying ultrasound; (2) Casein micelles downsizing which increases the instability of milk and increases the rennet enzyme effects; (3) Creating a complex between hydrophobic parts of serum proteins and casein with fat globules that as well as increasing the serum proteins in cheese it also increases the yield and the nutritional value of cheese.

The effects of ultrasound treatment on the cheese textural features:

Rheological properties of cheese are evaluated by determining its response to stressor strain applied during processes such as compression, shear or cut. Rheological properties such as elasticity, viscosity and viscoelastic properties of cheese are primarily related to the structure, composition and strength of attraction between structural elements. Rheological properties of cheese are usually assessed by measuring rheological parameters in experimental tests. Cheese rheology is a function of the composition, microstructure (e.g. structural composition), physical and chemical state of the components and macro molecular characteristics of (Composite structure consisting of casein clots gaps). Physical and chemical properties include parameters such as the ratio of solid to liquid fat, hydrolysis degree and matrix para-casein hydration and the amount of intermolecular attractions between molecules of para-casein. Texture profile

analysis (TPA) is a simulated test and a very important indicator for determining changes in the cheese texture) (O'Callaghan and Guinee, 2004). TPA parameters can be observed in Tables 3 and 4 as well as (hardness, adhesiveness, cohesiveness, springiness and chewiness) control samples and samples of cheese produced by ultrasound treatment on raw milk and cheese matrix.

Hardness parameter is the amount of force required to achieve the desired change in the shape of the sample (O'Callaghan and Guinee, 2004). The amount of hardness in control samples was N35.04 and in samples treated with baths and probes ultrasound treatment it was ranged 24.02-15.22 and 19.86-14.94 N, respectively (Tables 3 and 4). In general it can be said that the hardness of the cheese after ultrasound treatment significantly reduced compared to control ($p<0.05$).

Reducing the hardness of the cheese in the ultrasound treatment can be attributed to several reasons. Ultrasound treatment leads to an increase in the moisture content of the samples. On the other hand, water can act as a plasticizer in the texture and reduce hardness; because water can be placed between bigger components and reduce friction (Hennelly *et al.*, 2006). Another reason of reducing the cheese hardness in the ultrasound can be attributed to a decrease in pH.Pastorino et al (Pastorino *et al.*, 2003) reported that lower pH leads to a decrease in Cheddar hardness parameter. They stated that pH 5 is due to the increased solubility of calcium and consequently electrostatic force between proteins reduced and smaller protein masses have been formed in the cheese and reduced hardness.

In Tables 3 and 4 it can be observed that samples treated with probe ultrasound have less hardness than the samples treated with bath ultrasound. The reason for this can be related to the more intense damaging effect of ultrasound probe on milk components. It was also found that ultrasound treatment applied to cheese matrix compared with its application to raw milk has led to a further reduction of cheese hardness. Ultrasound treatment time and temperature rise resulted in a significant decrease of the cheese hardness ($p<0.05$). This can be due to more severe destruction of the protein network.

Adhesiveness parameters are used to describe a state of the food sticking to the teeth when chewing (Hennelly *et al.*, 2006). The amount of the control sample adhesiveness was 1.30 mJ and in samples treated with baths and probes ultrasound it was in the range of0.2-1.1 mJ and 0.2-1.1 mJ, respectively (Tables 3 and 4). In fact, ultrasound treatment resulted in a significant reduction of sample adhesiveness compared to control samples ($p<0.05$). The reason for this can probably be due to the moisture content in the samples followed by ultrasound treatment. Cohesiveness parameter helps to achieve a comprehensive understanding of the viscoelastic properties such as tensile stability of the materials (Hennelly *et al.*, 2006). The control sample cohesiveness was in the range of 0.56 and for the samples treated with bath and probe ultrasound it was range 0.60-0.76 and 0.62-0.78 (Tables 3 and 4). We can say that cohesiveness of cheese samples significantly increased after ultrasound treatment compared to control samples ($p<0.05$). Also with changes in temperature, time and type of treatment ultrasound no specific changes were observed. Springiness indicates the characteristics of elasticity and the ability to recover the structure of the samples. As can be seen in Tables 3 and 4, no certain changes took place for ultrasound treatment compared with the control sample.

Chewiness is a combination parameter and it is obtained by multiplying hardness, cohesiveness and springiness. There is an inverse relationship between tenderness, fragility, and chewiness parameter (Hennelly *et al.*, 2006). According to Tables 3 and 4, the amount of the control sample chewiness was 118.32 mJand in samples treated with baths and probes ultrasound it was in the range of 70.42-123.74 mJ and 58.54-101.42 mJ, respectively (Tables 3 and 4).

It can be said that the ultrasound

treatment significantly reduced chewiness and actually increases the cheese tenderness ($p<0.05$). Results related to the cheese samples chewiness completely overlaps with the data related to hardness. And generally harder samples have higher chewiness.

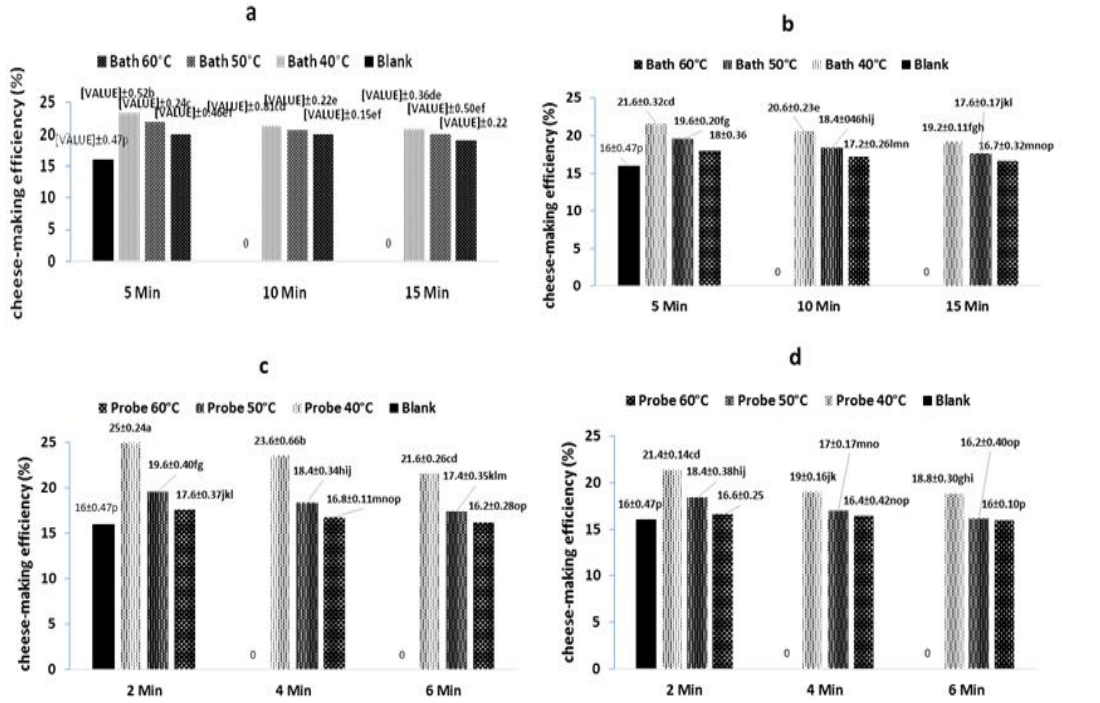

Fig. 1. The effect of ultrasound on the cheese-making efficiency of: raw milk treated by bath US (a), cheese matrix treated by bath US (b), raw milk treated by probe US (c), cheese matrix treated by probe US (d).
Mean ($n=3$) values with different letters represents the significant case at P<0.05.

Table 3- The effect of bath ultrasound on the texture parameters of raw milk and cheese matrix

Type of ultrasound treatment		Hardness (N)	Adhesiveness(mJ)	Cohesiveness	Springiness (mm)	Chewiness (mJ)
Raw milk	*5 min, 30 °C*	24.02±1.22^{b}	0.60±0.21^{f}	0.65±0.23^{d}	7.58±0.42^{c}	118.34±1.94^{c}
	5 min, 40°C	21.92±1.55^{d}	0.20±0.19^{b}	0.72±0.25^{bc}	7.75±0.26^{b}	122.32±2.16^{b}
	5 min, 50°C	19.68±2.04^{h}	0.85±0.12^{cd}	0.64±0.18^{d}	7.38±0.18^{d}	92.95±3.12^{i}
	10 min, 30 °C	20.85±1.88^{f}	0.50±0.32^{g}	0.74±0.10^{b}	8.02±0.32^{a}	123.74±2.17^{a}
	10 min, 40°C	19.23±2.11^{i}	0.80±0.02^{cd}	0.69±0.19^{cd}	7.10±0.20^{g}	94.21±2.55^{a}
	10 min, 50°C	17.76±1.34^{j}	0.21±0.10^{fg}	0.65±0.05^{d}	7.45±0.21^{d}	86.01±1.46^{h}
	15 min, 30 °C	17.96±2.15^{j}	0.60±0.12^{f}	0.60±0.05^{c}	6.28±0.27^{j}	92.98±3.05^{j}
	15 min, 40°C	16.74±2.22^{k}	1.10±0.25^{b}	0.67±0.24^{d}	6.34±0.18^{j}	70.44±3.18^{i}
	15 min, 50°C	15.32±1.64^{l}	0.50±0.15^{g}	0.64±0.15^{d}	6.66±0.22^{i}	65.30±2.11^{o}
Cheese matrix	*5 min, 30 °C*	23.55±2.44^{c}	0.90±0.31^{c}	0.65±0.12^{d}	7.43±0.21^{d}	113.74±2.74^{d}
	5 min, 40°C	21.46±2.13^{e}	1.10±0.25^{b}	0.76±0.02^{a}	6.94±0.26^{h}	113.20±3.36^{d}
	5 min, 50°C	19.65±1.58^{h}	0.40±0.27^{e}	0.72±0.18^{bc}	7.30±0.34^{e}	103.28±3.10^{f}
	10 min, 30 °C	20.12±2.43^{g}	0.20±0.40^{f}	0.71±0.15^{f}	7.76±0.15^{b}	112.28±3.44^{e}
	10 min, 40°C	18.88±1.56^{i}	1.00±0.19^{b}	0.73±0.23^{bc}	6.11±0.20^{k}	84.22±2.12^{k}
	10 min, 50°C	18.82±1.66^{i}	0.10±0.15^{fg}	0.74±0.22^{b}	7.55±0.05^{c}	99.56±2.46^{g}
	15 min, 30 °C	17.44±1.86^{j}	0.90±0.32^{c}	0.74±0.08^{b}	7.21±0.05^{f}	73.51±1.28^{l}
	15 min, 40°C	16.33±1.76^{k}	0.60±0.26^{g}	0.71±0.15^{c}	6.34±0.18^{j}	70.44±3.18^{n}
	15 min, 50°C	15.22±2.44^{l}	0.70±0.30^{e}	0.71±0.18^{c}	6.72±0.11^{i}	72.62±3.14^{l}
Untreated samples		35.04±2.44^{a}	1.30±0.18^{a}	0.56±0.02^{e}	6.03±0.20^{l}	118.32±1.44^{c}

Mean ($n=3$) values with different letters represents the significant case at P<0.05.

Table 4- The effect of probe ultrasound on the texture parameters of raw milk and cheese matrix

Type of ultrasound treatment		Hardness (N)	Adhesiveness(mJ)	Cohesiveness	Springiness (mm)	Chewiness (mJ)
Raw milk	*2 min, 30 °C*	19.86±1.52^{b}	0.40±0.01g	0.63±0.23^{f}	7.36±0.36^{d}	92.08±1.90^{c}
	2 min, 40°C	18.45±1.50^{e}	0.70±0.19^{e}	0.66±0.15^{de}	6.45±0.66^{ij}	78.54±2.16^{q}
	2 min, 50°C	16.82±2.04^{f}	0.80±0.15^{d}	0.76±0.20^{ab}	7.68±0.25^{b}	58.54±3.12^{q}
	4 min, 30 °C	18.24±1.88^{f}	0.30±0.02^{h}	0.66±0.10^{de}	6.52±0.23^{hi}	78.49±1.11^{j}
	4 min, 40°C	16.98±1.14^{g}	1.00±0.12^{b}	0.69±0.14^{a}	7.78±0.28^{a}	87.64±2.25^{e}
	4 min, 50°C	15.43±2.15^{m}	1.02±0.10^{b}	0.70±0.05^{c}	7.13±0.19^{e}	77.01±1.46^{l}
	6 min, 30 °C	16.43±1.15^{b}	0.30±0.05^{h}	0.68±0.05^{d}	6.87±0.27^{a}	76.77±1.64^{m}
	6 min, 40°C	15.78±1.48^{k}	0.90±0.06^{g}	0.56±0.24^{c}	6.76±0.18^{g}	59.74±1.18^{p}
	6 min, 50°C	14.94±2.04^{o}	0.80±0.05^{d}	0.62±0.15^{f}	6.32±0.22^{k}	58.54±1.21^{q}
Cheese matrix	*2 min, 30 °C*	19.32±2.22^{c}	0.20±0.01^{c}	0.66±0.16^{de}	7.40±0.08^{cd}	94.36±1.70^{d}
	2 min, 40°C	18.42±2.06^{e}	0.30±0.25^{h}	0.64±0.30^{b}	6.55±0.26^{h}	77.22±2.70^{k}
	2 min, 50°C	17.04±1.84^{g}	0.10±0.27^{e}	0.78±0.18^{a}	7.63±0.26^{b}	101.42±1.66^{b}
	4 min, 30 °C	17.02±1.78^{g}	0.30±0.02^{h}	0.68±0.26^{d}	7.40±0.15^{cd}	80.45±2.18^{h}
	4 min, 40°C	18.88±1.56^{d}	0.30±0.19^{h}	0.66±0.34^{de}	7.48±0.14^{c}	84.03±2.12^{f}
	4 min, 50°C	15.42±2.14^{m}	0.40±0.05^{g}	0.74±0.04^{b}	7.08±0.05^{e}	80.78±3.56^{g}
	6 min, 30 °C	16.24±1.55^{j}	0.40±0.12^{c}	0.71±0.30^{c}	6.92±0.05^{f}	79.79±1.28^{i}
	6 min, 40°C	15.66±2.44^{l}	0.50±0.26^{f}	0.62±0.02^{f}	6.81±0.18^{g}	66.12±1.28^{n}
	6 min, 50°C	15.12±1.64^{n}	0.40±0.03^{g}	0.68±0.18^{d}	6.38±0.35^{jk}	65.60±2.24^{o}
Untreated samples		35.04±2.44^{a}	1.30±0.18^{a}	0.56±0.02^{g}	6.03±0.20^{l}	118.32±1.44^{a}

Mean (*n=3*) values with different letters represents the significant case at P<0.05.

Conclusion

In summary, it can be stated that ultrasound treatment increases the cheese making yield and moisture content and decreases the cheese pH. It was found that with increasing temperature and time of treatment ultrasound, cheese yield and moisture content decreased. In relation to the pH, with increasing ultrasound treatment time, pH decreased but with increasing ultrasound treatment temperature, first pH slightly increases and then decreases. According to the TPA results, the hardness of cheese samples with increasing time and temperature of ultrasound treatments significantly decreased compared to control samples. Adhesiveness and chewiness parameters decreases by ultrasound treatment compared to control samples. But parameters of cohesiveness and springiness faced no discernable change trends. It can be concluded that ultrasound treatment increases the cheese making yield and improves the quality and texture of the cheese

Resources

Alarcon-Rojo, A., Janacua, H., Rodriguez, J., Paniwnyk, L., & Mason, T., 2015, Power ultrasound in meat processing. *Meat science*, 107**,** 86-93.

Benedito, J., Carcel, J., Sanjuan, N., & Mulet, A., 2000, Use of ultrasound to assess Cheddar cheese characteristics. *Ultrasonics*, 38**,** 727-730.

Bermúdez-Aguirre, D., Mawson, R., & Barbosa-Cánovas, G., 2008, Microstructure of fat globules in whole milk after thermosonication treatment. *Journal of Food Science*, 73**,** E325-E332.

Britz, T. & Robinson, R. K. Advanced Dairy Science and Technology, Wiley, 2008.

Cameron, M., Mcmaster, L. D., & Britz, T. J., 2009, Impact of ultrasound on dairy spoilage microbes and milk components. *Dairy Science and Technology*, 89**,** 83-98.

Chandrapala, J., Martin, G. J. O., Zisu, B., Kentish, S. E., & Ashokkumar, M., 2012, The effect of ultrasound on casein micelle integrity. *Journal of Dairy Science*, 95**,** 6882-6890.

Chemat, F., & Khan, M. K., 2011, Applications of ultrasound in food technology: processing, preservation and extraction. *Ultrasonics sonochemistry*, 18**,** 813-835.

Hennelly, P., Dunne, P., O'sullivan, M., & O'riordan, E., 2006, Textural, rheological and

microstructural properties of imitation cheese containing inulin. *Journal of food engineering*, 75**,** 388-395.

Marchesini, G., Balzan, S., Montemurro, F., Fasolato, L., Andrighetto, I., Segato, S., & Novelli, E., 2012, Effect of ultrasound alone or ultrasound coupled with CO2 on the chemical composition, cheese-making properties and sensory traits of raw milk. *Innovative Food Science & Emerging Technologies*, 16**,** 391-397.

Meyer, S., Berrut, S., Goodenough, T., Rajendram, V., Pinfield, V. & Povey, M., 2006, A comparative study of ultrasound and laser light diffraction techniques for particle size determination in dairy beverages. *Measurement Science and Technology*, 17**,** 289.

O'callaghan, D. & Guinee, T., 2004, Rheology and texture of cheese. *Cheese: Chemistry, physics and microbiology*, 1**,** 511-540.

Pastorino, A., Hansen, C., & Mcmahon, D. J., 2003, Effect of pH on the chemical composition and structure-function relationships of Cheddar cheese. *Journal of dairy science*, 86**,** 2751-2760.

Piyasena, P., Mohareb, E., Mckellar, R., 2003, Inactivation of microbes using ultrasound: a review. *International journal of food microbiology*, 87**,** 207-216.

Villamiel, M., & De Jong, P., 2000, Influence of high-intensity ultrasound and heat treatment in continuous flow on fat, proteins, and native enzymes of milk. *Journal of Agricultural and Food Chemistry*, 48**,** 472-478.

Villamiel, M., Van hamersveld, E., & De Jong, P., 1999, Effect of ultrasound processing on the quality of dairy products. *Milchwissenschaft*, 54**,** 69-73.

Walstra, P., Walstra, P., Wouters, J. T. M., & Geurts, T. J., 2005, *Dairy Science and Technology*, Second Edition, CRC Press.

نشریه پژوهشهای علوم و صنایع غذایی ایران
جلد 14، شماره 3، مرداد - شهریور 1397، ص. 51-41

Iranian Food Science and Technology Research Journal
Vol. 14, No. 3, Aug. Sep. 2018, p. 41-51

اثرات امواج فراصوت بر راندمان، بافت و برخی خصوصیات کیفی پنیر

سید مهدی حسینی بحری[1]- رضا اسماعیل زاده کناری[2*]

تاریخ دریافت: 1396/04/20
تاریخ پذیرش: 1396/12/24

چکیده

در تحقیق حاضر، تاثیرات تیمار اولتراسوند حمام و پروب بر راندمان، خصوصیات بافتی (سختی، چسبندگی، انسجام، فنریت و قابلیت جویدن)، pH و محتوای رطوبت پنیرسفید تازه مورد ارزیابی قرار گرفت. زمان‌های 2، 4، 6 دقیقه و 5، 10، 15 دقیقه به‌ترتیب در روش پروب (فرکانس 20 کیلوهرتز) و حمام (فرکانس 37 کیلوهرتز) در دماهای 40، 50 و 60 درجه سانتی‌گراد در دو مرحله (شیر خام گاو و ماتریکس پنیر) استفاده گردید. نتایج نشان دادند که اعمال تیمار اولتراسوند در مقایسه با نمونه شاهد باعث افزایش معنی‌دار ($P<0.05$)راندمان پنیرسازی، محتوای رطوبت و کاهش pH گردید. به‌طوری که بالاترین محتوای رطوبت و راندمان پنیرسازی مربوط به تیمار اولتراسوند پروب و زمان 2 دقیقه و دمای 30 درجه سانتی‌گراد بود. نتایج مربوط به آنالیز بافت نشان دادند که میزان سختی نمونه‌های پنیر در مقایسه با نمونه شاهد و همچنین با افزایش زمان و دمای تیمار اولتراسوند به‌طور معنی‌دار کاهش یافت ($P<0.05$). همچنین پارامترهای چسبندگی و قابلیت جویدن در اثر اعمال تیمار اولتراسوند نسبت به نمونه‌های شاهد کاهش یافتند، ولی پارامترهای انسجام و فنریت روند تغییرات مشخصی نداشتند.

واژه‌های کلیدی:اولتراسوند حمام و پروب، راندمان، ویژگی‌های کیفی، ویژگی های بافتی، پنیر

1- دانشجوی دکتری، گروه علوم و صنایع غذایی، دانشگاه علوم کشاورزی و منابع طبیعی ساری و عضو هیئت علمی مرکز آموزش و تحقیقات منابع طبیعی و کشاورزی،ورامین،ایران
2-دانشیار، گروه علوم و صنایع غذایی، دانشگاه علوم کشاورزی و منابع طبیعی ساری ،ساری، ایران.
(*- نویسنده مسئول: Email: reza_kenari@yahoo.com)

Iranian Food Science and Technology Research Journal
Vol. 14, No. 3, Aug. Sep. 2018, p. 53-62

نشریه پژوهشهای علوم و صنایع غذایی ایران
جلد 14، شماره 3، مرداد - شهریور 1397، ص. 62-53

Convective drying of garlic (*Allium sativum* L.): Artificial neural networks approach for modeling the drying process

Majid Rasouli*[1]

Received: 2017.07.20
Accepted: 2018.04.09

Abstract

In this study, artificial neural networks (ANNs) was utilized for modeling and the prediction of moisture content (MC) of garlic during drying. The application of a multi-layer perceptron (MLP) neural network entitled feed forward back propagation (FFBP) was used. The important parameters such as air drying temperature (50, 60 and 70°C), slice thickness (2, 3 and 4 mm) and time (min) were considered as the input parameters, and moisture content as the output for the artificial neural network. Experimental data obtained from a thin-layer drying process were used testing the network. The optimal topology was 3-25-5-1 with LM algorithm and TANSIG threshold function for layers. With this optimized network, R^2 and mean relative error were 0.9923 and 9.67 %, respectively. The MC (or MR) of garlic could be predicted by ANN method, with less mean relative error (MRE) and more determination coefficient compared to the mathematical model (Weibull model).

Key words: Artificial neural networks; Back propagation; Convective drying; Garlic; Moisture Content

[1]Introduction

Garlic (*Allium sativum* L.) is an important Allium spice that is a strong source of phenolic compounds, phosphorus, potassium, sulfur, zinc, selenium and vitamins A and C and lower levels of calcium, magnesium, sodium, iron, manganese and B complex vitamins elements (Brewester, 1997). It has antiseptic properties and is used in a number of medicinal preparations. Various garlic powder pills and garlic oil pills are now commercially available (Sharma & Prasad, 2006). It has been cultivated for centuries all over the world especially cultivated widely in Iran. Most of garlic has been used as a fresh vegetable without any preprocessing operation. It is also used for seasoning of foods because of its typical pungent flavor. Garlic is a semi-perishable product. Due to lack of suitable storage and transportation facilities, about 30% of fresh crop is wasted in postharvest stages by respiration and microbial spoilage (Sharma, Prasad, & Chahar, 2009). More recently, it has been used in its dried form, as an ingredient of precooked foods and instant convenience foods including sauces, gravies and soups. These lead to a sharp increasing in the demand of dried garlic. To cater the demand of dried garlic and to overcome its storage problems, it should be processed quickly and optimally to maintain the quality.

Drying is the most common food preservation method used in practice (Midilli, Kucuk, & Yapar, 2002) and dried garlic exists into different products such as powders, flakes and slices (Abbasi Souraki & Mowla, 2008). The optimization of drying operation leads to an improvement in the quality of the output product, a reduction in the cost of processing as well as the optimization of the throughput (Madamba, Driscoll, & Buckle, 1994). There are various methods for prediction of drying characteristics of agricultural products. The simplest way is to use the available empirical correlations, which based on relatively large number of experimental data to identify unknown parameters. However, this approach generally gives the most accurate results only in specific experiments and they are not valid in other conditions (Movagharnejad & Nikzad, 2007). Artificial neural network (ANN)

1. Assistant Professor, Department of Biosystem Engineering, Faculty of Agricultural Engineering, Bu-Ali Sina University, Hamedan, Iran.
(Corresponding Author Email: m.rasouli@basu.ac.ir)
DOI: 10.22067/ifstrj.v14i3.66235

modeling is an advanced computational method that can be used to handle complicated relationships between physical properties of foods and process parameters. A major advantage of this approach is that it requires less computational time compared to the finite-element or finite-difference methods because the outputs are calculated using basic algebra. This is beneficial in the development of an on-line predictive control system (Poonnoy, Tansakul, & Chinnan, 2007). Several studies demonstrated the significance and usefulness of the artificial neural network (ANN) in modeling the drying process (Khazaei & Daneshmandi, 2007; Nazghelichi, Kianmehr, & Aghbashlo, 2010; Satish & Pydi Setty, 2005), prediction of bulk density and residual moisture content (Chegini *et al.*, 2008), temperature and moisture content prediction (Mittal & Zhang, 2000; Poonnoy *et al.*, 2007), modeling of tomato drying (Movagharnejad & Nikzad, 2007), drying process of carrot (Erenturk & Erenturk, 2007), prediction of physical property changes of carrot during drying (Kerdpiboon *et al.*, 2006), energy consumption (Zhang, Yang, Mittal, & Yi, 2002) and moisture content modeling of thin-layer corn during the drying process (Trelea *et al.*, 1997).

The objective of the present study was to build up and evaluate the predictive performance of an ANN model to approximate a nonlinear function relating moisture content of garlic during the drying process under different drying conditions. The prediction of moisture ratio in the drying systems is helpful to find out the optimum drying time to reach optional moisture content in the final product.

Materials and methods

Fresh garlic (*Allium sativum* L.) bulbs were obtained from a field located in Azarshahr (East Azarbaijan Province), Iran; and stored in a refrigerator at 4°C until experiments started. After 2h stabilization period at the ambient temperature, the bulbs by uniform size were selected and separated into cloves and peeled, then were cut using a rotating disc slicer into 2, 3 and 4 mm thickness (L) mm.

The initial moisture content of pre-treated garlic was determined using a mechanical convection oven at 102±1°C until constant weight was attained (AOAC, 1990). The initial moisture content of pre-treated garlic was 2.03 ($g_{water}.g_{dry\ solid}^{-1}$). The samples weight was measured by an electronic balance with a sensitivity of 0.001 g. Four replications were conducted to obtain a reasonable average.

Drying equipment

Drying experiments were performed in a pilot plant tray- dryer. A schematic view of the dryer is shown in Figure 1. The dryer mainly consists of three basic units, a fan providing desired drying air velocity, electrical heaters controlling the temperature of drying air and drying chamber. The dryer was equipped with a data acquisition system and a controlling unit of temperature, air flow velocity and relative humidity. Air was flowed by an axial flow blower (90 W) and the velocity of air flow was controlled by changing the rotating speed of fan (SPC1-35, Autonics, Taiwan) and measured using a vane probe type anemometer (AM-4202, Lutron, Taiwan) with an accuracy of ± 0.1 $m.s^{-1}$. Air was heated, while flowing through three spiral type electrical heaters, having 5, 5 and 2 kW capacity. These electrical heaters turned off or on separately via a temperature control unit (TZ4ST-Autonics, Taiwan) depending on the changes in the temperature, to stabilize a constant air temperature during each experiment with an accuracy of ±0.1°C. The weighing system consisted of an electronic balance (AND GF3000, Japan) having an accuracy of ±0.01 g. During the drying process, the air temperature and relative humidity in the drying chamber were logged on a data acquisition system (Delta T, England).

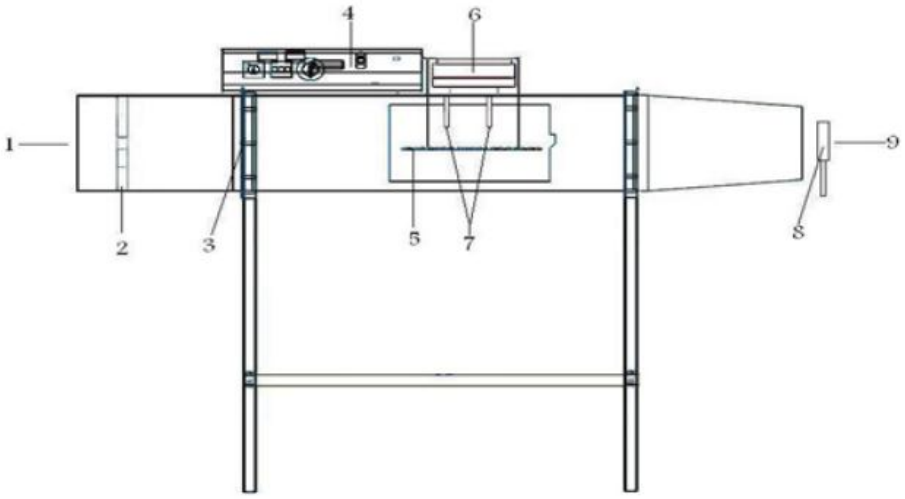

Fig. 1. Schematic diagram of the convectional drying equipment (1) Air inlet; (2) Fan; (3) Heaters; (4) Temperature and air flow velocity controlling; (5) Perforated tray; (6) Digital balance; (7) Relative humidity sensor and thermocouple to data logger; (8) Digital anemometer; (9) Air outlet.

Experimental procedure

The dryer was adjusted to the selected temperature for about half an hour before starting of the experiments in order to achieve steady state conditions. Then, the samples (about 120 g) were spread in a single layer on a tray that connected to the balance in the dryer. Weight loss of samples was measured and recorded every 120 s. Drying time was defined as the time required to reduce the moisture content of samples to 0.09 ($g_{water}. g_{dry\ solid}^{-1}$) (equilibrium moisture content). Additional samples (180g) were put on a separate tray within drying chamber without connecting to the balance. These samples were used to observe and measure the color changes of garlic slices during and at the end of drying process when the moisture content of samples fell to 1.06, 0.43, 0.13 and 0.09 ($g_{water}. g_{dry\ solid}^{-1}$). Drying experiments were performed at the drying air temperatures of 50, 60 and 70°C, a constant air flow rate of 1.5 $m.s^{-1}$ using garlic slices with different thickness, 2, 3 and 4 mm. Each experiment was repeated three times. The moisture content data obtained at different drying air temperatures and slice thicknesses during drying process were converted to the moisture ratio (MR). However, the MR was simplified to M/M_i instead of the $(M - M_e)/(M_i - M_e)$, because the values of the M_e are relatively small compared to M or M_i. Hence the error involved in the simplification is negligible (Ertekin & Yaldiz, 2004; Rasouli *et al*., 2011).

Artificial neural networks (ANNs)

The artificial neural networks are basically computational models, which simulate the function of biological networks, composed of neurons. Most research studies using artificial neural networks apply a multilayered, feed forward, fully connected network of perceptions. Among the reasons for using this kind of ANN is the simplicity of its theory, ease of programming and good results. If topology of the network is allowed to vary freely, it can take the shape of any broken curve (Topuz, 2010). The network had three layers; input, hidden and output. The numbers of neurons in the input layer and the output layer were equal to the number of input and output parameters, respectively. Each input unit of the input layer receives input signal X_i and broadcasts this signal to all units in the hidden layer. Each hidden unit Y_j sums its weighted input signal and applies its activation function to compute output signal as identified in Equal (1):

$$Y_j = f_{act}\left(\sum_{i=1} W_{ij} X_i + b_j\right) \quad (1)$$

where W_{ij} is the weight of the connection from the i^{th} input unit to the j^{th} hidden unit, b_j is the weight of bias connection for j^{th} hidden unit. The output signal of the hidden unit Y_j is sent to all units in the output layer. Each output unit O_k sums its weighted input signal and applies its activation function to compute its output signal as identified in equal (2):

$$O_k = f_{act}\left(\sum_{j=1} V_{jk} Y_j + b_k\right) \quad (2)$$

Where V_{jk} is the weight of the connection from the j^{th} hidden unit to the k^{th} output unit. The parameter of bias (b) in Equals. (1) and (2), also called the threshold value, is permanently set to 1 in the hidden layer as well as in the output layer, so that corresponding weight shifts the activation function along the x axis. The activation functions used in this study were tangent sigmoid and logistic sigmoid that are defined respectively as:

$$f_{act}(x) = \frac{1}{1+\exp(x)} \quad (3)$$

$$f_{act}(x) = \frac{2}{(1+\exp(-2x))-1} \quad (4)$$

(Demuth & Beale, 2003; Erenturk & Erenturk, 2007).

The BP training algorithm is an iterative gradient descent algorithm, designed to minimize the mean of square error (MSE) which is averaged over all patterns and is calculated as follows:

$$MSE = \frac{\sum_{p=1}^{m}\sum_{i=1}^{n}\left(S_{ip} - T_{ip}\right)^2}{n_p n_0} \quad (5)$$

Where S_{ip} is the desired or actual output, T_{ip} is the predicted output for the pattern, n_0 is the number of neurons in the output layer, and n_p is the number of patterns.

In order to facilitate the comparisons between predicted values for different network parameters (learning rate, momentum coefficient and neuron number in hidden layer, different activation functions and the training algorithm) and desired values, there is a need for secondary criteria which were used as follow:

$$R^2 = 1 - \frac{\sum_{i=1}^{n}\left[S_{ip} - T_{ip}\right]}{\sum_{i=1}^{n}\left[S_{ip} - \frac{\sum_{i=1}^{n} S_{ip}}{n}\right]} \quad (6)$$

$$MAE = \frac{1}{n}\sum_{i=1}^{n}\left|S_{ip} - T_{ip}\right| \quad (7)$$

$$MRE = \frac{1}{n}\sum_{i=1}^{n}\left|\frac{S_{ip} - T_{ip}}{S_{ip}}\right| \times 100 \quad (8)$$

During training, an ANN is the presented with the data for thousands of times, which is referred to as epochs. After each epoch the error between the ANN output and the desired values is propagated backward to adjust the weight in a manner mathematically guaranteed to converge. Adjustment of the weights ΔW_{ij} can be calculated as:

$$\Delta W_{ij} = -\alpha \frac{\partial E}{\partial W_{ij}} + \beta \Delta W_{ij}(s-1) \quad (9)$$

(Topuz, 2010).

Where α is the learning rate, β is the momentum coefficient and s is the current step. Training is the act of continuously adjusting the connection weights until they reach unique values that allow the network to produce outputs that are close enough to actual desired outputs. The accuracy of the developed model, therefore, depends on these weights. Once optimum weights are reached, the weights and biased values encode the network state of knowledge (Topuz, 2010).

Considering and applying the tree inputs in all experiments, the MC value was derived for different conditions. Networks with tree neurons in input layer (drying air temperature (°C), thickness of slices (mm) and time (s)) and one neuron in output layer (MC) were designed. Figure 2 shows the considered neural network topology and input and output

parameters. Boundaries and levels of input parameters are shown in Table 1. Using experimental data obtained in the thin-layer dryer, an optimized ANN model was developed to predict the outlet moisture content of the garlic. In order to determine the optimal number of hidden units of the proposed neural network architecture, pilot experiments were done. In order to avoid over fitting, two common methods were used. These were: (i) early stopping; and (ii) minimizing the number of hidden units (Erenturk & Erenturk, 2007). In this study, Back propagation (BP) algorithm, which is one of the most famous training algorithms for multi-layer perceptions, was implemented using the neural network toolbox of MATLAB (R2009a) software. The available data set was partitioned into three parts, 70% for training, 20% for test and 10% corresponding to the validation of the model. The training process was carried on until a minimum of the error was reached in the second (validation) partition. The estimation of the performance of the trained network was based on the accuracy of the network on the test partition (Erenturk & Erenturk, 2007).

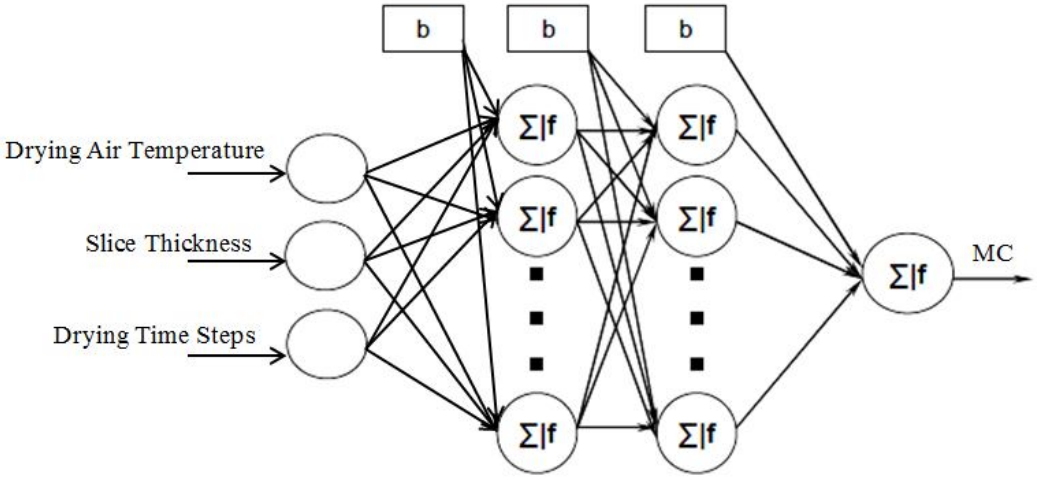

Fig. 2. Artificial neural network topology used for predicting the moisture content.

Table 1- Input parameters for ANNs and their boundaries

Parameters	Minimum	Maximum	No. of Levels
Air Temperature (° C)	50	70	3
Slice Thickness (mm)	2	4	3
Time Steps (min)	45	249	-

Result and discussion

In present ANN model, three independent variables, such as drying time, drying air temperature and slice thickness have been chosen as input parameters, and moisture content (dependent variable) of products has been regarded as the output parameter. In order to obtain the optimum structure of FFBP neural network, the ANN model was trained with varying number of neurons in hidden layer, TANSIG and LOGSIG threshold function and LM, CGF and OSS learning algorithms. Several topologies were tested and the best results which used from each training algorithm and Threshold function are represented in Table 2. Minimization of error was accomplished using the Levenberg–Marquardt (LM) algorithm. Training was completed after 200 epochs. The numbers of neurons in hidden layers were varied from 5 to 30. The networks were simulated with the learning rate equal to 0.05.

The best results for FFBP network with LM algorithm belonged to TANSIG threshold

function and 3-25-5-1 topology. This composition produced *MSE*=0.00131, R^2=0.9923 and *MRE* =9.67 and converged in 200 epochs.

The best results for FFBP network with CGF algorithm belonged to LOGSIG threshold function and 3-3-2-1 topology. This composition produced *MSE*=0.00399, R^2=0.9901 and *MRE* =12.27 and converged in 200 epochs.

The best results for FFBP network with OSS algorithm belonged to TANSIG threshold function and 3-25-5-1 topology. This composition produced *MSE*= 0.00399, R^2=0.9919 and *MRE* =11.34 and converged in 200 epochs.

Finally, application of LM algorithm has better result than CGF and OSS algorithms because it produced less *MRE* and more R^2 values. The results are presented in table 2. Experimental and predicted data set are shown in figure 3 and *MSE* for training patterns in figure 4. Results showed that *MRE* is the least value for this network, so this network selected as an optimized one.

Besides, in order to compare the results against the existing predictive models, a thin layer drying mathematical model was selected from the literature. Rasouli *et al*. (2011) used a nine thin layer drying models to describe the drying characteristics of garlic were evaluated according to the statistical criteria such as R^2, RMSE and SSE. The Weibull model was selected as a suitable model to represent the thin layer drying behavior of garlic slices.

The coefficients of the accepted model and the final MR equation of thin layer drying of garlic slices were as follows (Rasouli *et al*., 2011):

$$k_1 = 5.994251 \times L^{-0.164} \exp\left(\frac{-516.322}{T_{abs}}\right)$$

$$\overline{R}^2 = 0.8128 \qquad (10)$$

$$k_2 = 6.02554 \times 10^{-6} \times L^{1.065} \exp\left(\frac{3429.964}{T_{abs}}\right)$$

$$\overline{R}^2 = 0.9721 \qquad (11)$$

$$MR = f(T, L, t) = \exp\left(-\left(\frac{t}{k_2}\right)^{k_1}\right) \qquad (12)$$

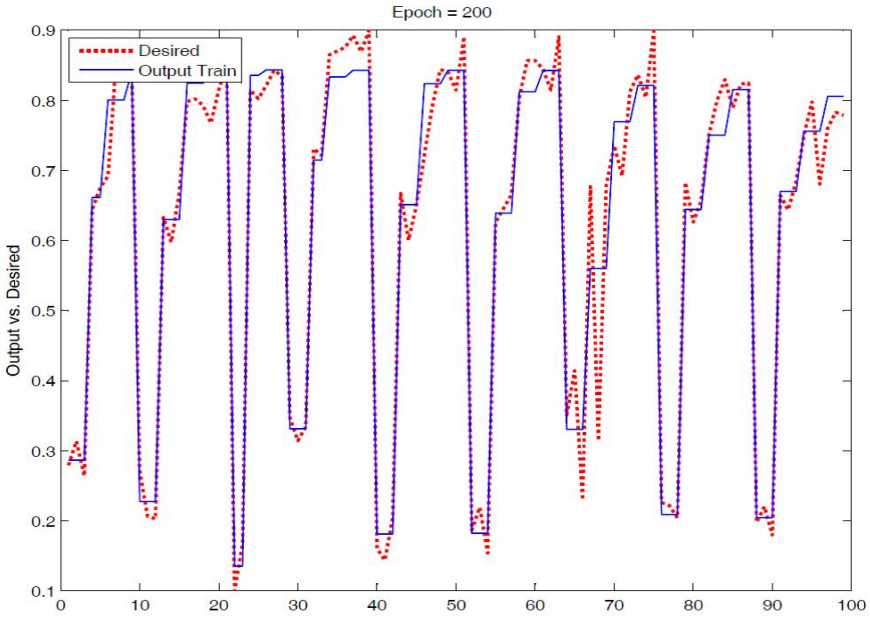

Fig. 3. Predicted Values of MR using ANNs versus experimental values

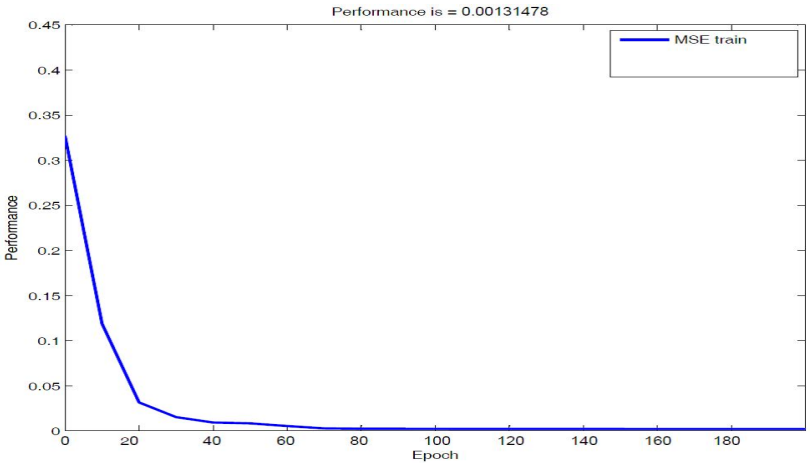

Fig. 4. Mean square error of training patterns for the best ANN

Table 2. Training algorithm for different neurons and hidden layers at the uniform threshold function for layers

Training Algorithm	Threshold Function	No. of Layers and Neurons	MSE	R^2	MRE	MAE
LM	TANSIG	3-3-2-1	0.00174	0.9912	10.76	0.054
		3-4-2-1	0.00127	0.9898	13.12	0.059
		3-10-5-1	0.00145	0.9901	11.18	0.044
		3-15-5-1	0.00227	0.9912	11.37	0.077
		3-20-5-1	0.00169	0.9854	13.87	0.073
		3-25-5-1	**0.00131**	**0.9923**	**9.67**	**0.041**
	LOGSIG	3-3-2-1	0.00123	0.9863	14.33	0.065
		3-4-2-1	0.00135	0.9899	12.57	0.064
		3-10-5-1	0.00314	0.9889	17.89	0.065
		3-15-5-1	0.00237	0.9866	16.56	0.140
		3-20-5-1	0.00278	0.9854	14.48	0.097
		3-25-5-1	0.00199	0.9911	10.25	0.076
CGF	TANSIG	3-3-2-1	0.00346	0.9822	18.74	0.023
		3-4-2-1	0.00447	0.9876	15.55	0.035
		3-10-5-1	0.00463	0.9791	16.79	0.040
		3-15-5-1	0.00681	0.9889	17.72	0.034
		3-20-5-1	0.00572	0.9831	21.34	0.165
		3-25-5-1	0.00519	0.9890	14.22	0.118
	LOGSIG	**3-3-2-1**	**0.00399**	**0.9901**	**12.27**	**0.087**
		3-4-2-1	0.00456	0.9827	16.55	0.061
		3-10-5-1	0.00423	0.9826	22.78	0.067
		3-15-5-1	0.00884	0.9766	15.67	0.091
		3-20-5-1	0.00727	0.9731	13.39	0.096
		3-25-5-1	0.00663	0.9890	17.92	0.074
OSS	TANSIG	3-3-2-1	0.00403	0.9913	12.34	0.063
		3-4-2-1	0.00289	0.9897	11.89	0.094
		3-10-5-1	0.00321	0.9799	13.67	0.083
		3-15-5-1	0.00462	0.9899	13.78	0.087
		3-20-5-1	0.00284	0.9905	11.91	0.077
		3-25-5-1	**0.00213**	**0.9919**	**11.34**	**0.059**
	LOGSIG	3-3-2-1	0.00236	0.9905	13.88	0.067
		3-4-2-1	0.00147	0.9908	13.11	0.017
		3-10-5-1	0.00755	0.9867	12.33	0.079
		3-15-5-1	0.00537	0.9897	16.69	0.089
		3-20-5-1	0.00574	0.9888	14.22	0.125
		3-25-5-1	0.00262	0.9877	11.37	0.083

Detailed information about this model can be found in (Rasouli *et al*., 2011). They have used this model to predict the drying characteristics of garlic. The ANN results

exhibit a good agreement with experimental results rather than mathematical model ones for garlic. These findings demonstrate that artificial neural networks produce better prediction and more useful results.

Conclusions

In this study, the drying behavior of the garlic slices as a thin layer was investigated experimentally. It was observed that the ANN model can be used to predict the drying characteristics of garlic undergoing different thin-layer drying conditions.

The best ANN for data training was FFBP with LM algorithm and TANSIG threshold function for layers, 25 neurons for the first hidden layer and 5 for the second one. With this optimized network, R^2 and mean relative error were 0.9923 and 9.67 %, respectively. The optimal models can predict the moisture content with high values of R^2.

The MC (or MR) of garlic could be predicted by ANN method, with less mean relative error (MRE) and more determination coefficient compared to the mathematical models (Weibull model). The methodology in this paper could be applied for other products as well. In addition, the developed ANN models are useful tool for estimating the on-line states and for controlling the drying process in industrial operations.

References

Abbasi Souraki, B., & Mowla, D. (2008). Experimental and theoretical investigation of drying behaviour of garlic in an inert medium fluidized bed assisted by microwave. *Journal of Food Engineering, 88*(4), 438-449. doi:10.1016/j.jfoodeng.2007.12.034

AOAC. (1990). *Official method of analysis of the Association of Official Analytical Chemists. NO. 934. 06, Arlington*: Virginia, USA.

Brewester, J. (1997). *Onions and Garlic. In: H.C. Wine(eds). The physiology of vegetable crops*: CAB International, Cambridge. UK.

Chegini, G. R., Khazaei, J., Ghobadian, B., & Goudarzi, A. M. (2008). Prediction of process and product parameters in an orange juice spray dryer using artificial neural networks. *Journal of Food Engineering, 84*(4), 534-543. doi:10.1016/j.jfoodeng.2007.06.007

Demuth, H., & Beale, M. (2003). *Neural Network Toolbox for Matlab-Users Guide Version 4.1. Natrick.* New York, UAS: The Mathworks Press.

Erenturk, S., & Erenturk, K. (2007). Comparison of genetic algorithm and neural network approaches for the drying process of carrot. *Journal of Food Engineering, 78*(3), 905-912. doi:10.1016/j.jfoodeng.2005.11.031

Ertekin, C., & Yaldiz, O. (2004). Drying of eggplant and selection of a suitable thin layer drying model. *Journal of Food Engineering, 63*, 349-359.

Kerdpiboon, S., Kerr, W. L., & Devahastin, S. (2006). Neural network prediction of physical property changes of dried carrot as a function of fractal dimension and moisture content. *Food Research International, 39*(10), 1110-1118. doi:10.1016/j.foodres.2006.07.019

Khazaei, J., & Daneshmandi, S. (2007). Modeling of thin-layer drying kinetics of sesame seeds: mathematical and neural networks modeling. *Int. Agrophysics, 21*, 335-348.

Madamba, P. S., Driscoll, R. H., & Buckle, K. A. (1994). Shrinkage, density and porosity of garlic during drying. *J Food Eng, 23*(3), 309-319.

Midilli, A., Kucuk, H., & Yapar, Z. (2002). A new model for single–layer drying. *Dry Technol, 20*(7), 1503-1513.

Mittal, G., & Zhang, J. (2000). Prediction of temperature and moisture content of frankfurters during thermal processing using neural network. *Meat Sci, 55*(1), 13-24.

Movagharnejad, K., & Nikzad, M. (2007). Modeling of tomato drying using artificial neural network. *Computers and Electronics in Agriculture, 59*(1-2), 78-85. doi:10.1016/j.compag.2007.05.003

Nazghelichi, T., Kianmehr, M. H., & Aghbashlo, M. (2010). Prediction of carrot cubes drying kinetics during fluidized bed drying by artificial neural network. *Journal of Food Science and Technology, 48*(5), 542-550. doi:10.1007/s13197-010-0166-2

Poonnoy, P., Tansakul, A., & Chinnan, M. (2007). Artificial neural network modeling for temperature and moisture content prediction in tomato slices undergoing microwave-vacuum drying. *Journal of food science, 72*(1), E042-047. doi:10.1111/j.1750-3841.2006.00220.x

Rasouli, M., Seiiedlou, S., Ghasemzadeh, H. R., & Nalbandi, H. (2011). Convective drying of garlic (Allium sativum L.): Part I: Drying kinetics, mathematical modeling and change in color. *Australian Journal of Crop Science, 5*(13), 1707-1714.

Satish, S., & Pydi Setty, Y. (2005). Modeling of a continuous fluidized bed dryer using artificial neural networks. *International Communications in Heat and Mass Transfer, 32*(3-4), 539-547. doi:10.1016/j.icheatmasstransfer.2004.06.005

Sharma, G. P., & Prasad, S. (2006). Optimization of process parameters for microwave drying of garlic cloves. *Journal of Food Engineering, 75*(4), 441-446. doi:10.1016/j.jfoodeng.2005.04.029

Sharma, G. P., Prasad, S., & Chahar, V. K. (2009). Moisture transport in garlic cloves undergoing microwave-convective drying. *Food and Bioproducts Processing, 87*(1), 11-16. doi:10.1016/j.fbp.2008.05.001

Topuz, A. (2010). Predicting moisture content of agricultural products using artificial neural networks. *Advances in Engineering Software, 41*(3), 464-470. doi:10.1016/j.advengsoft.2009.10.003

Trelea, I. C., Courtois, F., & Trystram, G. (1997). Dynamic models for drying and wet-milling quality degradation of corn using neural networks. *Drying Technol, 15*, 1095-1102.

Zhang, Q., Yang, S., Mittal, G., & Yi, S. (2002). Ae-automation and emerging technologies:prediction of performance indices and optimal parameters of rough rice drying using neural networks. *Biosystems Engineering, 83*(3), 281.

نشریه پژوهشهای علوم و صنایع غذایی ایران
جلد 14، شماره 3، مرداد - شهریور 1397، ص. 62-53

Iranian Food Science and Technology Research Journal
Vol. 14, No. 3, Aug. Sep. 2018, p. 53-62

خشک شدن همرفتی سیر (*Allium sativum L.*): رویکرد شبکه های عصبی مصنوعی برای مدل‌سازی فرآیند خشک کردن

مجید رسولی*[1]

تاریخ دریافت: 1396/04/29
تاریخ پذیرش: 1397/01/20

چکیده

در این مطالعه، شبکه عصبی مصنوعی برای مدل‌سازی و پیش‌بینی میزان رطوبت سیر در طی خشک کردن سیر استفاده شد. برای این منظور شبکه عصبی مصنوعی پرسپترون چند لایه تحت عنوان پس انتشار پیشرو به‌کار گرفته شد. پارامترهای مهم از جمله دمای هوای خشک کردن (50، 60 و 70 درجه سانتی‌گراد)، ضخامت ورقه‌ها (2، 3 و 4 میلی‌متر) و زمان خشک کردن به‌عنوان ورودی و محتوای رطوبت به‌عنوان خروجی شبکه در نظر گرفته شد. داده‌های آزمایشگاهی به‌دست آمده از فرآیند خشک کردن لایه نازک سیر برای آموزش و تست شبکه استفاده شد. توپولوژی بهینه 3-25-5-1 با الگوریتم LM و تابع آستانه TANSIG برای لایه‌ها بود. با این شبکه بهینه، مقدار R^2 و خطای نسبی به‌ترتیب 0/9923 و 9/67 درصد بود. مقدار MC برای سیر را می‌توان با استفاده از شبکه عصبی، با میانگین خطای متوسط کمتر و ضریب تبیین بیشتر نسبت به مدل ریاضی ویبل پیش‌بینی کرد.

واژه‌های کلیدی: شبکه‌های عصبی مصنوعی، انتشار اولیه، خشک کردن همرفتی، سیر، محتوای رطوبت.

1- استادیار، گروه مهندسی بیوسیستم، دانشگاه بوعلی سینا.
(*- نویسنده مسئول: Email: m.rasouli@basu.ac.ir)

Iranian Food Science and Technology Research Journal
Vol. 14, No. 3, Aug. Sep. 2018, p. 63-73

نشریه پژوهشهای علوم و صنایع غذایی ایران
جلد 14، شماره 3، مرداد - شهریور 1397، ص. 73-63

Quality and sensory profiling of gluten free bread as a function of quinoa, corn and xanthan content: Statistical analysis and modeling study

Simin Ghasemizadeh[1], Behzad Nasehi[2*], Mohammad Noshad[1]

Received: 2017.06.03
Accepted: 2017.12.27

Abstract

In the study, the effect of compositional parameters (Xanthan, Corn flour and quinoa flour content) on sensory characteristics and image features of gluten free bread were evaluated. Results showed, addition of quinoa and corn flour significantly decreased L^* value and increased a^* value of crust and crumb of gluten free bread. Also, increased percentage of corn flour has led to decreased amount of FD_{L^*} that indicates the area appears less nonhomogeneous on surface of gluten- free bread. The results also showed that using complete flour of quinoa causes softness in bread due to the presence of bran and networking, therefore, resulting in increased contrast, homogeneity and entropy, and decreased energy and correlation of produced breads. The results of sensory analysis showed that all samples containing quinoa flour have higher overall acceptance score than that of the control treatment. Correlation analysis showed a good linear relationship between image features and overall acceptance of gluten- free bread. Results showed that the optimized Adaptive Neuro-Fuzzy Inference System (ANFIS model) provide best accurate prediction method for overall acceptance of gluten-free bread (R^2= 0.994 and MSE= 0.0015) and it could be a useful tool in the food industry to design and develop novel products.

Key words: Image processing; Sensory analyzer; Gluten free bread; ANFIS model.

Introduction

Patients with coeliac disease should avoid regular consumption of grain-based products such as wheat, barley because they are intolerance to the gliadin fraction, so taking food products made with wheat flour for these patients is not recommended. As a result, gluten-free products were produced for these patients. Low quality, poor mouth feel and flavor are the most challenges in producing these products. This is due to removal of gluten from the flour. The important rheological characteristics of dough, such as elasticity, extensibility, resistance to stretch, mixing tolerance, and gas holding ability depend on the quality of gluten matrix (Lazaridou *et al.*, 2007; Stikic *et al.*, 2012; Yazar *et al.*, 2017).

Quinoa flour is one of the compounds used as a substitute for wheat flour in gluten free productions. Quinoa (*Chenopodium quinoa* Willd.), is distinguished as being a cereal with high-quality protein and absence of gluten and it has high levels of essential fatty acids, with good oxidative stability. Therefore, partially replaced wheat flour with quinoa in gluten- free products, increases its nutritional value in terms of dietary fibre, minerals, proteins of high biological value and healthy fats (Alvarez-Jubete *et al.*, 2009; Stikic *et al.*, 2012; Świeca *et al.*, 2014).

Xanthan, guar gum, galactomannans, are the most common hydrocolloids which are being used in gluten-free formulations for a variety of purposes including texture improvement and water retention. In this study, the xanthan gum (XG) was selected because it forms a high-viscosity pseudo plastic semisolid. XG produces a viscose solution with shear thinning flow behavior when dissolved in cold water. The shear thinning property of XG is important during dough preparation, i.e. kneading and rolling(Matuda *et al.*, 2008; Naji-Tabasi and

1. Department of Food Science & Technology, Faculty of Animal Science and Food Technology, Khuzestan Agricultural Sciences and Natural Resources University, Mollasani, Iran.
2. Department of Agricultural Engineering and Technology, Payame Noor University (PNU), Iran.
*-Corresponding author Email: Nasehi.b@pnum.ac.ir

Mohebbi, 2015).

A multiple regression analysis such as the response surface method has been applied for modeling and predicting the different procedures. An adaptive neuro-fuzzy inference system or adaptive network-based fuzzy inference system (ANFIS) is based on Takagi–Sugeno fuzzy inference system. The technique was developed in the early 1990s. Since it integrates both neural networks and fuzzy logic principles, it has potential to capture the benefits of both in a single framework. Once the ANFIS is trained using experimental data, it can be used in a predictive mode to calculate the dependent variable(s) for any values of input variables. ANFIS techniques appear to be very applicable tools to overcoming some of the difficulties in sensory evaluation(Al-Mahasneh *et al.*, 2016).

Overall acceptance of a new product considers as one of the important parameters is a food products' quality. This can be assessed by trained sensory panels or by consumer tests. But, organizing a sensory panel needstoo much time and is labour consuming. To solve this problem, computer vision as a novel technology used for extracting quantitative information of morphology, structure and microstructure from digital images in order to provide objective, rapid, non-contact, and non-destructive quality evaluation(Katina *et al.*, 2006; Soukoulis *et al.*, 2010).

The aim of this study was to develop new techniques for the investigation and modeling the effect of quinoa and XG on color and macrostructure (porosity, fractal dimension and crumb texture) and overal acceptance of gluten-free bread and for the first time, as well as the efficiency of ANFIS simulation for prediction of overall acceptance of this product.

Material and methods

Bread ingredient

Rice flour (powderineh North group, Iran), Corn flour (Tarkhineh group, Iran), Xanthan gum (Rhodia Food, France), fast active dry yeast (Razavi group, Iran), salt, sugar and sunflower oil (Oila group, Iran) were the materials used in the study. Also, quinoa flour mill grains variety of *Santamaria* were cultivated and obtained at Ramin university of Agriculture and Natural Resources field.

Preparation of breads

The materials used in formulation for gluten- free bread consist of rice flour, corn flour (0-30 % base on flour), quinoa flour (0-30 % base on flour), Xanthan gum (0-1.5 % base on flour), fast active dry yeast (2%), salt (2%), sugar (2%), sunflower oil (3%) and the amount of water used in all sample breads was kept the same (80%).

The method of Foste *et.al* (2014) was used to produce of gluten– free bread. All ingredients were mixed at 100 rpm for 2 min and kneaded at 200 rpm for 2 min (MHM-X3P, Mayson, Japan). After weighing 250 g into baking tins (resulting in 4 tins per recipe), samples were proofed at 30°C and 80% relative humidity for 30 min and baked at 220°C for 35 min with initial 0.5 L steam in a deck oven (Karl Walker, Germany) *(Föste et al.*, 2014).

2.3. Sensory evaluation

Gluten- free breads were evaluated for their organoleptic characteristics (color, flavor, taste, texture, and overall acceptability) by performing a five-point hedonic test using trained panelists. The panelists were asked to evaluate the samples and score them between 1 (most disliked) to 5 (most liked) (Stone, *et al.*, 2012).

2.4. Image processing

A computer vision system consisted four fluorescent lights (8W; 60 cm in length) with a color index close to 95% was employed. The illuminating lights were placed (45 cm above the sample and at the angle of 45° with sample) in a wooden box and the interior walls of the wooden box were painted black to give a uniform light intensity over the bread. A color digital camera (Canon PowerShot SX60 HS, Japan) with lens focal length of 35 mm for color analysis and 45 mm for investigation of pore properties was located vertically. The iris was operated in manual mode, with the lens

aperture of 5.6, ISO 100 and shutter speed of 1/100 s to achieve high uniformity and repeatability.

The image analysis was carried out using MATLAB (version 2011 b). The features of crust and crumb color, porosity, fractal dimension of crust color and crumb texture were investigated(Mogol and Gökmen, 2014; Naji-Tabasi and Mohebbi, 2015).

Fractal texture Fourier image

A methodology similar to the one developed by Noshad *et al* (2015) was followed: first, color image was transformed form RGB space color to L*a* b* space color. Second, pixel coordinates (x,y) were plotted against their L* levels in the z-axis. Surface intensity obtained from L* channel, was called "SI_{L^*}", corresponding to L* channel. Third, SIL* was quantified using the fractal theory. The Fourier fractal method was used to compute the fractal dimension of a 2-D image came from the L* channel. A fractal dimension (FDL*) was determined from the Fourier power spectrum of image data (Noshad *et al*., 2015).

Image texture analysis

The Grey-level co-occurrence matrix (GLCM) was used to obtain the statistical texture features. A GLCM is a matrix where the number of rows and columns is equal to the number of gray levels, G, in the image. The GLCM's are very sensitive to the size of the texture samples on which they are estimated. Thus, the number of gray levels is often reduced. The center of each slice was cropped in a square of 1400 * 1400 pixels and converted to grey-level image (8 bits). During our study, the features were investigated in four directions (0°, 90 °, 180° and 270°) and a distance of 1 pixel. The GLCM analysis was managed using MATLAB (version 2011 b). The average of five textural features: angular second moment, contrast, correlation, inverse difference moment and entropy were studied (Jackman and Sun, 2013; Naji-Tabasi and Mohebbi, 2015).

Adaptive Neuro-Fuzzy Inference System (ANFIS) Architecture

Hybrid neuro-fuzzy system (ANFIS) combines a Neural Networks (NN) and a fuzzy system together. ANFIS has been proved to have significant results in modeling nonlinear functions. In ANFIS, the membership functions (MF) are extracted from a data set that describes the system behavior. The ANFIS learns features in the data set and adjusts the system parameters according to given error criterion (Mohebbi, *et al.,* 2013). In a fused architecture, NN learning algorithms are used to determine the parameters of fuzzy inference system. Among many Fuzzy Inference System (FIS) models, the Sugeno fuzzy model is the most widely used for its high interpretability and computational efficiency, and built-in optimal and adaptive techniques (Al-Mahasneh, *et al.*, 2016;Mohebbi,*et al*., 2013).

For a first-order Sugeno fuzzy model, a common rule set with two fuzzy if-then rules can be expressed as:

Rule 1: If x is A_1 and y is B_1, then $Z_1 = p_1x+q_1y+r_1$

Rule 2: If x is A_2 and y is B_2, then $Z_2= p_2x + q_2y+r_2$

Where Ai, $B_i(i=1,2)$ A_i and B_i are fuzzy sets in the antecedent, and p_i, q_i,r_i (i=1,2) are the design parameters that are determined during the training process.

As in Fig.1, the ANFIS consists of five layers:

Layer 1, every node i in this layer is an adaptive node with a node function:

$O_i^1 = \mu A_i (x)$, i=1,2

$O_i^1 = \mu B_i (y)$, i=3,4

Where x,y are the input of node i, and $\mu A_i(x)$ and $\mu B_i(y)$ can adopt any fuzzy membership function (MF). In this paper, generalized membership function was used.

Layer 2, every node in the second layer represents the ring strength of a rule by multiplying the incoming signals and forwarding the product as:

$O_i^2 = w_i = \mu A_i(x) \mu B_i(y)$, i=1,2

Layer 3, the i^{th} node in this layer calculates the ratio of the i^{th} rule's ring strength to the

sum of all rules' ring strenghs:

$O_i^3=\omega_i=\frac{w_i}{w_1+w_2}$, i=1,2

Where ω i is referred to as the normalized ring strengths.

Layer 4, the node function in this layer is represented by:

$O_i^4=\omega_i z_i=\omega_i(p_ix+q_iy+r_i)$, i=1,2

Where ω_i is the output of layer 3, and $\{p_i, q_i, r_i\}$7 are the parameter set. Parameters in this layer are referred to as the consequent parameters.

Layer 5, the single node in this layer computs the overall output at the summation of all incoming signals.

$O_1^5=\sum_{i-1}^{2}\omega_i z_i=\frac{w_1z_1+w_2z_2}{w_1+w_2}$

It is seen from the ANFIS architecture that when the values of the premise parameters are fixed, the overall output can be expressed as a linear combination of the consequent parameters:

$Z=(\omega_1x)p_1+(\omega_1y)q_1+(\omega_1)r_1+(\omega_2x)p_2+(\omega_2y)q$

The Matlab (2011 b) software was used to obtain the results, and to build a fuzzy model for overall acceptance of gluten- free bread.

Statistical analysis

Response surface methodology (Box-Behnken) was applied for the determination of the main effects of the investigated independent factors (quinoa flour, corn flour and xanthan gum) and their interactions on the image features and overall acceptance.

Also, ANFIS for modeling , the relationship between image features and overall acceptance using the correlation coefficient (r), which is a measure of the linear relationship between two variables, were first evaluated. All statistical treatments were carried out using Minitab 16 (statistical software, USA).

Results

Crust and crumb color

The results of variance analysis of the bread crust color were shown in table1. The results of variance analysis showed that second-level models fitted to responses of crust color were significant ($p<0.05$) (table 1). Also, the non-fitness indexes of significant models for responses of crust color were significant ($p<0.05$). Statistical analysis showed that Quinoa and corn flour had a considerable effect on the value of crust color. As shown in figure 2, adding Quinoa and corn flour significantly decreased L^* value ($p<0.05$). The increased L^* value (brightness) enhanced the non-enzyme browning of Millard reaction due to higher level of lysine amino acid in Quinoa flour(Alencar *et al*., 2015).

Table 1. ANOVA evaluation of linear, quadratic, and interaction terms for each response variable and coefficient of prediction models

source	Energy	Contrast	Entropy	Correlation	homogeneity	L*crust	a*	L* crumb	FD $_{L^*}$	Porosity	Overall acceptance
Model	0.54	0.17	5.66	0.64	0.92	67.02	-6.16	65.9	0.64	0.096	**6.33**
$_1\beta$	0.01^{ns}	-0.05^{ns}	-0.48^{ns}	0.09^{ns}	0.05^{ns}	-0.09^{*}	-0.21*	-0.19*	0.6^{ns}	0.18*	**0.064^{ns}**
$_2\beta$	-0.17*	0.08^{ns}	0.075*	-0.013*	0.03^{*}	-0.25*	-0.03*	-0.5*	0.08*-	0.02^{ns}	**-1.94***
3β	-0.02^{ns}	0.011^{ns}	0.17*	-0.03*	-0.025^{ns}	-2.13*	0.71*	-8*	0.01^{ns}	3.8*	**0.74***
$_2\beta_1\beta$	0.07^{ns}	-0.012^{ns}	0.019^{ns}	0.04^{ns}	0.06^{ns}	0.01*	0.001*	-0.04^{ns}	-0.09^{ns}	0.01^{ns}	**0.36^{ns}**
$_3\beta_1\beta$	-0.08^{ns}	0.02^{ns}	0.036^{ns}	0.06^{ns}	-0.034^{ns}	0.09*	0.01*	0.01^{ns}	0.13^{ns}	0.06*	**-.38^{ns}**
$_3\beta_2\beta$	-0.03^{ns}	0.03^{ns}	0.014^{ns}	-0.07^{ns}	0.065^{ns}	2.85^{ns}	0.76^{ns}	5.44*	0.01^{ns}	0.04*	**0.49*-**
$_1^2\beta$	-0.01^{ns}	-0.04^{ns}	0.057^{ns}	-0.06^{ns}	0.01^{ns}	0.01*	0.01^{ns}	0.01^{ns}	-0.4^{ns}	0.03*	**0.16^{ns}**
$_2^2\beta$	0.04^{ns}	0.06^{ns}	-0.034^{ns}	-0.01^{ns}	-0.04^{ns}	0.2^{ns}	-0.01^{ns}	0.01^{ns}	-0.08^{ns}	1.74^{ns}	**-0.078^{ns}**
$_3^2\beta$	0.04^{ns}	-0.04_{ns}	-0.07^{ns}	-0.037^{ns}	-0.007^{ns}	0.06^{ns}	-0.06^{ns}	0.18*	0.28^{ns}	0.82*	**0.28^{ns}**
Model (p-value)	0.006	0.005	0.007	0.013	0.028	0.001	0.001	0.001	0.042	0.001	**0.002**
Lack of fit (p-value)	0.489	0.09	0.18	0.76	0.27	0.842	0.59	0.482	0.14	0.54	**0.406**
R^2	0.9	0.84	0.82	0.84	0.86	0.94	0.94	0.95	0.81	0.96	**0.925**
Adj-R^2	0.81	0.79	0.77	0.76	0.75	0.9	0.88	0.89	0.74	0.91	**0.857**

^{ns} is not significant at α=0.05; * is significant at α=0.05; lack of fit is not significant at p>0.05

Bran or crust of quinoa also causes darkness in bread crumb. Considering the fact that complete flour of quinoa is darker that wheat flour and the color of bread crumb depends on ingredients rather than browning reactions, adding quinoa flour into free-gluten bread formulation would decrease the brightness of bread crumb (L^* value). Moreover, the results showed that added xanthan hydrocolloid leads to increase lightness and yellowing index, and decrease redness (Naji-Tabasi and Mohebbi, 2015).

Fractal dimension

To represent how distributing spatial L* values on the area analyzed, FD_{L*} value can be used and it does not have physical significance here. Decreasing FD_{L*} value showing decreasing irregularity of SI_{L*} in other word distribution of L* values on the area appears less nonhomogeneous during the browning kinetics (Noshad et al., 2015). The results of variance analysis of the data from FD_{L*} showed that the only linear effect of corn flour was significant ($p<0.05$) (table 1). Figure 1 shows that increased percentage of corn flour has led to decreased amount of FD_{L*}. The decrease in the amount of FD_{L*} indicates the area appears less nonhomogeneous on surface of gluten- free bread.

Porosity of bread texture

The results from figure 2 show that Quinoa four is more effective in increasing the porosity of bread texture than xanthan gum thus the linear effect of Quinoa flour in porosity factorial was significant ($p<0.05$) and positive and linear effect of corn flour was significant ($p<0.05$) and negative and xanthan gum was not significant. Furthermore, the second-level effect of Quinoa was insignificant and the second-level effects of corn flour and xanthan gum were significant ($p<0.05$). The results showed that linear effect of Quinoa flour and xanthan gum on cells circularity was significant ($p<0.05$) and the second-level effects of Quinoa flour and xanthan were significant ($p<0.05$) and the second-level effect of corn flour was significant ($p<0.05$). The interaction of Quinoa and xanthan and also the interaction of corn and xanthan were significant ($p<0.05$) (table 1). Adding xanthan to bread causes reduction in cell area and increased number of pores compared to control. The parameter of pore number to cell area was considered as porosity. Therefore, adding xanthan increased the porosity while increased quinoa flour caused reduction in cell density and cell number. Additionally, increased xanthan gum and quinoa flour resulted in increasing the volume. The increased volume compared with control is due to the increased viscosity by quinoa flour, improved water gas distribution in the paste trapping more produced bubbles in bread resulting to increased porosity *(Elgeti et al*., 2014).

Crumb texture: evaluation by gray level co-occurrence matrix (GLCM)

Resulted shows that adding Quinoa flour to free-gluten bread formulation leads to increased homogeneity in all treatments compared to control. Also, energy and correlation of all treatments showed reduction in comparison to control. The decreased amount of contrast indicates the softer texture of product while the increased amount of energy, correlation and homogeneity, results in increased softness of texture (Karimi *et al.*, 2012).

The results showed that increased percentage of Quinoa has led to decreased amount of energy and correlation while homogeneity and entropy were increased. The increase in the amount of contrast and homogeneity indicates the softer texture of product on one hand, and decreased energy and correlation, on the other hand, resulted in increased texture softness. It seems that using complete flour of Quinoa causes softness in bread due to the presence of bran and networking, therefore, resulting in increased contrast, homogeneity and entropy, and decreased energy and correlation of produced breads.

Overall acceptances

The results of variance analysis of the data

from overall acceptances showed that the linear effect of corn flour and xanthan gum were significant ($p<0.05$). The second effect of xanthan gum was also positive and significant ($p<0.05$). Moreover, the interaction of them was not significant (Table 1). Figure 3 shows the response-surface chart of overall acceptance.

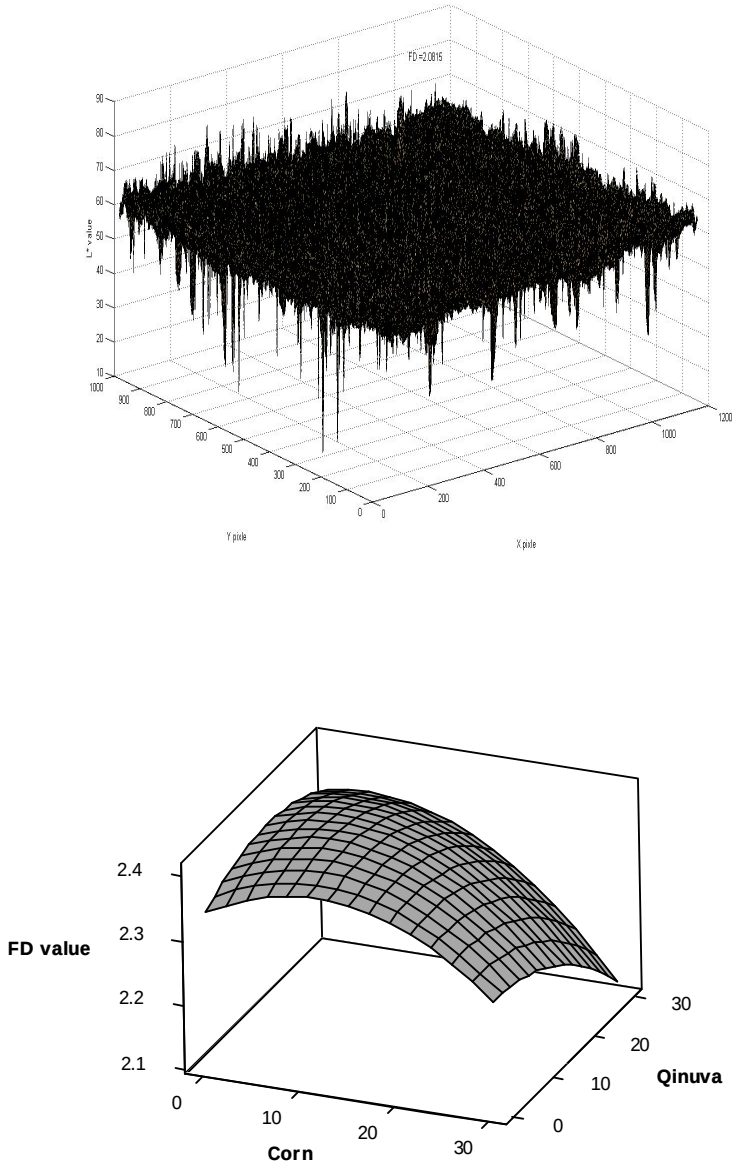

Fig. 1. Surface intensity and Response surface plots for FD L^* value

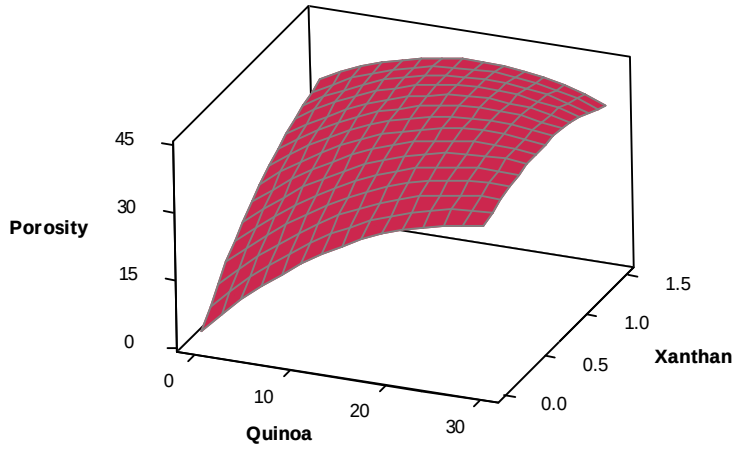

Fig. 2. Response surface (3D) plot for porosity

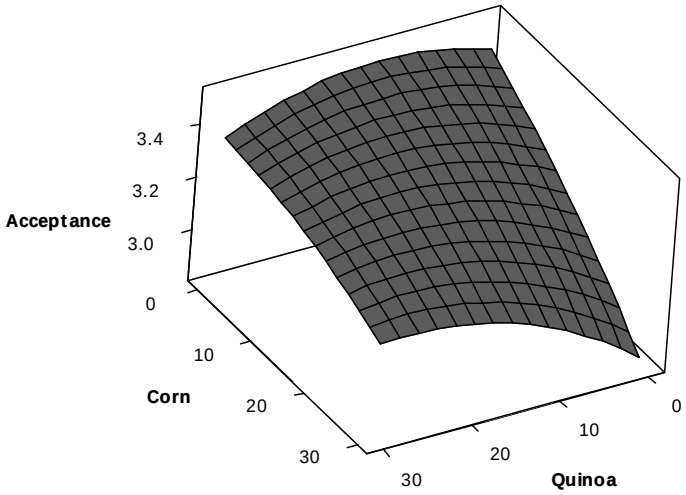

Fig. 3. Response surface (3D) for overall acceptance

The results of sensory analysis show that in most of the treatments, sense response received from panelists had increase in comparison to free-quinoa samples. Finally,

the score of overall acceptances for all treatments containing Quinoa flour were higher than control treatment sample indicating higher acceptance of tested samples among consumers and panelists. Generally, the breads with formulations containing quinoa flour were different in terms of smell and taste. The bread crust color was yellow to bright red and texture contained small pores and bran particles of quinoa and in all breads containing quinoa flour, the sweet smell and taste were enjoyable to consumers. Furthermore, adding xanthan gum resulted in better texture and more sensory analysis for consumers(Naji-Tabasi and Mohebbi, 2015).

Correlation analysis

In evaluating the correlation analysis, negative coefficient indicates an inverse relationship, and a positive coefficient indicates a direct relationship between variables. Correlation analysis showed a good linear relationship between image features and overall acceptance of gluten- free bread. Thus, according to the results of correlation analysis (table2), machine vision and image processing techniques can be a useful tool in predicting and evaluating overall acceptance of gluten-free bread.

Table 2. Correlation coefficients between overall acceptance and image features

	FD $_{L^*}$	L* crumb	a*	L*crust	homogeneity	Correlation	Entropy	Contrast	Energy	porosity
Overall acceptance	-0.14*	0.79*	-0.56*	0.73*	0.69*	0.1*	0.12*	-0.68*	0.73*	0.71*

* is significant at α=0.05

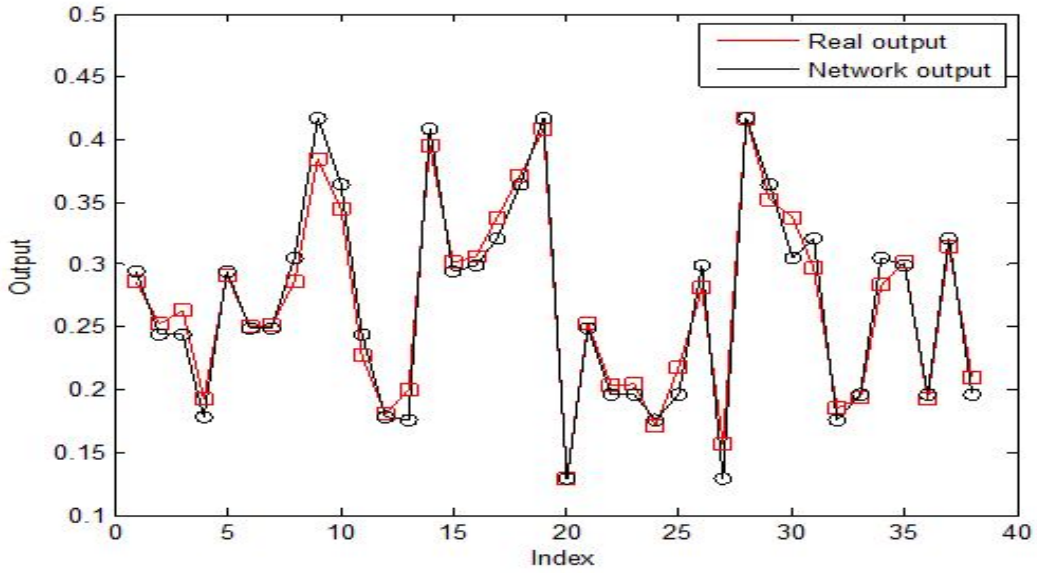

Fig. 4. The actual values of the overall acceptance versus predicted values by ANSIF (R^2=0.994)

ANFIS model

An experimental data was used for building a fuzzy model and training the system to predict the overall acceptance of gluten-free bread. A comparison between the actual and ANFIS predicted overall acceptance for testing data is shown in figure 4, which shows that the system is well-trained to model the actual chemical outputs. It must be mentioned randomizing the data set done before training the ANFIS prediction system and Gaussian curve built-in membership function (gaussmf) was chosen. The experimental values of overall acceptance versus ANFIS predictions

for each test data sets were plotted for estimation the performance of developed ANFIS model. Resulted showed that the optimized ANFIS model provide best accurate prediction method for overall acceptance of gluten-free bread (R^2= 0.994 and MSE= 0.0015). Therefore, this method can be applied to model the operating conditions.

Conclusion

According to this study, adding quinoa flour decreased L^* value, amount of energy and correlation and increased a* value, homogeneity, entropy and the score of overall acceptances. Also, addition of corn flour significantly decreased L^* value and amount of FD_{L^*} but increased a* value. The increase in the amount of contrast and homogeneity indicates the softer texture of product on one hand, and decreased energy and correlation, on the other hand, resulted in increased texture softness. Correlation analysis showed a good linear relationship between image features and overall acceptance of gluten- free bread. Results showed that the optimized ANFIS model provide best accurate prediction method for overall acceptance of gluten-free bread (R^2= 0.994 and MSE= 0.0015). Therefore, this method can be applied to model the operating conditions.

References

Al-Mahasneh, M., Aljarrah, M., Rababah, T., Alu'datt, M., 2016. Application of Hybrid Neural Fuzzy System (ANFIS) in Food Processing and Technology. *Food Engineering Reviews* 8, 351-366.

Alencar, N.M.M., Steel, C.J., Alvim, I.D., de Morais, E.C., Bolini, H.M.A., 2015. Addition of quinoa and amaranth flour in gluten-free breads: Temporal profile and instrumental analysis. *LWT-Food Science and Technology* 62, 1011-1018.

Alvarez-Jubete, L., Holse, M., Hansen, A., Arendt, E., Gallagher, E., 2009. Impact of Baking on Vitamin E Content of Pseudocereals Amaranth, Quinoa, and Buckwheat. *Cereal chemistry* 86, 511.

Elgeti, D., Nordlohne, S.D., Föste, M., Besl, M., Linden, M.H., Heinz, V., Jekle, M., Becker, T., 2014. Volume and texture improvement of gluten-free bread using quinoa white flour. *Journal of Cereal Scienc*e 59, 41-47.

Föste, M., Nordlohne, S.D., Elgeti, D., Linden, M.H., Heinz, V., Jekle, M., Becker, T., 2014. Impact of quinoa bran on gluten-free dough and bread characteristics. *European Food Research and Technology* 239, 767-775.

Jackman, P., Sun, D.-W., 2013. Recent advances in image processing using image texture features for food quality assessment. *Trends in Food Science & Technology* 29, 35-43.

Karimi, M., Fathi, M., Sheykholeslam, Z., Sahraiyan, B., Naghipoor, F., 2012. Effect of different processing parameters on quality factors and image texture features of bread. *J Bioproces Biotech* 2, 2-7.

Katina, K., Heiniö, R.-L., Autio, K., Poutanen, K., 2006. Optimization of sourdough process for improved sensory profile and texture of wheat bread. *LWT-Food Science and Technology* 39, 1189-1202.

Lazaridou, A., Duta, D., Papageorgiou, M., Belc, N., Biliaderis, C., 2007. Effects of hydrocolloids on dough rheology and bread quality parameters in gluten-free formulations. *Journal of Food Engineering* 79, 1033-1047.

Matuda, T.G., Chevallier, S., de Alcântara Pessôa Filho, P., LeBail, A., Tadini, C.C., 2008. Impact of guar and xanthan gums on proofing and calorimetric parameters of frozen bread dough. *Journal of Cereal Science* 48, 741-746.

Mogol, B.A., Gökmen, V., 2014. Computer vision-based analysis of foods: A non-destructive colour measurement tool to monitor quality and safety. *Journal of the Science of Food and Agriculture* 94, 1259-1263.

Mohebbi, M., Mehraban, M., Noshad, M., 2013. Adaptive Neuro Fuzzy Modeling of Moisture and Oil Content of Fried Mushroom. 1 st I*nternational e-Conference on novel Food Processing*; IECFP 2013.

Naji-Tabasi, S., Mohebbi, M., 2015. Evaluation of cress seed gum and xanthan gum effect on macrostructure properties of gluten-free bread by image processing. *Journal of Food Measurement and Characterization* 9, 110-119.

Noshad, M., Mohebbi, M., Ansarifar, E., 2015. Quantification of enzymatic browning kinetics of quince preserved by edible coating using the fractal texture Fourier image. *Journal of Food Measurement and Characterization* 9, 375-381.

Soukoulis, C., Lyroni, E., Tzia, C., 2010. Sensory profiling and hedonic judgement of probiotic ice cream as a function of hydrocolloids, yogurt and milk fat content. LWT-*Food Science and Technology* 43, 1351-1358.

Stone, H., R. Bleibaum, and H.A. Thomas, *Sensory evaluation practices*. 2012: Academic press. 40-90.

Stikic, R., Glamoclija, D., Demin, M., Vucelic-Radovic, B., Jovanovic, Z., Milojkovic-Opsenica, D., Jacobsen, S.-E., Milovanovic, M., 2012. Agronomical and nutritional evaluation of quinoa seeds (*Chenopodium quinoa Willd*.) as an ingredient in bread formulations. *Journal of Cereal Science* 55, 132-138.

Świeca, M., Sęczyk, Ł., Gawlik-Dziki, U., Dziki, D., 2014. Bread enriched with quinoa leaves–The influence of protein–phenolics interactions on the nutritional and antioxidant quality. *Food chemistry* 162, 54-62.

Yazar, G., Duvarci, O., Tavman, S., Kokini, J.L., 2017. Non-linear rheological behavior of gluten-free flour doughs and correlations of LAOS parameters with gluten-free bread properties. *Journal of Cereal Science* 74, 28-36.

نشریه پژوهشهای علوم و صنایع غذایی ایران
جلد 14، شماره 3، مرداد - شهریور 1397، ص. 73-63

Iranian Food Science and Technology Research Journal
Vol. 14, No. 3, Aug. Sep. 2018, p. 63-73

بررسی آماری و مدل‌سازی کیفیت و ویژگی‌های حسی نان بدون گلوتن به‌عنوان تابعی از مقادیر آرد کینوا، ذرت و گزانتان

سیمین قاسمی‌زاده[1]– بهزاد ناصحی[2*]– محمد نوشاد[1]

تاریخ دریافت: 1396/03/13
تاریخ پذیرش: 1396/10/06

چکیده

در این پژوهش اثر افزودن آرد کامل کینوا، ذرت و صمغ زانتان به فرمولاسیون نان بدون گلوتن بر ویژگی‌های حسی و کیفی مورد بررسی قرار گرفت. نتایج این پژوهش نشان داد که افزودن آرد کینوا و ذرت باعث افزایش معنی‌دار شاخص L^* و کاهش شاخص a^* پوسته و مغز نان شد. همچنین افزایش درصد آرد ذرت باعث کاهش شاخص FD_L^* در نمونه‌ها شد که این امر نشان‌دهنده کاهش ظاهر ناهمگن سطح نان است. یافته‌ها نشان داد با افزایش درصد کینوا، میزان انرژی و همبستگی کاهش یافته و همگنی و انتروپی و تباین افزایش می‌یابد. افزایش میزان تباین و همگنی نشان دهنده بافت نرم‌تر محصول بوده، از سوی دیگرکاهش انرژی، همبستگی نیز سبب افزایش نرمی در بافت می‌شود. به‌نظر می‌رسد استفاده از آرد کامل کینوا به دلیل وجود سبوس و ایجاد شبکه، سبب نرم‌تر شدن نان نسبت به نمونه شاهد و در نتیجه سبب افزایش تباین، همگنی و آنتروپی و کاهش انرژی و همبستگی نان‌های تولیدی گردید. نتایج داده‌های حسی نشان می‌دهد که امتیاز پذیرش کلی تمامی تیمارهای حاوی آرد کینوا نسبت به تیمار نمونه کنترل بیشتر بود که نشان‌دهنده بالا بودن مقبولیت نمونه‌های مورد آزمایش در بین مصرف‌کنندگان و ارزیاب‌ها بود. نتایج آنالیز همبستگی به‌خوبی نشان داد شاخص‌های بینایی، همبستگی بالایی ($p<0/05$) با ویژگی‌های حسی نان بدون گلوتن داشتند که بیان‌کننده توانایی تکنیک‌های پردازش تصویر در پیش بینی پذیرش مصرف کننده بود. مقادیر بالای ضریب همبستگی (0/994) و کم MSE (0/0015) گویای کارایی بالای سیستم استنتاج تطبیقی فازی- عصبی (ANFIS) در پیش‌بینی میزان پذیرش کلی نان‌های بدون گلوتن می باشد. که می‌تواند به‌عنوان یک ابزار دقیق برای طراحی و توسعه محصولات جدید در صنعت مواد غذایی استفاده شود.

واژه‌های کلیدی: پردازش تصویر، ارزیابی حسی، نان بدون گلوتن، سیستم استنتاج تطبیقی فازی- عصبی (ANFIS)

1- گروه علوم و مهندسی صنایع غذایی، دانشکده علوم دامی و صنایع غذایی، دانشگاه علوم کشاورزی و منابع طبیعی خوزستان.
2- دانشیار، گروه مهندسی و فناوری کشاورزی، دانشگاه پیام نور، ایران
(*- نویسنده مسئول: Email: mo. Nasehi.b@pnum.ac.ir)

Contents

Iranian Food Science and Technology Research Journal

Vol. 14 No. 3 2018

Published by: Ferdowsi University of Mashhad

Printed by: Ferdowsi University of Mashhad Press, Iran.

Address: The Iranian Food Science & Technology Research Journal, Scientific Publication Office, Food Science and Technology Department, Agriculture Faculty, Ferdowsi University of Mashhad, Iran.

P.O.BOX: 91775- 1163

Phone: (98)511-8795618-20(321)

Fax: (98)511-8787430

E-Mail: ifstrj@um.ac.ir

Web Site: http://jm.um.ac.ir/index.php/food_tech/index

This journal is indexed in ISC, SID, and MAGIRAN.

Ferdowsi University of Mashhad

Iranian Food Science and Technology Research Journal

Iranian food science and technology Association

Vol.14 No.3

2018

ISSN:1735-4161

نشریه علمی - پژوهشی پژوهشهای علوم و صنایع غذایی ایران جلد ۱۴ شماره ۳ سال ۱۳۹۷

Iranian Food Science and Technology Research Journal Vol.14 No.3 2018

Contents